

Traversing the pyrochlore stability diagram: Microwave-assisted synthesis and discovery of mixed *B*-site Ln_2InSbO_7 family

Brenden R. Ortiz^{1,2,*†}, Paul M. Sarte^{1,3,‡}, Ganesh Pokharel¹, Michael Garcia, Marcos Marmolejo¹, and Stephen D. Wilson^{1,§}
Materials Department and California Nanosystems Institute, University of California Santa Barbara, Santa Barbara, California 93106, USA



(Received 28 June 2022; accepted 11 August 2022; published 12 September 2022)

The lanthanide pyrochlore oxides $Ln_2B_2O_7$ are one of the most intensely studied classes of materials within condensed matter physics, firmly centered as one of the pillars of frustrated magnetism. The extensive chemical diversity of the pyrochlores, coupled with their innate geometric frustration, enables realization of a wide array of exotic and complex magnetic ground states. Thus, the discovery of new pyrochlore compositions has been a persistent theme that continues to drive the field in exciting directions. The recent focus on the mixed *B*-site pyrochlores offers a unique route towards tuning both local coordination chemistry and sterics, while maintaining a nominally pristine magnetic sublattice. Here, we present a broad overview of the pyrochlore stability field, integrating recent synthetic efforts in mixed *B*-site systems with the historically established $Ln_2B_2O_7$ families. In parallel, we present the discovery and synthesis of the entire Ln_2InSbO_7 family ($Ln = La, Pr, Nd, Sm, Eu, Gd, Tb, Dy, Ho, Er, Tm, Yb, Lu$) located near the boundary of the pyrochlore stability field using a rapid, hybrid mechanochemical and microwave-assisted synthesis technique. Magnetic characterization on the entire class of compounds draws striking parallels to the stannate analogs, suggesting that these compounds may host a breadth of exotic magnetic ground states.

DOI: 10.1103/PhysRevMaterials.6.094403

I. INTRODUCTION

The cubic pyrochlore structure $A_2B_2O_7$ (Fig. 1) is considered as one of the canonical frustrated lattices in three dimensions [1–5]. In the case of the lanthanide pyrochlore oxides ($Ln_2B_2O_7$), the trivalent lanthanide Ln^{3+} ions form the hallmark frustrated network of corner-sharing tetrahedra (Fig. 1). Even considering only the *lanthanide* pyrochlore oxides, the number of possible combinations of Ln^{3+} and B^{4+} is staggering [1,2,6,7]. The flexibility to decorate the frustrated lattice with lanthanide elements of varying single-ion anisotropy, moment size, and radii, combined with the steric and chemical flexibility offered by the *B* site, have cemented the pyrochlore family as a fruitful arena for the pursuit of the emergence of exotic and novel magnetic ground states. Experimental and theoretical studies alike have proposed the $Ln_2B_2O_7$ pyrochlores as a means to realize a myriad of properties ranging from unconventional long-range order [2–5,8–15], unconventional spin-glass behavior [3,16–27], topologically nontrivial electronic states [28–36], spin ices [12,37–47], magnetic monopole quasiparticles [48–52], quantum spin liquids [53–63], cooperative paramagnetism [64–68], and other spin-liquid-like states [69,70].

Considering the rich interplay between chemistry and physics present in the pyrochlore materials, the discovery of new pyrochlore compositions has been a constant theme

over the last few decades [1,2,4,5]. Given the vast chemical space, the community naturally sought out empirical “rules” to predict the relative stability of pyrochlore structures using simple chemical metrics. These approaches are reminiscent of the Goldschmidt tolerance factor for perovskites [71], and aim to provide simple guidelines and chemical intuition. Within pyrochlores, the “radius-ratio rules” have been the most successful, which constrain $R_{\min} \leq R_{Ln^{3+}}/R_{B^{4+}} \leq R_{\max}$ [1,2,72,73]. Despite the apparent simplicity and variations in the specifics of R_{\min} and R_{\max} , the radii-ratio rules have been applied with great success [1,2]. Naturally, the diversity of experimentally accessible $Ln_2B_2O_7$ pyrochlore phases saw a rapid expansion in the 1960s [72], particularly with rapid technological advances in extreme synthesis conditions (e.g. high pressure). Human ingenuity has also continued to produce metastable $Ln_2B_2O_7$ phases outside the pyrochlore stability field, including the germanates [74–78] and plumbates [79].

Beyond the search for the prototypical $Ln_2B_2O_7$ phases, one can also consider permutations that build upon the basic structure while maintaining the hallmark frustrated Ln^{3+} sublattice. The first mention of mixed *B*-site pyrochlore phases emerged with Blöte [80], where the six-coordinate B^{4+} ion was replaced by the isoelectronic combination of $B_i^{3+}B_{ii}^{5+}$. This is reminiscent of exploratory searches for more complex diamondlike semiconductors where silicon can be split iteratively into increasingly complex chemical compositions (e.g., Si, GaAs, CuGaSe₂) bound by charge balance. Unlike the diamondlike semiconductors, where the permutations reduce the global symmetry of the unit cell (Si: $Fd\bar{3}m$, GaAs: $F\bar{4}3m$), the *B* site in $Ln_2B_i^{3+}B_{ii}^{5+}O_7$ is nominally disordered, yielding an average structure with the same global symmetry

*These authors contributed equally to this work.

†ortiz.brendenr@gmail.com

‡pmsarte@gmail.com

§stephendwilson@ucsb.edu

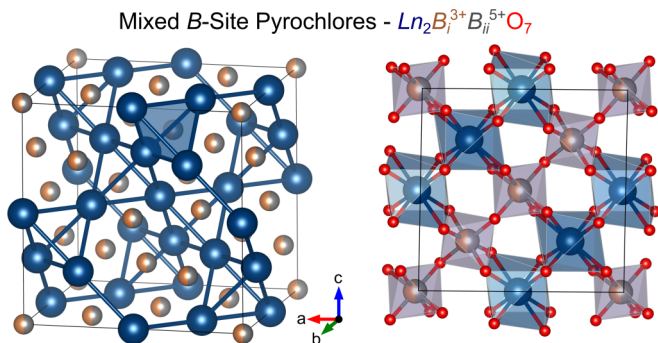


FIG. 1. Isometric view of the cation sublattice of the cubic $Fd\bar{3}m$ pyrochlore lattice (left), where the lanthanide sublattice consists of a 3D network of corner-sharing tetrahedra. The pyrochlore structure is an ordered superstructure variant of the defect fluorite structure, where the eight-coordinate A and six-coordinate B sites are structurally distinct (right).

as the ternary “parent” pyrochlore structure ($Fd\bar{3}m$). Despite the potential for a large number of additional permutations on the pyrochlore structure, systematic studies of the mixed B-site pyrochlores have been scarce so far [1].

Part of the historical hesitation behind the mixed B-site pyrochlores comes from the negative connotation of “disorder” and its association with “dirty” samples [81]. Recently, however, there has been a surge of renewed interest in the mixed B-site pyrochlores [82–87], driven by the emerging picture of the profound effects that disorder can play on cooperative magnetic properties. Recent experimental studies on $Pr_2Zr_2O_7$ suggest the possibility that disorder may in fact provide a key route in the realization of both exotic, and possibly novel, magnetic ground states [55,81]. The studies that do exist for mixed B-site pyrochlores are fascinating in their own right, and the most thorough investigations have indicated that the mixed $Ga^{3+}Sb^{5+}$ compositions are remarkably similar to the $Ln_2Ti_2O_7$ titanates in both structure and properties [80,82–84]. As such, we postulate that the richness of the $Ln_2B_2O_7$ phases may be mirrored in their mixed B-site counterparts, but with additional chemical degrees of freedom.

In this work we aim to provide the first systematic study of a mixed B-site family throughout the entire *f* block in the context of the rich history of the lanthanide $Ln_2B_2O_7$ phases. We begin by providing an updated pyrochlore stability field diagram, integrating recent synthetic efforts in the metastable $Ln_2B_2O_7$ phases and mixed B-site $Ln_2B_i^{3+}B_{ii}^{5+}O_7$ pyrochlores. Simultaneously, we present our synthesis and discovery of the Ln_2InSbO_7 series of compounds. These compounds serve as a structural analog to the $Ln_2Sn_2O_7$ stannates, much as the Ln_2GaSbO_7 family corresponds to the respective titanates. The Ln_2InSbO_7 compounds straddle the pyrochlore stability window, and producing high-quality powders using classical synthesis methods is difficult [88]. As such, we also present a hybrid mechanochemical-microwave synthesis method for pyrochlore oxides which can produce phase-pure crystalline material in <30-min heat treatments. We discuss the magnetic properties of the entire Ln_2InSbO_7 series down to 60 mK, analyzing the data in the context of other $Ln_2B_2O_7$ analogs and other mixed B-site pyrochlores. Our work demonstrates the rich and diverse role the mixed B-site materials can play

when deciphering complex structure-property relationships in the lanthanide pyrochlores.

II. EXPERIMENTAL METHODS

A. Synthesis

Polycrystalline samples of the Ln_2InSbO_7 family ($Ln = La, Pr, Nd, Sm, Eu, Gd, Tb, Dy, Ho, Er, Tm, Yb, Lu$) were synthesized from stoichiometric amounts of the dried lanthanide oxides: La_2O_3 99.999% Alfa, Pr_6O_{11} 99.99% Alfa, Nd_2O_3 99.99% Alfa, Sm_2O_3 99.9% Alfa, Eu_2O_3 99.9% Alfa, Gd_2O_3 99.99% Alfa, Tb_4O_7 99.9% Alfa, Dy_2O_3 99.9% Alfa, Ho_2O_3 99.99% Alfa, Er_2O_3 99.9% Alfa, Er_2O_3 99.9% Alfa, Tm_2O_3 99.9% Alfa, Yb_2O_3 99.998% Alfa, Lu_2O_3 99.999% Alfa, and the two metalloid oxides: In_2O_3 (99.9% Alfa) and Sb_2O_5 (99.998% Alfa). Two synthetic routes were investigated.

The first route corresponds to a method building on the classical heating profiles previously reported for similar pyrochlores, while integrating mechanochemical methods. Stoichiometric mixtures of the dried lanthanide oxide and the two metalloid oxides were combined into a tungsten carbide ball-mill vial and milled for 60 min. The resulting powders were extracted, ground in an agate mortar, and sieved through a 50- μ m sieve. These powders were loaded into 2-mL high-density alumina crucibles (CoorsTek) and annealed in a box furnace at 1250 °C for 48 h.

The second route involves abandoning classical heating profiles and instead combines mechanochemical methods with microwave-assisted synthesis. Stoichiometric mixtures of the dried lanthanide oxide and the metalloid oxides were combined into tungsten carbide ball-mill vials and milled for an initial 60-min cycle. The resulting powder was extracted, ground in an agate mortar to break up any agglomerates, and milled again for an additional 90 min. After this second cycle, 10 mL of anhydrous ethanol was added to the vial, and the sample was milled a third time for an additional 30 min. The resulting slurry was dried in a 80 °C oven, resulting in an extremely fine, homogeneous powder.

Each precursor powder was loaded directly into a 2-mL alumina crucible (CoorsTek), which was subsequently nested within a larger 10-mL alumina crucible filled with 7 g of granular activated charcoal (DARCO 12-20 mesh, Sigma-Aldrich). The crucibles were then placed within an assembly of low-density alumina foam measuring approximately 15 × 15 × 15 cm. Finally, the total assembly was placed in a 2.45-GHz multimode microwave oven with a maximum output of 1.2 kW (Panasonic model NN-SN651B). For samples containing large lanthanide ions (La-Gd), the alumina crucible was exposed directly to air. For smaller lanthanide ions (Tb-Lu), an alumina frit and secondary 2-mL crucible were used as an effective “lid” to reduce heat loss and increase the maximum temperature.

Phase purity was examined with powder x-ray diffraction (XRD) measurements at room temperature on a Panalytical Empyrean diffractometer ($Cu K_{\alpha 1,2}$) in standard Bragg-Brentano (θ -2 θ) geometry. Rietveld refinements of the powder XRD patterns were performed using TOPAS ACADEMIC v6 [89]. Structural models and visualization utilized the VESTA software package [90].

B. Magnetic characterization: dc and ac magnetic susceptibility

Measurements of the temperature- and field-dependent dc magnetization were performed on a 7 T Quantum Design Magnetic Property Measurement System (MPMS3) SQUID magnetometer in vibrating-sample magnetometry (VSM) mode. Powder of each Ln_2InSbO_7 sample was placed in a polypropylene capsule and subsequently mounted in a Quantum Design brass holder. The zero-field-cooled (ZFC) and field-cooled (FC) dc magnetization was collected continuously in sweep mode with a ramp rate of 2 K/min in the presence of an external dc field of 100 Oe. The ZFC isothermal dc magnetization was collected continuously in sweep mode with a ramp rate of 100 Oe/s.

The temperature dependence of the ac magnetization was measured on a Quantum Design 14 T Dynacool Physical Property Measurement Systems (PPMS) employing the ac susceptibility option for the dilution refrigerator (ACDR). Phase-pure powder of each member of the Ln_2InSbO_7 was cold pressed with a Carver press, and a portion of the resulting pellet with approximate dimensions of $1 \times 1 \times 0.5$ mm was adhered to a sapphire sample mounting post with a thin layer of GE varnish. All ac measurements were collected under ZFC conditions in the absence of an external dc magnetic field.

III. RESULTS AND DISCUSSION

A. Pyrochlore stability field

Part of the allure of the pyrochlore lattice is the chemical diversity offered by the choice of A-site and B-site elements [1,2,4,5,7,72,73,91,92]. As established previously, the community leverages the empirically derived “radius-ratio rules” to predict and synthesize new pyrochlore materials. For trivalent lanthanide oxide pyrochlorides $Ln_2B_2O_7$, the relationship was previously established decades ago as $1.46 \leq R_{Ln^{3+}}/R_{B^{4+}} \leq 1.80$ [1]. More recently, the rules are often quoted as $1.36 \leq R_{Ln^{3+}}/R_{B^{4+}} \leq 1.71$ [2,72,73]. The pyrochlore stability rules have been applied with great success in the discovery of new $Ln_2B_2O_7$ phases and continues to guide materials discovery in the pyrochlorelike phases.

While the applicability of the “radii-ratio rules” within the mixed B-site systems is assumed, there has not been a exhaustive review of the B-site systems in the context of the pyrochlore stability field. In addition to any steric considerations (e.g. ionic radii), mixed B-site alloys must also observe charge neutrality conditions. As such, there are a relatively finite number of combinations that can be expected to obey both the radii-rules and charge-neutrality conditions. Figure 2 provides a graphical review of known trivalent lanthanide pyrochlorelike oxide (gray) compositions of the form $Ln_2B_2O_7$ or $Ln_2B_i^{3+}B_{ii}^{5+}O_7$ [1,74–80,82,88,93–157].

In our search for lanthanide pyrochlore oxides, we have chosen to maintain the nominal purity of both the Ln^{3+} and oxygen sublattices, although many other variants on the pyrochlore lattice (e.g., mixed anion oxyfluoride [158,159], oxynitrides [17], alkali A site [160], etc.) have been reported. For graphical simplicity, compositions with a limited number (<4) of members reported (e.g., Ln_2AlSbO_7 [161]) have been omitted. White boxes mark compositions with no reported synthetic data. Nonpyrochlore compositions are

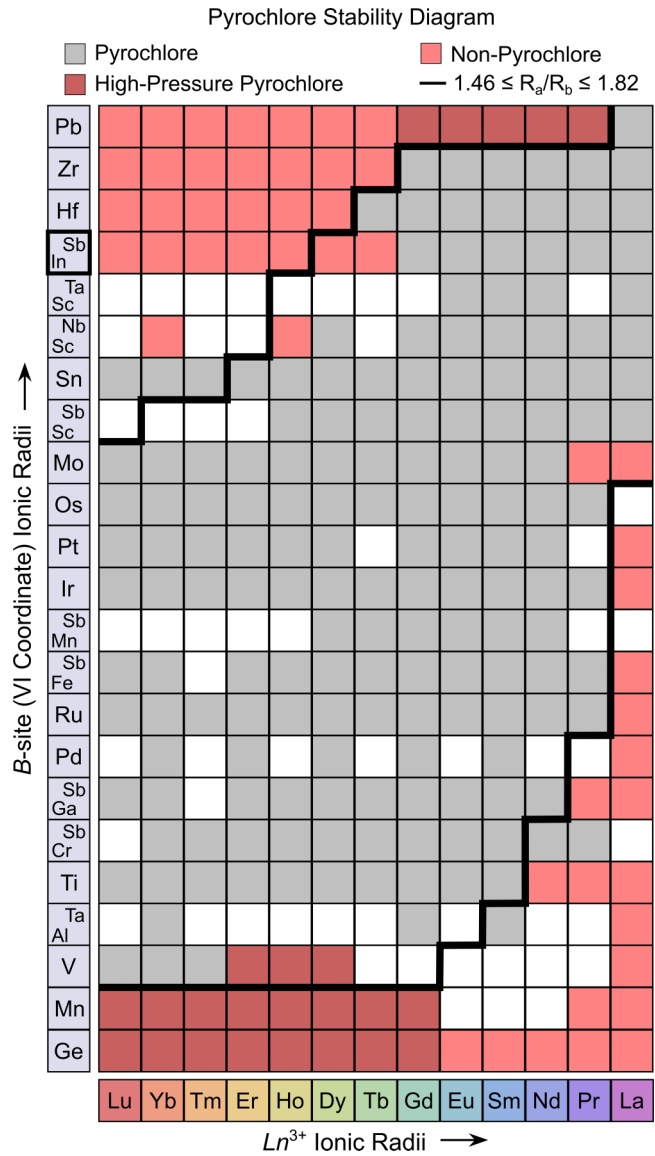


FIG. 2. Stability-field map for $Ln_2B_2O_7$ and $Ln_2B_i^{3+}B_{ii}^{5+}O_7$ lanthanide pyrochlore oxides. Known pyrochlore structures reported in the literature are superimposed with a minimized stability field (black border). “Non-pyrochlore” null results (red) and pyrochlorides stabilized with high pressure (dark red) are distinguished from “no data” (white).

marked in red, and include (1) phase competition with other compounds, (2) polymorph competition with fluorite-type or lower-symmetry structures, or (3) persistent (substantial) phase impurity and off stoichiometry. Special attention has been paid to pyrochlore phases that have been stabilized in the pyrochlore structure through the application of hydrostatic pressure > 1 MPa (e.g., $Ln_2Ge_2O_7$ [74–78], $Ln_2Pb_2O_7$ [79]). These metastable compositions are distinguished by a dark red coloration.

Using a simple scoring algorithm, we have recalculated the limits of $R_{\min} \leq R_{Ln^{3+}}/R_{B^{4+}} \leq R_{\max}$. Contrary to the often quoted range $[R_{\min}, R_{\max}]$ of $[1.36 \text{ \AA}, 1.71 \text{ \AA}]$ [2,72,73], the best fit, denoted by the black boundary in Fig. 2, was calculated to be $[R_{\min}, R_{\max}]$ of $[1.46 \text{ \AA}, 1.82 \text{ \AA}]$, in excellent

agreement with the historical estimate provided by Subramanian *et al.* [1]. Our updated stability diagram suggests that the mixed *B*-site pyrochlores largely abide by the empirical radii rules discovered decades prior. This is interesting, as one could reasonably expect that the bond strain and disorder induced by the mixed *B* site could negatively impact the energetics of the ordered pyrochlore structure. The predictive accuracy of the model for all known compounds is $\sim 94\%$. We note that the range $[R_{\min}, R_{\max}]$ of $[1.36 \text{ \AA}, 1.71 \text{ \AA}]$ [2,72,73] performs substantially worse, only capturing the known pyrochlore phases with 75% accuracy.

Upon closer inspection of Fig. 2, many compositions that border the edge of the stability field were noted to have mixed results reported in the literature, where coexistence and competition of the pyrochlore and defect fluorite phases is contested [7,162]. While we have tried to survey the results independently, the binary demarcation of pyrochlore or nonpyrochlore is an oversimplification at best. The literature is rife with such results that highlight the complexity of defect formation [163,164] throughout the stability field. Informally, our review of the literature serves as a reminder that the stability field, although convenient, is an oversimplified construct. One must respect that the defect thermodynamics and kinetics will be unique for each composition. These defect mechanisms are crucial for many key systems (e.g., $\text{Yb}_2\text{Ti}_2\text{O}_7$ [5,165–173], $\text{Tb}_2\text{Ti}_2\text{O}_7$ [64,174–182]) whose ground-state properties are intimately tied with the nuances of both defects and disorder. It is important to note that such considerations must be taken into account, particularly when moving into compositions with *intentional* disorder on the *B* site.

B. $\text{Ln}_2\text{InSbO}_7$: Synthesis and structure

While the effective radii of the combination of InSb is approximately 0.70 \AA , nearly identical to that of Sn (0.69 \AA) [183], the discrepancy is large enough such that the InSb compositions straddle the limits of pyrochlore stability field in Fig. 2. This is consistent with previous work by Strobel [88], where only $\text{Gd}_2\text{InSbO}_7$ was able to be synthesized in a phase-pure form. In contrast to the case of the much smaller combination of GaSb, approximating that of Ti, preliminary work by Strobel suggested that smaller Ln^{3+} cations appeared to destabilize the cubic pyrochlore structure in favor of lower-symmetry derivatives [88].

Even within compositions which were nominally stable, prior reports in the GaSb and InSb systems [88] commonly referenced impurity phases that were persistent and often unidentifiable. Considering that mixed *B*-site compositions are quaternary alloys, they require excellent mixing and homogeneity to produce phase-pure samples. Ensuring good mixing, accelerating kinetics, and producing phase-pure powders often requires several cycles of classical “shake-and-bake” processing, consisting of multiple heating cycles with intermittent grinding. However, often these methods are insufficient to produce phase-pure powders. Such is the case for $\text{Ln}_2\text{InSbO}_7$ [80,88], and some select $\text{Ln}_2\text{GaSbO}_7$ compositions [80,82], where impurities persist indefinitely. As an attempt to circumvent the limitation of slow reaction kinetics, we incorporated mechanochemical methods (see Methods

Sec. II A), creating extremely fine, homogeneous, glassy precursor phases. In the case of $\text{Ln}_2\text{InSbO}_7$ (La...Gd), a single annealing treatment (18 h) on the glassy precursor phase is sufficient to produce phase-pure powders. The successful synthesis of phase-pure $\text{Ln}_2\text{InSbO}_7$ cubic pyrochlore oxides suggests that prior limitations [88] were a consequence of the classically established processing methods commonly employed to synthesize pyrochlore oxides, and not limitations of thermodynamics.

However, $\text{Ln}_2\text{InSbO}_7$ compositions with small lanthanide ions (Tb...Yb) did not produce cubic pyrochlores, and instead exhibited diffraction patterns fraught with numerous additional reflections, reminiscent of previous exploratory work [88]. A combination of scanning electron microscopy (SEM) and energy dispersive spectroscopy (EDS) confirmed the heated powders remained chemically homogeneous and single phase, suggesting a reduction in symmetry from cubic to monoclinic or triclinic crystal systems. We noted an extreme sensitivity of the additional peaks with anneal time and temperature, suggestive of complex crystallization kinetics in the trans-Gd compounds.

To probe the crystallization process *ex situ*, we designed a series of quenching experiments to generate a crude time-temperature phase diagram. We determined that the precursor, which is largely amorphous, first crystallizes into a cubic phase within a very short time frame ($\sim 1 \text{ h}$). As the anneal proceeds further, the cubic phase gradually degrades and transforms into the lower-symmetry structure. Additional experiments to control atmospheric conditions and test potential volatility issues failed to stymie the decomposition of the cubic phase, suggesting that the symmetry reduction is a thermodynamic effect. In this respect, although the emergence of the cubic phase from the glassy precursor is *kinetically* favored, the high-symmetry phase is ultimately *thermodynamically* unstable for the smaller Ln^{3+} ions.

The synthetic observations summarized above are consistent with Fig. 2, where $\text{Ln}_2\text{InSbO}_7$ compositions for early lanthanides are predicted to be cubic, while destabilizing midway through the lanthanide series. However, the observation that the cubic phase was kinetically favored provided a means to stabilize pyrochlorelike phases for the heavier lanthanides. As described in Sec. II A, microwave-assisted heating [184–188] of the mechanochemically synthesized amorphous precursors provided a direct experimental means of achieving the extreme heat and cooling rates required to successfully quench in the cubic $\text{Ln}_2\text{InSbO}_7$ phases [Fig. 3(a)]. It is worth noting that trans-Gd compounds often benefit from small amounts of excess Sb_2O_5 to compensate for increased volatility during the extreme ramp rates. We note that the microwave-assisted mechanochemical methods also work for pyrochlore phases that are accessible through classical heating methods. Thus, the combination of microwave-assisted heating and mechanochemical methods enables the rapid synthesis of the pyrochlore oxides, on the order of minutes *in lieu* of days, allowing for wide experimental surveys of chemical spaces in a short amount of time.

At first glance, it appears that the entire $\text{Ln}_2\text{InSbO}_7$ series can be stabilized as cubic pyrochlores. In Fig. 3(a), XRD illustrates that all $\text{Ln}_2\text{InSbO}_7$ compositions crystallize in the cubic crystal system. The corresponding Rietveld analysis

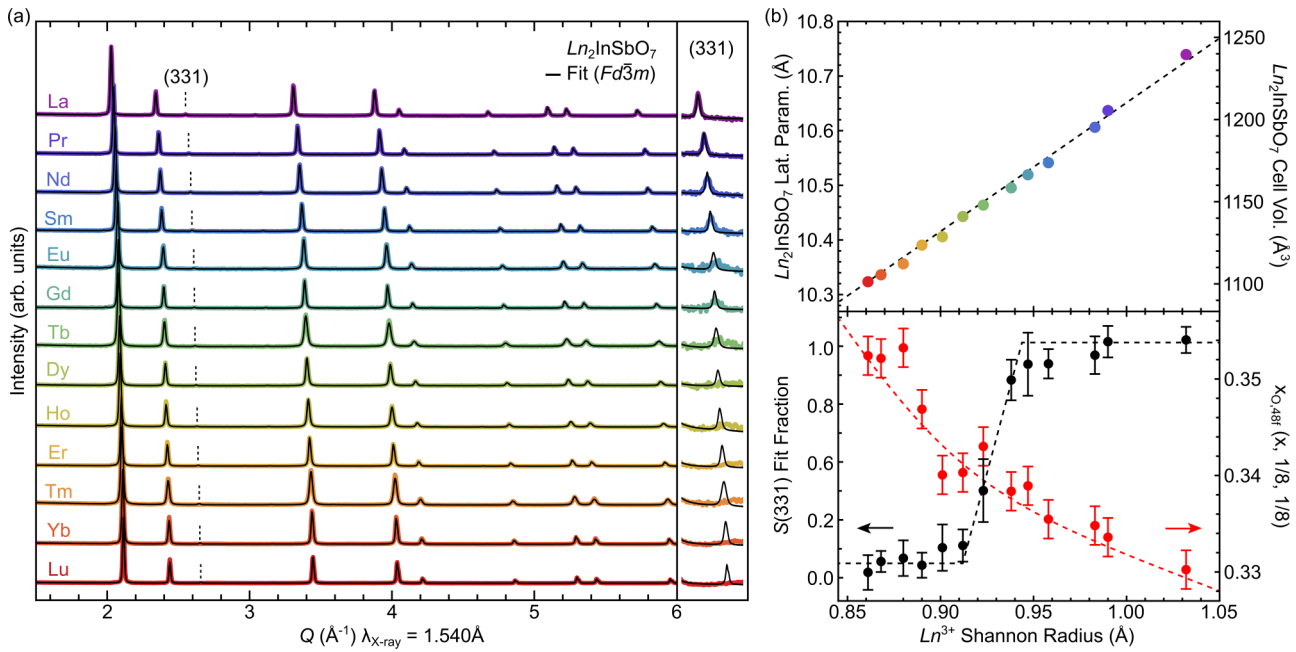


FIG. 3. (a) Room-temperature x-ray diffraction patterns and corresponding Rietveld fits (black) in the $Fd\bar{3}m$ space group for Ln_2InSbO_7 family. All compounds crystallize in cubic symmetry with pre-Gd compositions (La...Gd) displaying characteristic pyrochlore superlattice reflections [e.g., (331) peak]. Due to the exceptionally weak structure factor of the (331) reflection, we have provided a magnified view [(a), right] to aid in graphical comparison. [(b), top] Linear dependence of the refined cubic lattice parameter and cell volume with trivalent lanthanide Shannon radius. [(b), bottom] Deviation between predicted and observed intensity of (331) superlattice reflection as a function of composition. The suspected crossover from the pyrochlore structure for pre-Gd compositions (La...Gd) to a defect fluoritelike structure for post-Gd compositions (Tb...Yb) is mirrored by the shift of the variable x coordinate of the 48 f oxygen.

(black) is shown for each compound using the pyrochlore $Fd\bar{3}m$ structure with an ordered cation sublattice. No impurity phases can be identified within the resolution of x-ray diffraction, and the lattice parameter and cell volume trend linearly with increasing Ln^{3+} radii [Fig. 3(b), top], consistent with reports for other pyrochlore families [1]. For lighter lanthanides (La...Gd), Ln_2InSbO_7 compositions are best described with the pyrochlore $Fd\bar{3}m$ structure, possessing the characteristic (311) and (331) “pyrochlore” superlattice reflections [1,2,189,190]. However, it is worth noting that due to the particular elements involved, these superlattice peaks in Ln_2InSbO_7 are extremely weak. For the ideal pyrochlore structure with no disorder present between the A and B sites, the (311) and the (331) superlattice reflections in La_2InSbO_7 are *predicted* to be 0.2% and 1.4% of the main (222) reflection, respectively.

In the case of trans-Gd compositions (Tb...Lu), assignment of the unit cell is more nuanced. Although these materials do maintain cubic symmetry [Fig. 3(a)], the (311) and (331) superlattice reflections become vanishingly small, as illustrated in Fig. 3(b), bottom. The black trace denotes the “fit fraction” of the (331) reflection, where the “fit fraction” is defined by

$$F = 100\% \times \left(1 - \frac{I_{hkl,\text{Calc.}} - I_{hkl,\text{Obs.}}}{I_{hkl,\text{Calc.}} - I_{hkl,\text{Bkg.}}} \right), \quad (1)$$

where F was constructed such that perfect agreement with the pyrochlore structure is defined as 100%, and complete suppression of the (331) corresponds to 0%. The loss of the (331) peak as the Ln^{3+} radius shrinks is mirrored by a gradual shift in the position of the 48 f oxygen ion to the higher-

symmetry point at $(\frac{3}{8}, \frac{1}{8}, \frac{1}{8})$. This shift towards a symmetric oxygen coordination is likely associated with a gradual disordering of the A and B sublattices [7,191]. However, we caution that oxygen is notoriously difficult to fully characterize with standard x-ray diffraction. Incremental increases in disorder are consistent with recent results in the pyrochlore zirconates, where a combination of XANES, synchrotron, and neutron diffraction indicate that the defect fluorite to pyrochlore transition across the series is gradual [164]. However, in the case of Ln_2InSbO_7 , the situation has an additional layer of complexity since the cubic phase is not the thermodynamic ground state for trans-Gd compositions. Thus, we move to conservatively classify the Ln_2InSbO_7 compositions from (Tb...Lu) as defect fluorite phases. Since the In^{3+} , Sb^{5+} , and Ln^{3+} ions all share relatively similar electron densities, it is difficult to directly quantify the degree of A - and B -site disordering. However, loss of the (311) and (331) superlattice reflections is typically sufficient to suggest suppression of pyrochlorelike domains.

Despite our tentative classification of the trans-Gd Ln_2InSbO_7 phases as defect fluorite phases, we feel it appropriate to highlight recent results that demonstrate how the transition from pyrochlore to defect fluorite is not always a simple matter. Recent work on $Tb_2Hf_2O_7$ [163] demonstrates that the loss of the pyrochlore superlattice reflections does not *necessarily* arise from cation disordering. In the case of the halfnate, a combination of neutron powder diffraction and resonant x-ray diffraction confirmed the presence of an ordered “pyrochlore” cation sublattice. Instead, the anionic sublattice experiences progressive disordering, marked by a high density of oxygen Frenkel defects [163]. Reflecting on

our observations in the Ln_2InSbO_7 compounds, such an effect could conceivably be convolved in our observation of shifts in the $48f$ oxygen position, but ultimately lies outside our experimental confidence at this time. Further experiments, including neutron diffraction, are underway. However, as we will demonstrate in our magnetization measurements, many of the trans-Gd compositions retain magnetic properties that are strikingly similar to their *pyrochlore* stannate and titanate analogs.

Revisiting Fig. 2, it is clear that the structural trends identified in the Ln_2InSbO_7 series are consistent with its location in the predicted pyrochlore stability field. Despite having a nearly identical effective *B*-site radius as the stannates (0.69 \AA) [183], the Ln_2InSbO_7 series (0.70 \AA) does not share the structural stability of the stannates. This striking drop in the phase stability of the pyrochlore structure is mirrored by other large mixed *B*-site pyrochlores such as Ln_2ScNbO_7 [109,110,192] (0.693 \AA) and Ln_2ScTaO_7 [105–108] (0.693 \AA), both of whom have effective Shannon radii [183] closely comparable to that of tetravalent tin. As our discussion shifts towards the magnetic properties of the Ln_2InSbO_7 family of compounds, we will aim to make comparisons between not only the stannates, but also with their heavier analogs (e.g., halfnates and zirconates), and other mixed *B*-site pyrochlores.

C. dc and ac magnetic susceptibilities

Drawing analogies to the stannates, members of the Ln_2InSbO_7 family have been organized into four categories based on their proposed magnetic ground state: (1) long-range antiferromagnetic order, (2) dynamic magnetic ground states, (3) dipolar spin ices, and (4) nonmagnetic singlet states. As shown below, despite mirroring a stability field similar to the halfnate counterparts [1,94,100–104], the properties of the Ln_2InSbO_7 series are remarkably consistent with the magnetic properties of the stannates, the nonmixed *B*-site family with whom they share the closest structural properties [1,111]. Remarkably, even in the cases of trans-Gd compositions where the structure would be conservatively classified as defect fluorite, the magnetic properties of the Ln_2InSbO_7 family remain reminiscent of the behavior exhibited by their pyrochlore stannate counterparts.

We stress that our comparison with existing pyrochlore families is a first-order approximation. We aim to frame the magnetic properties of the Ln_2InSbO_7 systems using familiar terminology derived from the breadth and depth of available pyrochlore research. Detailed investigations utilizing other thermodynamic (e.g., heat capacity) and scattering (e.g., inelastic or elastic neutron) will always be required to unambiguously determine complex ground states.

1. Long-range antiferromagnetic order: Nd_2InSbO_7 , Gd_2InSbO_7 , and Er_2InSbO_7

Nd_2InSbO_7 : As illustrated in Fig. 4, a λ -type peak at $T_N = 0.37 \text{ K}$ is present in the ac susceptibility of Nd_2InSbO_7 . Exhibiting no clear frequency dependence, such a peak is consistent with a transition into a long-range magnetic ordered state. As the isothermal magnetization suggests the presence of $\langle 111 \rangle$ Ising single-ion anisotropy [193], combined with

the small magnitude of the Curie-Weiss temperature, our data support the possibility that Nd_2InSbO_7 assumes noncoplanar all-in-all-out magnetic order that has been reported for all other Nd-based pyrochlores [82,87,194–203].

While possessing many of the generic features of Nd-based pyrochlores, Nd_2InSbO_7 exhibits a key distinguishing property: an exceptionally low Curie-Weiss temperature of $+0.1 \text{ K}$. Recently, Gomez *et al.* [82] proposed that chemical pressure plays a crucial role in realization of moment fragmentation [204]. The authors argue that any contraction of the lattice would decrease the value of the Curie-Weiss constant as a result of the enhancement of the antiferromagnetic Nd^{3+} - O^{2-} - Nd^{3+} superexchange pathways, which would exclude moment fragmentation in favor of long-range antiferromagnetic order [195,205]. Solely utilizing the lattice parameter, both T_N and θ_{CW} for Nd_2InSbO_7 compare favorably to the general trends observed among all Nd-based pyrochlores summarized by Fig. 8 in Gomez *et al.* [82].

We suspect that Nd_2InSbO_7 may exhibit the same rich physics present in the $ScNb$ [87,194], Hf [206], Zr [205,207,208] analogs due to its proximity to the crossover point in the sign of the Curie-Weiss temperature. Recently, Scheie *et al.* [194] suggested that both Nd_2ScNbO_7 and $Nd_2Zr_2O_7$ share a common, unusual, fluctuating magnetic ground state. This presents the exciting possibility that Nd_2InSbO_7 may exhibit moment fragmentation. With the presence of controlled chemical disorder, Nd_2InSbO_7 may provide additional insights into the physical origins of the strong quantum fluctuations [205,209,210] underlying both the nature of moment fragmentation and the magnetic ground state present in the heavier Nd-based pyrochlores.

Gd_2InSbO_7 : With a half-filled $4f^7$ electronic configuration ($L = 0$, $S = \frac{7}{2}$) [211], Gd^{3+} is expected to possess minimal spin anisotropy, particularly smaller than Ho^{3+} , Dy^{3+} , and Tb^{3+} [14,212,213]. Combined with dominant antiferromagnetic exchange when placed on a pyrochlore lattice, Gd-based pyrochlores are excellent candidates for the experimental realization of a classical Heisenberg pyrochlore antiferromagnet and its predicted ground-state degeneracy [214–221].

As is the case for the other $Gd_2B_2O_7$ pyrochlores (Ti [212,222,223], Sn [222–224], Sc/Nb [86], Hf [225], Zr [225], Pb [79]), the presence of minimal single-ion anisotropy results in a Curie-Weiss-type magnetization response over a large temperature range. The presence of dominant antiferromagnetic interactions with a $\theta_{\text{CW}} = -8.7 \text{ K}$, results in the deviation of the isothermal magnetization from the Brillouin function in the low-field limit before its saturation at $g_J J = 7 \mu_B$ [226].

In stark contrast with Gd_2ScNbO_7 [86], Gd_2InSbO_7 exhibits a frequency-independent λ -type anomaly at $T_N = 0.78 \text{ K}$ in the ac susceptibility, corresponding to the onset of long-range order. In the case of $ScNb$ [86], a Mydosh parameter of $0.020(1)$ places Gd_2ScNbO_7 in the conventional spin-glass regime [19,227]. The glassy nature of Gd_2ScNbO_7 is consistent with the bifurcation of the ZFC/FC dc magnetization, linear low-temperature specific heat, and μ SR results. Instead, Gd_2InSbO_7 has a sharp λ -type anomaly which is highly reminiscent of $Gd_2Sn_2O_7$ [222,228]. Unlike the titanate, which exhibits two closely spaced transitions [222,229,230], the stannate assumes the $\mathbf{k} = (0,0,0)$

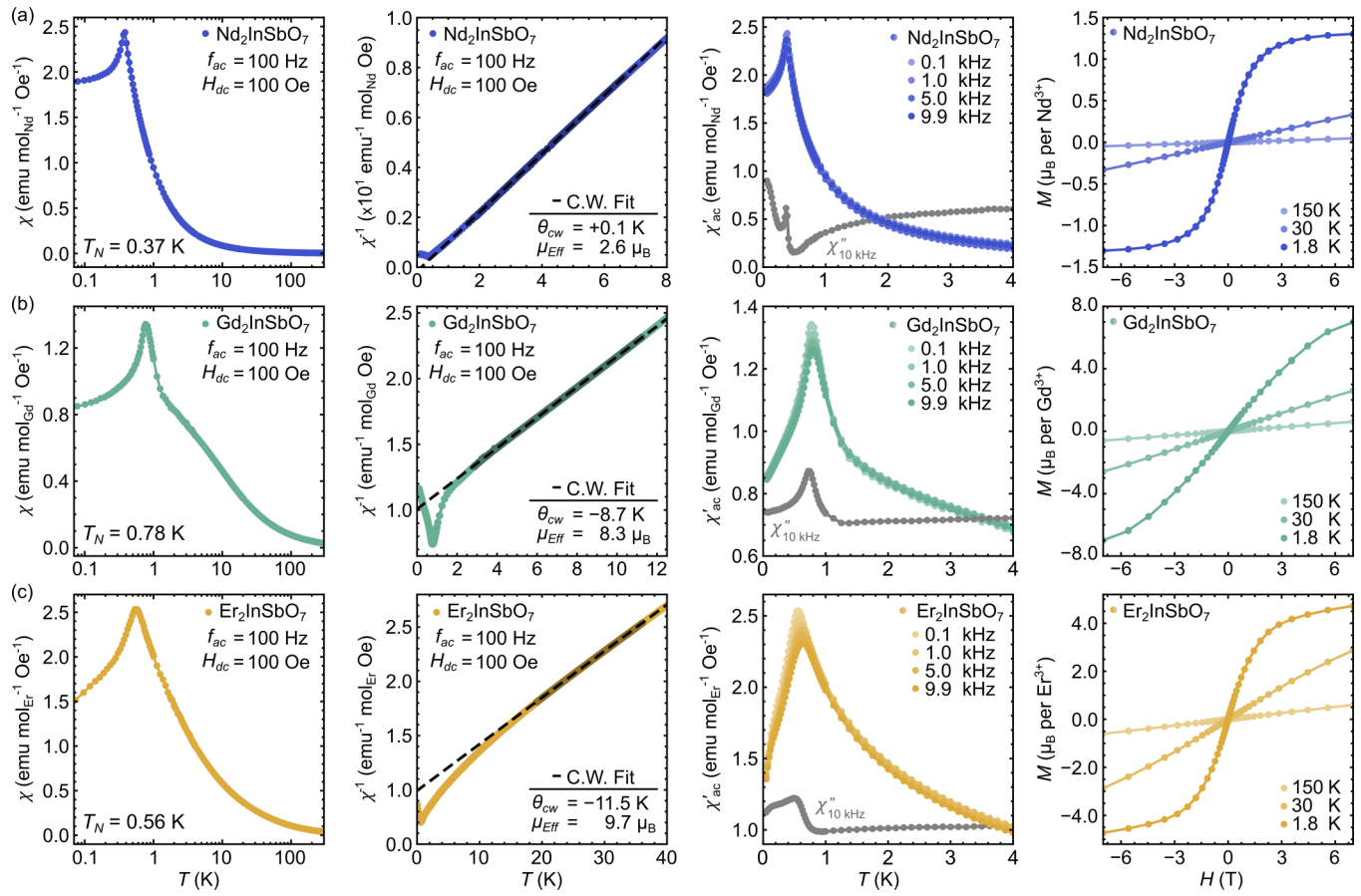


FIG. 4. Combined temperature dependence of the ac and dc magnetizations with corresponding Curie-Weiss fits, and the isothermal dc magnetization of (a) $\text{Nd}_2\text{InSbO}_7$, (b) $\text{Gd}_2\text{InSbO}_7$, and (c) $\text{Er}_2\text{InSbO}_7$. For temperatures $T < 4$ K, the ac susceptibility was measured at various frequencies f_{ac} in the absence of a dc field. For $T > 1.8$ K, the dc susceptibility was measured in an external field H_{dc} of 100 Oe. Data ranges used in Curie-Weiss fits correspond to darkly shaded data.

Γ_7 “Palmer-Chalker” state [228,231]. In fact, such a collinear antiferromagnetic state is theoretically predicted for a Heisenberg antiferromagnet with dipolar interactions [232], and corresponds to the proposed state for $\text{Gd}_2\text{Pt}_2\text{O}_7$ [233]. Such a magnetic structure is much simpler to determine experimentally when compared to the proposed multi- \mathbf{k} structure of the titanate that still remains the subject of debate [14,229,230,234–237].

The presumed long-range antiferromagnetic order of $\text{Gd}_2\text{InSbO}_7$ is particularly interesting in the context of the spin-glass ScNb [86]. A generic mixed B -site Gd-based pyrochlore generally exhibits the three key ingredients of a spin glass: (1) frustration, (2) disorder, and (3) competing interactions. However, our conceptual intuition may be limited, particularly in the face of a recent report of the effects of sample quality in $\text{Gd}_2\text{Zr}_2\text{O}_7$ [225,238]. The clear absence of glassy behavior in $\text{Gd}_2\text{InSbO}_7$, despite substantial (intentional) chemical disorder, demonstrates that other subtle perturbative terms such as beyond-nearest-neighbor exchange terms [228,239] may be particularly influential in the selection of its magnetic ground state.

$\text{Er}_2\text{InSbO}_7$: As is the case for their Heisenberg Gd $^{3+}$ counterparts, the inclusion of dipolar interactions to the isotropic exchange Hamiltonian for XY pyrochlores (e.g., Er $^{3+}$) with dominant antiferromagnetic interactions is pre-

dicted to lift any extensive classical degeneracy, and uniquely select the Palmer-Chalker state [8,232,240]. Experimentally, however, this is not the case for the majority of XY pyrochlores [78,166,168,241–245]. Exemplified by $\text{Er}_2\text{Ti}_2\text{O}_7$, where long-range magnetic order is realized via a quantum order-by-disorder mechanism [8–12], XY pyrochlores present a versatile experimental platform for the effects of multiphase competition [5].

The presence of multiphase competition has been used extensively to account for key experimental signatures that are characteristic of the XY pyrochlores [5]. These include multiple heat capacity anomalies, suppression of the ordering temperature, unconventional spin dynamics, defect sensitivity, and pressure-dependent magnetic ground states. Recently, the application of multiphase competition has been extended [246–249] further to address the vastly different magnetic ground states observed among each of the two families of XY pyrochlores.

In Er-based pyrochlores, members with a smaller lattice parameter tend to select for long-range antiferromagnetic order in Γ_5 [241,242], while their larger counterparts assume the Palmer-Chalker state at significantly lower Néel temperatures [250,251]. The effects of multiphase competition becomes particularly apparent when comparing the titanate that orders at 1.23 K with ψ_2 (Γ_5) [8,242,252],

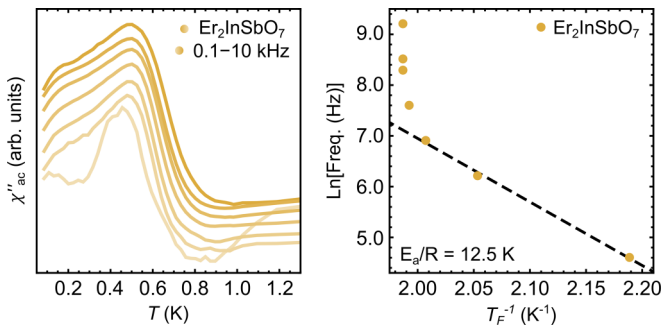


FIG. 5. Temperature dependence of the out-of-phase component χ'' of the ac susceptibility of $\text{Er}_2\text{InSbO}_7$ (left) with corresponding Arrhenius analysis (right) for frequencies below 1 kHz.

while its stannate counterpart begins to order at 108 mK in the Palmer-Chalker state [240,251,253]. The significant suppression of the second-order magnetic transition, combined with the multiscale dynamics, is consistent with the placement of $\text{Er}_2\text{Sn}_2\text{O}_7$ in close proximity to the Γ_7/Γ_5 boundary [5,240,246]. The titanate, however, exhibits little sample dependence and a robust ground state as it is located deep within ψ_2 of Γ_5 [246,254].

As illustrated in Fig. 4(c), both the temperature-dependent and isothermal magnetization mirrors the titanate [8,255–257] and the stannate [224,258–260]. Above 20 K, the magnetic susceptibility follows the Curie-Weiss law for dominant antiferromagnetic interactions ($\theta_{\text{CW}} = -11.5$ K) between large Er^{3+} moments ($\mu_{\text{eff}} = 9.7 \mu_B$). The isothermal magnetization does not follow a Brillouin curve, saturating at $\sim 4.2 \mu_B \ll g_J J$. The large moment suggests a large dipolar term, and when combined with the XY single-ion anisotropy of Er^{3+} , a Palmer-Chalker state theoretically should be realized [8,8,232,240,242]. In the case of Er-based pyrochlores, B -site disorder does not preclude the assumption of long-range magnetic order. Samples produced along the $\text{Er}_2\text{Sn}_{2-x}\text{Ti}_x\text{O}_7$ solid solution retained the ψ_2 (Γ_5) ground state of the titanate until a quantum crossover at $x = 1.7$ to Γ_7 of the stannate [261].

In $\text{Er}_2\text{InSbO}_7$, the transition to a long-range ordered state is consistent with the distinct peak at $T_N = 0.56$ K present in the ac susceptibility. However, unlike the Nd and Gd analogs, the prominent peak exhibits a clear frequency dependence at low frequencies. In $\text{Er}_2\text{Sn}_2\text{O}_7$, the frequency dependence was attributed to spins located at magnetic domain boundaries [262,263]. As illustrated in Fig. 5, the frequency dependence does not follow Arrhenius-type behavior. Instead, our data exhibit extreme nonlinearity for frequencies above 1 kHz. We note that this behavior may still be consistent with the stannate, as all published ac data are collected over a narrow low-frequency regime from 5–200 Hz [240,251]. We hypothesize that the non-Arrhenius behavior in $\text{Er}_2\text{InSbO}_7$ may be a reflection of the slow dynamics that have previously identified in $\text{Er}_2\text{Sn}_2\text{O}_7$ [240,251]. Ultimately, it would be interesting to determine if both the stannate and titanate analogs exhibit nonlinearity in the high-frequency limit.

While $\text{Er}_2\text{InSbO}_7$ does exhibit clear linear behavior for lower frequencies, its activation energy of 12.5 K is over an

order of magnitude larger than that of its stannate analog (0.9 K) [240,251]. Such an increase is consistent with the effects of disorder, as has been proposed in A -site disordered pyrochlores [264–266], although it has been noted that B disorder may have the opposite effect [267]. Regardless, the distinct similarities between $\text{Er}_2\text{InSbO}_7$ and its stannate analogs suggest the existence of multiscale dynamics, where slow dynamics may persist and coexist with static long-range magnetic order below T_N .

The Néel temperature of $\text{Er}_2\text{InSbO}_7$ is unique among those values reported for all other Er^{3+} -based pyrochlores. Naïvely, with a lattice constant comparable to the stannate, it is expected that the resulting weaker exchange tensor would depress the Néel temperature of $\text{Er}_2\text{InSbO}_7$ towards the 0 K limit [5]. Instead, its large $T_N = 0.56$ K is comparable to that of the much smaller titanate [8,255–257]. Such a large Néel temperature suggests that $\text{Er}_2\text{InSbO}_7$ is located far from a phase boundary in the classical ground-state phase diagram [5,240,246], although it is important to note that without neutron diffraction, the identity of Γ and its respective ψ both remain an open question.

2. Dynamic magnetic ground states: $\text{Yb}_2\text{InSbO}_7$, $\text{Tb}_2\text{InSbO}_7$, and $\text{Sm}_2\text{InSbO}_7$

$\text{Yb}_2\text{InSbO}_7$: Corresponding to the second, and arguably most prominent, family of the XY pyrochlores [5], Yb-based pyrochlores have been subject to intense interest since the proposal of quantum spin-ice behavior in $\text{Yb}_2\text{Ti}_2\text{O}_7$ [60,249,268–271]. The subsequent explosion of experimental and theoretical studies have propelled research into Yb-based magnetism in various frustrated geometries, including the triangular [59,272–279] and Shastry-Sutherland lattices [280–285]. Fueled by the enhanced quantum fluctuations that are a result of the $J_{\text{eff}} = \frac{1}{2}$ degrees of freedom originating from the thermally well-isolated Kramers doublet single-ion ground state [2,5,78,246,286–288], Yb-based magnetism has remained a fruitful arena for the search of quantum spin-liquid states [5,58,61,268,289–292].

As is the case for their Er^{3+} counterparts, multiphase competition in Yb-based pyrochlores is particularly influential on the magnetic properties of the selected ground state [247,249]. In addition to extremely depressed transition temperatures ($T_N, T_C \ll 1$ K), Yb-based pyrochlores have demonstrated particular sensitivity to sample preparation and defect formation [5,166,167,169,171,173,293–299]. The case of $\text{Yb}_2\text{Ti}_2\text{O}_7$ is perhaps the most infamous. Minute changes in the Yb stoichiometry have been demonstrated to broaden, depress, or completely suppress any signature of long-range static magnetic order in heat capacity and magnetization [5,165–173]. Interestingly enough, the application of a moderate amount of pressure [300] is sufficient to recover the $\mathbf{k} = 0$ splayed ferromagnetic state. Altogether, these results are consistent with the placement of the titanate near the ferromagnetic Γ_9 /antiferromagnetic Γ_5 phase boundary [60,246,247].

Given the extreme fragility of the magnetic ground state in $\text{Yb}_2\text{Ti}_2\text{O}_7$, one would expect full suppression of the long-range order in the mixed B -site $\text{Yb}_2\text{GaSbO}_7$. Indeed, $\text{Yb}_2\text{GaSbO}_7$ does not exhibit the characteristic λ -type anomaly in its heat capacity [80,83] indicative

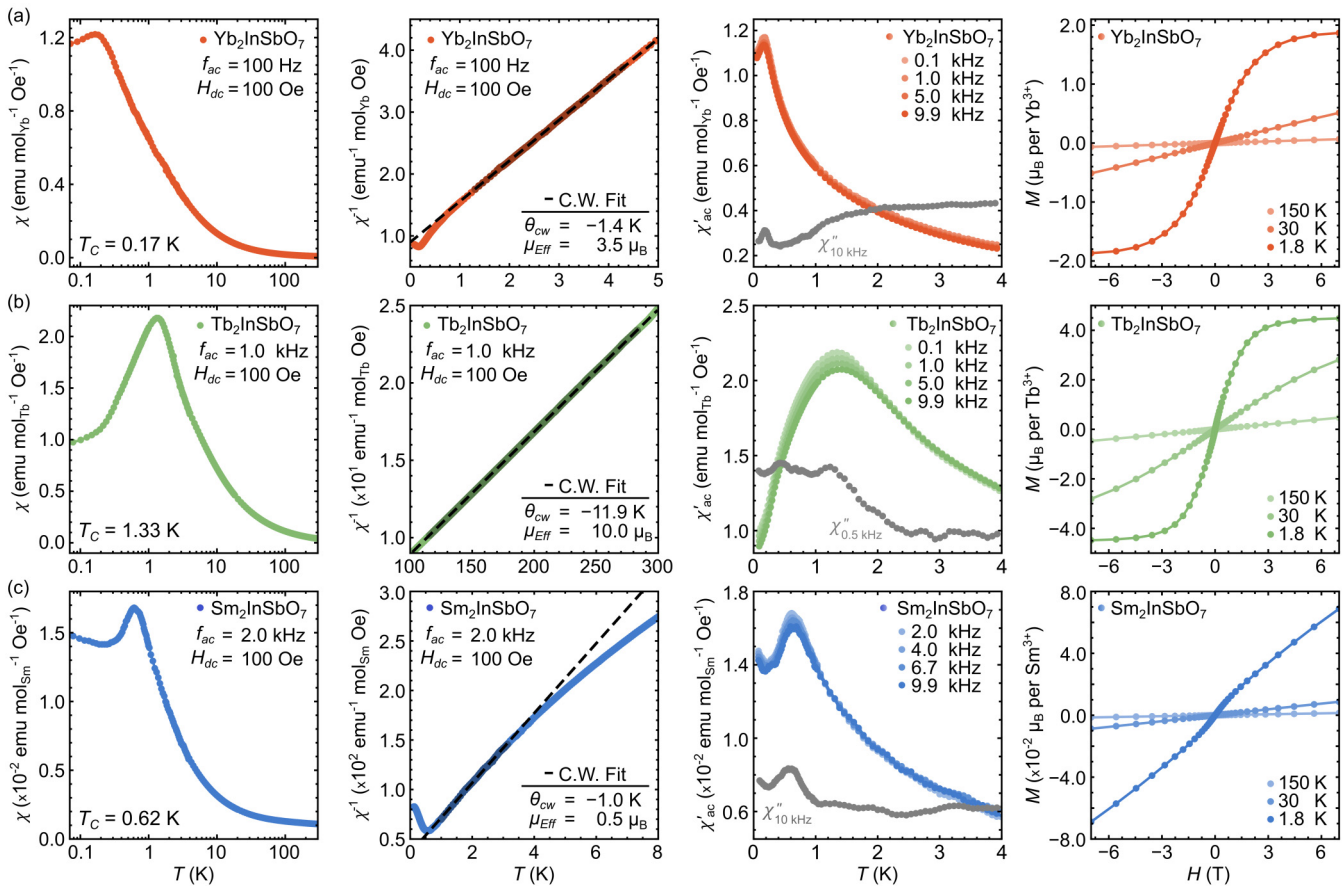


FIG. 6. Combined temperature dependence of the ac and dc magnetizations with corresponding Curie-Weiss fits, and the isothermal dc magnetization of (a) $\text{Yb}_2\text{InSbO}_7$, (b) $\text{Tb}_2\text{InSbO}_7$, and (c) $\text{Sm}_2\text{InSbO}_7$. For temperatures $T < 4$ K, the ac susceptibility was measured at various frequencies f_{ac} in the absence of a dc field. For $T > 1.8$ K, the dc susceptibility was measured in an external field H_{dc} of 100 Oe. Data ranges used in Curie-Weiss fits correspond to darkly shaded data.

of static long-range magnetic order in Yb^{3+} -based pyrochlores [165–168,229,243–245,293,294,301,302]. At a cursory glance, this seems consistent with the deleterious effect of disorder, though more thorough investigations demonstrate that only a minority of spins freeze, with the majority remaining dynamic to base temperatures as confirmed by both inelastic neutron scattering [83] and μ SR spectroscopy [303].

In fact, strong dynamical correlations appear ubiquitous among the Yb^{3+} -based pyrochlores [5,294], developing coherence at a temperature $T^* > T_N, T_C$ centered about a broad feature present in the heat capacity [78,244,245,294,302]. These unconventional dynamics correspond to gapless $\mathbf{Q} = 0$ excitations [166,250,251,294,301] and are remarkably robust against disorder and doping effects, regardless of the presence (or suppression) of long-range magnetic order [5,258,294]. Similar effects have been particularly well documented in Tb^{3+} -based pyrochlores [4,175,304–309].

In the case of $\text{Yb}_2\text{GaSbO}_7$, the application of a modest 1 T field shifts spectral weight from these low-energy fluctuations into magnetic Bragg peaks corresponding to Γ_9 long-range magnetic order [83]. Although corresponding to the zero-field magnetic structure of the titanate, the appearance of such static magnetic order despite the presence of maximal B -site disorder at first is not expected, particularly when considering stuffing of the order of 1%–2% in the $\text{Yb}_2\text{Ti}_2\text{O}_7$ suppresses

long-range ordering [5,167,169–171,173]. While mechanical pressure can be used to recover the magnetic order in $\text{Yb}_2\text{Ti}_2\text{O}_7$ [300], the energy scale is quite disparate from the application of a 1 T field in $\text{Yb}_2\text{GaSbO}_7$. This is evidence that *antisite* disorder (stuffing) and *B*-site disorder operate independently, and should be experimentally discernible.

As summarized in Fig. 6(a), the low-temperature magnetic properties of $\text{Yb}_2\text{InSbO}_7$ are reminiscent of its GaSb analog [83] with comparable Curie-Weiss parameters ($3.5 \mu_{\text{eff}}/\text{Yb}^{3+}$ and $\theta_{\text{CW}} = -1.4$ K). In the low-temperature limit, a frequency-independent peak at 0.17 K dominates, reminiscent of both $\text{Yb}_2\text{GaSbO}_7$ and the relatively sharp features present in pristine samples of both the titanate [165,166,168,172,173,310,311] and stannate [243,244,301]. The energy scale is comparable to the stannate ($T_C \sim 0.11\text{--}0.15$ K [243,244,301]) which is proximal in terms of both average B -site radius [183] and cell volume. The comparison between InSb:Sn is analogous to GaSb:Ti, where the smaller GaSb (0.35 K [83]) mimics the respective titanate (0.26 K [166–168]).

Exploiting the analogy to its GaSb analog, it is more probable that the sharp peak in both χ' and χ'' corresponds to a freezing of a minority of spins instead of long-range ferromagnetic order. The striking similarities between $\text{Yb}_2\text{InSbO}_7$ and $\text{Yb}_2\text{GaSbO}_7$ are particularly noteworthy since $\text{Yb}_2\text{InSbO}_7$

is outside the pyrochlore stability field (Fig. 2) and may be intermediate between the pyrochlore and defect fluorite structures. The analogous behavior of InSb and GaSb may suggest that the cation sublattice (up to a certain correlation length) remains intact, despite a highly disordered anionic sublattice, as is the case for $\text{Tb}_2\text{Hf}_2\text{O}_7$ [163].

Although it remains to be seen whether $\text{Yb}_2\text{InSbO}_7$ will exhibit properties consistent with $\text{Yb}_2\text{GaSbO}_7$ or its stannate analogs, the interaction between long-range magnetic order and the mixed B -site pyrochlores is interesting. Given that 1%–2% of Yb disorder suppresses long-range magnetic order [5,167,169–171,173], the observation that such suppression can be reversed by a modest field in $\text{Yb}_2\text{GaSbO}_7$ [83], with its much larger structural and steric changes, suggests that B -site disorder may present a unique (and very distinct) chemical means of reliably suppressing long-range ferromagnetic order in Yb-based pyrochlores, while preserving the Yb^{3+} sublattice and its underlying persistent dynamics [5,294].

$\text{Tb}_2\text{InSbO}_7$: Despite possessing a wealth of complex phenomena that rivals the Yb-based pyrochlores, theoretical efforts to address their Tb-based counterparts have remained an enduring challenge [2,4]. In contrast to the other lanthanide ions presented so far, the non-Kramers doublet of the $J = 6$ free-ion ground-state manifold of Tb^{3+} is separated from its first excited doublet by only ~ 1.4 meV [2,64,176,312–314]. Corresponding to a gap roughly an order of magnitude smaller than Yb^{3+} , the application of the pseudospin- $\frac{1}{2}$ model is not necessarily straightforward, necessitating the incorporation of more subtle effects, possibly even on equal footing with $\hat{\mathcal{H}}_{\text{CEF}}$ [315–317]. Such subtle effects include virtual crystal-field transitions, secondary corrections that introduce anisotropic exchange and may potentially stabilize a quantum spin-ice ground state in the cooperative paramagnet $\text{Tb}_2\text{Ti}_2\text{O}_7$ [176,268,315,316,318–320].

As is the case for its Yb^{3+} counterpart, multiphase competition is particularly influential on the magnetic ground state of $\text{Tb}_2\text{Ti}_2\text{O}_7$ [4,321–324]. Highly reminiscent of $\text{Yb}_2\text{Ti}_2\text{O}_7$, the magnetic ground state of $\text{Tb}_2\text{Ti}_2\text{O}_7$ is extremely sample dependent [64,174–182] with deviations in stoichiometry on the level of 1%–2% yielding quadrupolar order [305,321,325], consistent with the placement of the titanate in close proximity to the boundary between quantum spin ice and quadrupolar order [4]. Contrast such behavior to that exhibited by the stannate which assumes “soft” (or dynamic) spin-ice ordering corresponding to Tb^{3+} moments oriented 13.3° relative to the local $\langle 111 \rangle$ [326,326–332].

As summarized in Fig. 6(b), the isothermal magnetization of $\text{Tb}_2\text{InSbO}_7$ is consistent with Ising single-ion anisotropy characteristic of Tb^{3+} -based pyrochlores [4,74,163,176,268,313]. The high-temperature dc magnetization is qualitatively similar to both its stannate [224,259,326,328] and titanate [64,176,223] analogs with comparable Curie-Weiss parameters of $\mu_{\text{eff}} = 10 \mu_B$ and $\theta_{\text{CW}} = -11.9$ K. However, the sharp feature indicative of long-range order in the stannate [328] is absent, replaced by a broad, frequency-independent feature centered about ~ 1.33 K in χ' . These properties are highly reminiscent of $\text{Tb}_2\text{SnTiO}_7$ [309]. In the titanate [175,180,223,333], stannate [326,328], and $\text{Tb}_2\text{GaSbO}_7$ [80], the broad feature

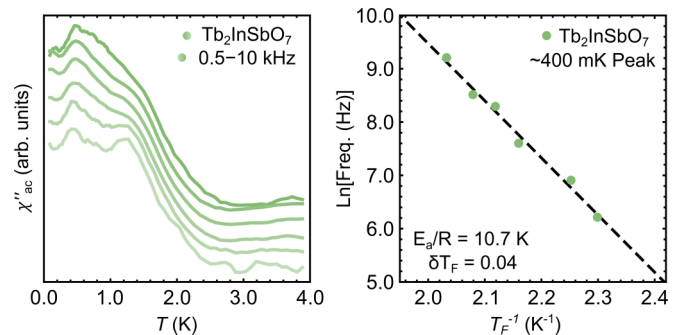


FIG. 7. The out-of-phase ac susceptibility (χ'') in $\text{Tb}_2\text{InSbO}_7$ exhibits a complex spectra with multiple peaks and strong frequency dependence (left). A subsequent Arrhenius fit to the frequency dependence of the 400-mK feature yields activation energy $E_a/R = 10.7$ K and Mydosh parameter $\delta T_F = 0.04$ (right).

has been attributed to the buildup of short-range magnetic correlations.

More complexity is evident in the out-of-phase χ'' ac magnetization signal (Fig. 7). We first observe an upturn in the magnetization around 2 K, normally associated with an increase in ferromagnetic interactions and mirrored by the broad feature in χ' . A shoulder peak in χ'' can be seen near 1.2 K, particularly in the low-frequency regime. This feature corresponds with the peak in the ac magnetization shown in Fig. 6. However, unlike the pristine $\text{Tb}_2\text{Sn}_2\text{O}_7$, our data lack the characteristic sharpness of the ferromagnetic ordering peak in the stannate, and it is difficult to extract a frequency dependence due to convolution with the rising signal. The general shape of χ'' agrees *remarkably well* with $x = 0.1$ Ti-doped $\text{Tb}_2\text{Sn}_{2-x}\text{Ti}_x\text{O}_7$ [328]. We postulate that the InSb disorder plays a similar role to the Ti doping, destroying the long-range ferromagnetic order. An additional feature emerges around 400 mK, a similar energy scale to a 300-mK feature observed in the pristine $\text{Tb}_2\text{Sn}_2\text{O}_7$. However, while prior reports observed an anomalously high Mydosh parameter (0.34) [328], we estimate that the 400-mK feature exhibits $\Delta T_f/T_f \Delta \ln(f) = 0.04$, an order of magnitude lower and more akin to results observed in the doped $\text{Tb}_2\text{Sn}_{2-x}\text{Ti}_x\text{O}_7$ samples.

Presuming that $\text{Tb}_2\text{InSbO}_7$ sits on the boundary between the defect fluorite and pyrochlore stability fields, the observation that $\text{Tb}_2\text{InSbO}_7$ exhibits behavior extremely reminiscent to lightly doped $\text{Tb}_2\text{Sn}_{2-x}\text{Ti}_x\text{O}_7$ is somewhat perplexing. However, if you consider the case of the corresponding halfnate $\text{Tb}_2\text{Hf}_2\text{O}_7$, where despite the presence of substantial anionic disorder (oxygen Frenkel defects), the cation sublattice remains ordered in the pyrochlore motif [1,103,104,163,224], the similarities of $\text{Tb}_2\text{InSbO}_7$ to its $\text{Tb}_2\text{Sn}_{2-x}\text{Ti}_x\text{O}_7$ analog can be somewhat reconciled. The question as to why χ'' retains such complex structure in $\text{Tb}_2\text{InSbO}_7$ that is so characteristic of both the titanate and stannate, despite the known sensitivity of Tb-based pyrochlores to chemical disorder [64,174–182], may assist in addressing the physics that underlies the distinct sample dependence in the selection of the magnetic ground state for Tb-based pyrochlores [4].

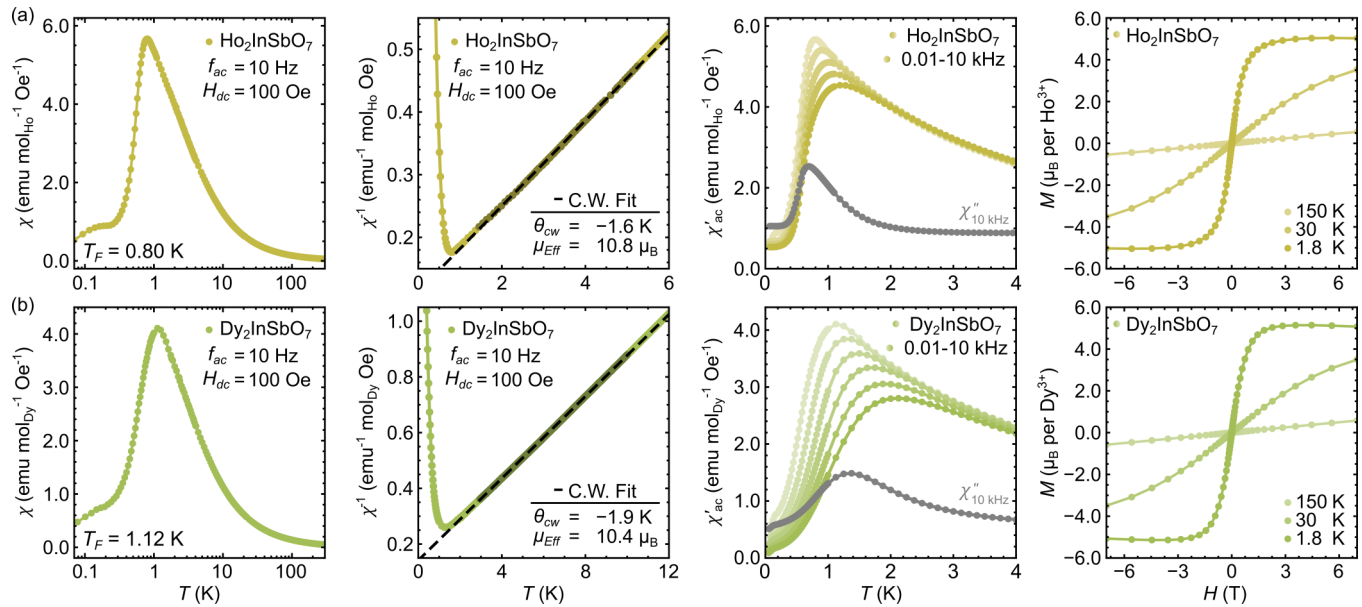


FIG. 8. Combined temperature dependence of the ac and dc magnetizations with corresponding Curie-Weiss fits, and the isothermal dc magnetization of (a) $\text{Ho}_2\text{InSbO}_7$ and (b) $\text{Dy}_2\text{InSbO}_7$. For temperatures $T < 4$ K, the ac susceptibility was measured at various frequencies f_{ac} ranging from 10 to 9984 Hz in the absence of a dc field. Here we show data collected for $T > 1.8$ K, the dc susceptibility was measured in an external field H_{dc} of 100 Oe. Data ranges used in Curie-Weiss fits correspond to darkly shaded data.

$\text{Sm}_2\text{InSbO}_7$: Despite exhibiting a frequency-independent peak at 0.62 K that compares favorably to both its titanate ($T_N = 350$ mK [334]) and stannate ($T_N = 440$ mK [335]) analogs, the peak observed in the case of $\text{Sm}_2\text{InSbO}_7$ is significantly broader. A natural suspicion is that the broad peak is a reflection of poor crystallinity, though this is not the case for $\text{Sm}_2\text{InSbO}_7$ which exhibits clear pyrochlore superstructure reflections and crystallinity comparable to all other pre-Gd InSb compounds. In fact, such behavior is highly reminiscent of its zirconate analog, which despite exhibiting excellent crystallinity with no detectable Sm/Zr antisite defects, does not exhibit a sharp λ -type anomaly in the heat capacity down to 0.1 K [238]. Instead, $\text{Sm}_2\text{Zr}_2\text{O}_7$ has a broad peak centered at 500 mK corresponding to the full $Rln2$ of the ground-state doublet, consistent with a buildup of short-range magnetic correlations [238,336].

Such a comparison to its zirconate analog is further strengthened by clear similarities in both the temperature and field dependence of the dc magnetization. As is the case for all Sm^{3+} -based pyrochlores, the temperature dependence of the dc magnetization in Fig. 6(c) does not exhibit a simple Curie-Weiss-type behavior due to crystal-field effects [335–337]. Restriction of the Curie-Weiss analysis to a narrow temperature range yields a Curie-Weiss temperature θ_{CW} of -1.0 K and an effective paramagnetic moment μ_{eff} of $0.5 \mu_B/\text{Sm}^{3+}$, comparing favorably with those values recently reported for the zirconate [238] ($\theta_{\text{CW}} = -1.27$ K and $\mu_{\text{eff}} = 0.39 \mu_B/\text{Sm}^{3+}$). As is the case for the zirconate, the isothermal magnetization does not saturate up to $\mu_0 H_{\text{ext}} \sim 7$ T. Instead, the magnetization is linear and consistent with a pseudospin- $\frac{1}{2}$ model assuming Ising anisotropy with a g factor significantly less than 1 [238,336]. Such single-ion anisotropy is consistent with the $|\pm \frac{3}{2}\rangle$ dipolar-octupolar doublet previ-

ously reported for the stannate [335], titanate [334,335], and zirconate [238].

Possessing a moment over a magnitude smaller relative to the dipolar spin-ice candidates Ho^{3+} and Dy^{3+} , the corresponding reduction in the dipolar term that is characteristic of all Sm^{3+} -based pyrochlores [259,334–336,338], suggests that exchange will be particularly influential in the magnetic ground state of $\text{Sm}_2\text{InSbO}_7$. When combined with the slightly larger lattice parameter, there is a possibility that quantum fluctuations may be strong enough to prohibit the assumption of the all-in-all-out long-range antiferromagnetic order that usually accompanies antiferromagnetically coupled Ising moments on the pyrochlore lattice [43,57,82,339–342]. As is the case for the zirconate [238], strong dynamics may persist in $\text{Sm}_2\text{InSbO}_7$ down to the lowest measurable temperatures, placing $\text{Sm}_2\text{InSbO}_7$ as a potential quantum spin-ice candidate.

3. Dipolar spin ices: $\text{Ho}_2\text{InSbO}_7$ and $\text{Dy}_2\text{InSbO}_7$

The discovery of the dipolar (“classical”) spin-ice state in both $\text{Ho}_2\text{Ti}_2\text{O}_7$ [37–39] and $\text{Dy}_2\text{Ti}_2\text{O}_7$ [40] spurred a flurry of interest in lanthanide pyrochlore oxides that has spanned the past two decades [2,4,5,42,343,344]. When decorated with large Ho^{3+} or Dy^{3+} moments that exhibit local $\langle 111 \rangle$ Ising single-ion anisotropy and net effective ferromagnetic exchange [80,345,345–348], $\text{Ho}_2\text{Ti}_2\text{O}_7$ and $\text{Dy}_2\text{Ti}_2\text{O}_7$ exhibit the macroscopically degenerate “two-in–two-out” motif fundamental to the dipolar spin ice [12,39,41–47].

As illustrated in Fig. 8, both $\text{Ho}_2\text{InSbO}_7$ and $\text{Dy}_2\text{InSbO}_7$ exhibit quantitative behavior highly reminiscent of both their titanate [37,40,72,182,193,212,257,349,350] and stannate [72,193,224,259,349,351] counterparts. The isothermal magnetization saturates to half of the theoretical value,

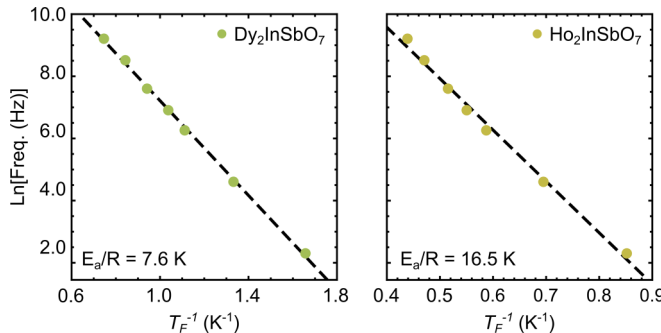


FIG. 9. Arrhenius fit of the frequency dependence of the freezing transition in $\text{Dy}_2\text{InSbO}_7$ (left) and $\text{Ho}_2\text{InSbO}_7$ (right), yielding activation energies $E_a/R = 7.6$ and 16.5 K, respectively, comparable to their stannate and titanate analogs.

consistent with a pseudospin- $\frac{1}{2}$ model assuming Ising anisotropy [193]. Temperature-dependent susceptibility measurements confirm the clear absence of long-range magnetic order. Above 3 K, both systems exhibit Curie-Weiss-type behavior with parameters similar to those reported for the titanate and stannate. Frequency-dependent maxima at 0.80 and 1.12 K appear in the ac susceptibility of $\text{Ho}_2\text{InSbO}_7$ and $\text{Dy}_2\text{InSbO}_7$, respectively, comparable to those temperatures reported for their stannate [349,349] and titanate [265,349,352–354] counterparts. Such behavior is also consistent with other Ho- and Dy-based spin ices, where frequency dependence is indicative of local spins freezing into the spin-ice state [75,76,265,349,352–358]. An Arrhenius analysis of the frequency-dependent ac susceptibility (Fig. 9) yielded activation energies E_a/R of 16.5 and 7.6 K for $\text{Ho}_2\text{InSbO}_7$ and $\text{Dy}_2\text{InSbO}_7$, respectively, that are comparable to those values reported [85,352,359–362] for the corresponding stannate and titanate systems.

The realization of a dipolar spin ice for two trans-Gd members of the $\text{Ln}_2\text{InSbO}_7$ family is not completely unexpected. Early studies on “stuffed” spin ice $\text{Ho}_2(\text{Ti}_{2-x}\text{Ho}_x)\text{O}_{7-x/2}$ ($0 \leq x \leq \frac{2}{3}$) demonstrated that the spin-ice state is remarkably robust against significant amounts of disorder [363–367]. The resistance to local disorder appears to persist up to the defect fluorite limit, where both A and B sites become indistinguishable. The presence of antisite disorder naturally accounts for both the negative Weiss temperature and reduced activation energy barrier [267,363]. However there are noteworthy differences between the $\text{Ln}_2\text{InSbO}_7$ systems and the “stuffed” spin ices. In particular, the magnitude of the normalized values of both χ' and χ'' are much larger than their stuffed spin-ice counterparts [363]. The freezing transitions of the InSb pyrochlores are also much sharper with minimal temperature suppression, reminiscent of their pure stannate [349,349] and titanate [265,349,352–354] analogs.

Recently, it was shown that in many Dy-based pyrochlores, antisite disorder between the A and B sites may destroy the spin-ice state. This effect was observed for the “stuffed” spin ice $\text{Dy}_2(\text{Dy}_x\text{Ti}_{2-x})\text{O}_{7-x/2}$ [368] and $\text{Dy}_2\text{Zr}_2\text{O}_7$, the latter of which hosts a disordered spin-liquid-like magnetic ground state [369]. Recall that $\text{Dy}_2\text{InSbO}_7$ is initially considered to be within the defect fluorite regime of the stability diagram, naively characterized by gradual disordering of the A and

B sites. In this sense, the prototypical spin-ice behavior seen in Fig. 8 is surprising. Potentially, both $\text{Ho}_2\text{InSbO}_7$ and $\text{Dy}_2\text{InSbO}_7$ may exhibit the same anionic sublattice disorder at $\text{Tb}_2\text{Hf}_2\text{O}_7$ [163], which would preserve the Dy^{3+} and Ho^{3+} cation sublattice and the requisite spin-ice state. Consistent with this thesis, the spin state has been shown to be remarkably robust against disorder isolated to the nonmagnetic B -site sublattice. Examples include the doped systems $\text{Ho}_2(\text{Ti}_{2-x}\text{Ho}_x)\text{O}_{7-x/2}$ ($x \lesssim 0.3$) [363], $\text{Dy}_2\text{Sn}_{2-x}\text{Sb}_x\text{O}_{7+x/2}$ [267], and $\text{Dy}_2\text{Ti}_{2-x}\text{Fe}_x\text{O}_7$ [370]. Similar effects are observed in the mixed B -site analogs $\text{Dy}_2\text{ScNbO}_7$ [85,267], $\text{Dy}_2\text{GaSbO}_7$ [84], and $\text{Dy}_2\text{FeSbO}_7$ [371] as well.

As is the case for all trans-Gd members, additional measurements (e.g., neutron diffraction and PDF, heat capacity, etc.) will be necessary to distinguish between which particular scenario: “stuffed” ($A_{B^{4+}}^{3+}$ antisite) or B -site (B_iB_{ii}) disordered spin ice applies to both the Ho^{3+} and Dy^{3+} members.

4. Nonmagnetic singlet ground states: $\text{Tm}_2\text{InSbO}_7$, $\text{Eu}_2\text{InSbO}_7$, and $\text{Pr}_2\text{InSbO}_7$

$\text{Eu}_2\text{InSbO}_7$: Both Eu- and Tm-based pyrochlores host trivial nonmagnetic spin-singlet ground states [121,259,372–374]. In the case of Eu^{3+} , the combination of the $4f^6$ electronic configuration, strong spin-orbit coupling, and D_{3d} point-group symmetry yields a nonmagnetic 7F_0 ground state [372,373,375]. With a gap of over 100 K to its first excited magnetic state 7F_1 , the Van Vleck term dominates the low-temperature magnetism of Eu^{3+} pyrochlores [88,259,376]. The dominance of the Van Vleck term for $\text{Eu}_2\text{InSbO}_7$ is consistent with the temperature independence of the magnetic susceptibility over a large temperature range below 100 K [Fig. 10(a)], in stark contrast to the behavior predicted by the Curie-Weiss law. As was the case for the titanate [372,373] and stannate [259] analogs, the isothermal magnetization does not saturate but continues linearly up to 7 T, consistent with antiferromagnetic exchange [372]. The increase in the magnetization in the low-temperature limit can be attributed to the presence of small amounts of magnetic impurities that eventually freeze.

$\text{Tm}_2\text{InSbO}_7$: In the case of Tm^{3+} , the ground state is a non-Kramers doublet that is weakly split due to crystal-field effects, resulting in a nonmagnetic singlet state at sufficiently low temperatures [80,259,374,377,378]. As is the case for both the stannate [259] and titanate [374] analogs, the isothermal magnetization of $\text{Tm}_2\text{InSbO}_7$ does not saturate, with values over an order of magnitude smaller than its predicted saturation magnetization [211]. The temperature dependence of the magnetic susceptibility illustrated in Fig. 10(b) does not exhibit Curie-Weiss-type behavior, instead it is reminiscent of the behavior predicted for a singlet-triplet level scheme [374,379]. The slight upturn and resulting nonlinearity at the low-temperature limit is attributed to the presence of small amounts of magnetic impurities. The frequency dependence of the ac susceptibility suggests that these impurities freeze in the low-temperature limit.

$\text{Pr}_2\text{InSbO}_7$: In contrast to their Tm^{3+} and Eu^{3+} counterparts, Pr-based pyrochlores can host a plethora of exotic magnetic ground states including the possibility

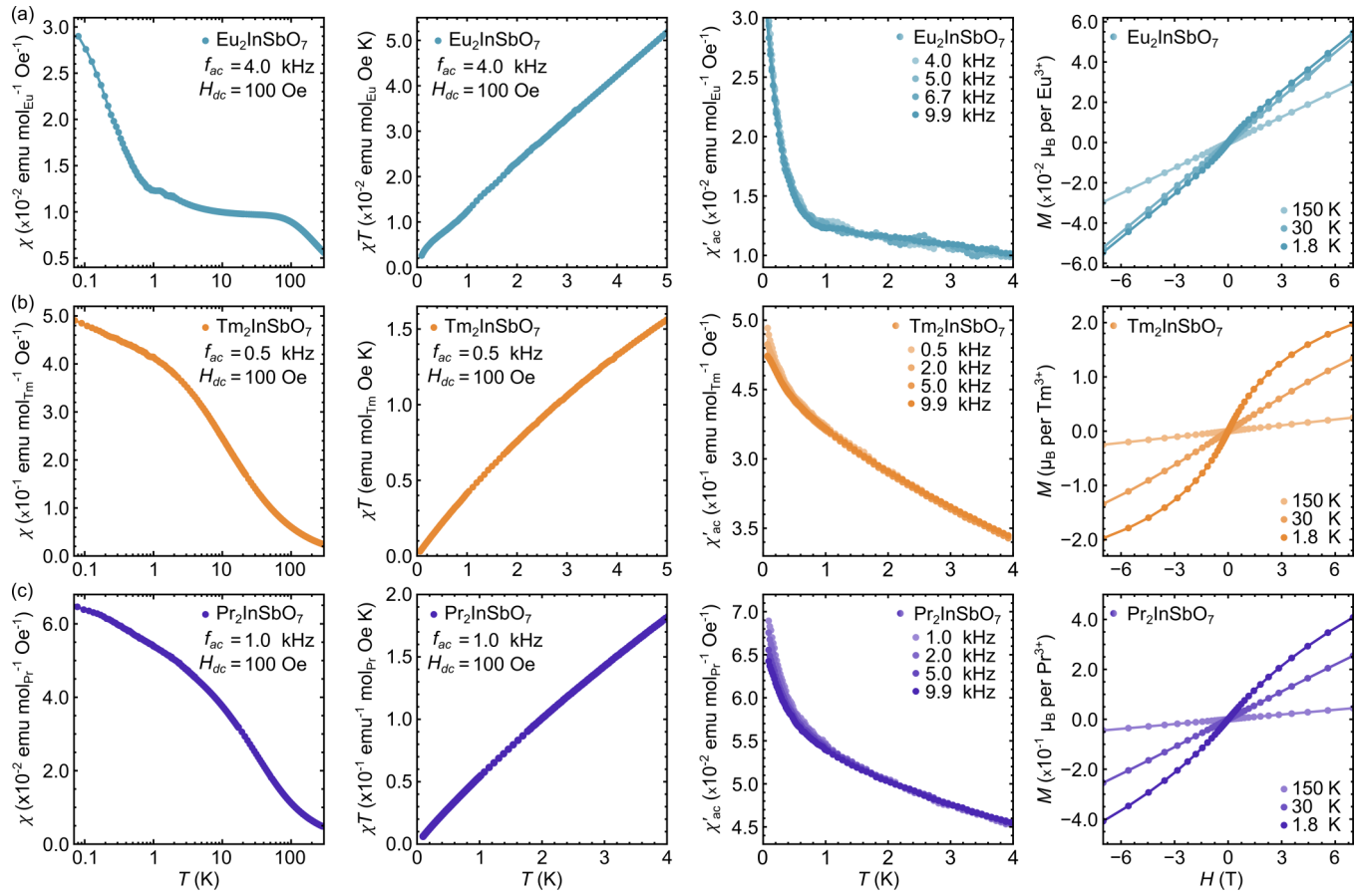


FIG. 10. Combined temperature dependence of the ac and dc magnetizations, and the isothermal dc magnetization of (a) $\text{Eu}_2\text{InSbO}_7$, (b) $\text{Tm}_2\text{InSbO}_7$, and (c) $\text{Pr}_2\text{InSbO}_7$. For temperatures $T < 4$ K, the ac susceptibility was measured at various frequencies f_{ac} in the absence of a dc field. For $T > 1.8$ K, the dc susceptibility was measured in an external field H_{dc} of 100 Oe.

of the experimental realization of quantum spin ice in the stannate [48,355], halfnate [206,380,381], and zirconate [55,81,210,382]. $\text{Pr}_2\text{Zr}_2\text{O}_7$ in particular has garnered significant attention as theoretical and experimental treatments have identified $J_{zz} > 0$ that is much larger than both $|J_{\pm}|$ and $|J_{\pm\pm}|$, placing $\text{Pr}_2\text{Zr}_2\text{O}_7$ near the QSI limit [81,210,382]. In these systems, the crystalline electric field acting on the $J = 4$ manifold yields a non-Kramers doublet that is well thermally isolated ($\Delta > 10$ meV), and thus can be projected onto an effective $J = \frac{1}{2}$ description [56,210,355,383]. Thus, Pr^{3+} -based pyrochlores can provide an experimental platform to investigate the complex, and often subtle interplay that result from geometric frustration, strongly correlated electrons, and orbital degrees of freedom [384].

However, the zirconate is also fraught with substantial chemical and structural disorder [55,81,92]. Although the physical origin of the disorder is still a subject of debate (e.g., lattice strain [81], Pr^{3+} off-centering [385]) the effect is to induce a temperature-independent continuum of scattering [55]. The profound influence of structural disorder in the zirconate is intuitive, considering that Pr^{3+} is a non-Kramers ion. It was shown that any perturbation away from ideal D_{3d} site symmetry can be mapped onto the introduction of transverse fields onto the pseudospin manifold [55,81]. Although such a strong random transverse theoretical treatment was shown to be con-

sistent with experimental observations, the role of exchange disorder plays remains an open question [4]. Theoretical attempts to address such a question have only focused on both extremes. In the case of strong exchange and weak exchange disorder, a disordered variant of a QSI is expected, while in the case of the exchange being significantly weaker than disorder, one would expect a frozen quadrupolar gas [54,56]. Instead, the intermediate regime, where the strength of the exchange and exchange disorder are comparable, has remained largely unexplored and represents an open question of great interest [4].

At a cursory level, $\text{Pr}_2\text{InSbO}_7$ presents an opportunity to address this intermediate regime. Its significantly smaller lattice parameter relative to the zirconate should result in an increase in strength of the $\text{Pr}^{3+}\text{-O}^{2-}\text{-Pr}^{3+}$ superexchange pathways. Instead, as illustrated in Fig. 10(a), both dc and ac magnetization results suggest a trivial nonmagnetic singlet state resembling that of $\text{Tm}_2\text{InSbO}_7$. The absolute magnitude of the isothermal magnetization is suppressed, and when combined with the lack of saturation in the isothermal magnetization, the results are inconsistent with a pseudospin- $\frac{1}{2}$ model assuming Ising anisotropy. Many quantum spin-ice candidates [355] exhibit a weakly frequency-dependent feature at base temperatures, but this feature is replaced with a Curie-type tail in $\text{Pr}_2\text{InSbO}_7$.

that may be attributed to the freezing of small amounts of impurities.

A natural conclusion would be that the splitting of the ground-state doublet into a nonmagnetic singlet state was a result of maximal *B*-site disorder, in strong contrast with the minimal levels of disorder in the zirconate [55,81,385]. However, other mixed *B*-site Pr-based pyrochlores such as $\text{Pr}_2\text{Sn}_{2-x}\text{Ti}_x\text{O}_7$ [48] and $\text{Pr}_2\text{ScNbO}_7$ [386] have been identified as spin-liquid-like candidates. It is possible that the various magnetic ground states stem from the deviation between the Shannon radii [183] of In^{3+} and Sb^{5+} ($\delta = 0.2$), which is substantially larger than that of $\text{Pr}_2\text{Sn}_{2-x}\text{Ti}_x\text{O}_7$ ($\delta = 0.085$) or $\text{Pr}_2\text{ScNbO}_7$ ($\delta = 0.105$). The role of the deviation δ in the selection of the magnetic ground state is a promising avenue for future investigation, with direct experimental routes in the form of the plethora of mixed *B*-site combinations currently synthetically available, each with differing values of δ .

IV. CONCLUSION

With a wide array of possible compositions and the hallmark frustrated lattice, mixed-site pyrochlores allow access to exotic properties ranging from moment fragmentation, quantum spin ices, spin liquids, magnetic monopoles, and many others [2,4,5,72]. In this work we analyzed the known stability field for the lanthanide oxide pyrochlores $\text{Ln}_2\text{B}_2\text{O}_7$. We merged recent synthetic results for the mixed *B*-site compositions with the previously established families, providing a broad review of the existing Ln -*B*-O compounds. We find the slightly modified “radius-ratio rule” of $1.43 \leq R_{\text{Ln}^{3+}}/R_{\text{B}^{4+}} \leq 1.82$ to perform across the entire family with a predictive accuracy of $\sim 94\%$.

In tandem with our review of pyrochlore compositions, we presented the phase-pure, rapid synthesis of the entire $\text{Ln}_2\text{InSbO}_7$ mixed *B*-site family. Our synthetic improvements enable synthesis of the entire family, improving upon prior reports wherein only the Gd and Nd variants were produced with sufficient purity [88]. Furthermore, we discuss how microwave-heating methods can stabilize the cubic phase throughout the entire family, despite small Ln^{3+} (Lu...Tb) showing the proclivity to crystallize in low-symmetry (monoclinic/triclinic) forms. We have provided empirical evidence that the InSb family may transition towards the defect fluorite phase for small Ln^{3+} (Lu...Tb) while compounds with larger Ln^{3+} (La...Gd) are consistent with the pyrochlore $Fd\bar{3}m$ structure.

This work additionally presents a broad survey of the magnetic properties throughout the entire $\text{Ln}_2\text{InSbO}_7$ mixed

B-site family. We provide analysis and comparisons to the relevant $\text{Ln}_2\text{B}_2\text{O}_7$ analogs, examining how the magnetic properties of the InSb compounds compare to the parent structures. We find that $\text{Nd}_2\text{InSbO}_7$, $\text{Gd}_2\text{InSbO}_7$, and $\text{Er}_2\text{InSbO}_7$ exhibit properties consistent with the long-range antiferromagnetic order typical of their analogous stannates. $\text{Yb}_2\text{InSbO}_7$, $\text{Tb}_2\text{InSbO}_7$, and $\text{Sm}_2\text{InSbO}_7$ show properties consistent with a dynamic ground state. $\text{Ho}_2\text{InSbO}_7$ and $\text{Dy}_2\text{InSbO}_7$ exhibit behavior consistent with the canonical dipolar spin ices, with energetics consistent with their stannate equivalents. Finally, $\text{Eu}_2\text{InSbO}_7$, $\text{Tm}_2\text{InSbO}_7$, and $\text{Pr}_2\text{InSbO}_7$ host nonmagnetic singlet ground states. Such behavior is expected for $\text{Eu}_2\text{InSbO}_7$ and $\text{Tm}_2\text{InSbO}_7$ due to their local crystal-field configurations. However, in the case of Pr^{3+} , the nonmagnetic ground state appears to arise from a splitting of the non-Kramers ground-state doublet due to the large Shannon radii contrast between In^{3+} (VI) and Sb^{5+} (VI).

Our survey of the existing lanthanide pyrochlore oxides combined with the magnetic characterization of the $\text{Ln}_2\text{InSbO}_7$ family provides a fresh perspective on the properties of mixed *B*-site pyrochlores. The chemical diversity of the mixed *B*-site systems has become a highlight of recent pyrochlore research, as the community reexamines the influence of disorder and local sterics on the realization of complex quantum phenomenon in the pyrochlore phases. Striking similarities between mixed *B*-site systems and the analogous mono-*B*-site pyrochlores continue to emerge, forcing us to reevaluate the presumed deleterious role of disorder. Instead, chemical disorder may become a tool that enables controlled changes in the local chemistry while maintaining a pristine Ln^{3+} magnetic sublattice.

ACKNOWLEDGMENTS

The authors acknowledge fruitful conversations with A. A. Aczel, J. A. M. Paddison, C. R. Wiebe, B. A. Frandsen, and A. Krajewska. B.R.O. and P.M.S. acknowledge financial support from the University of California, Santa Barbara, through the Elings Fellowship. This work was supported by DOE, Office of Science, Basic Energy Sciences under Award No. DE-SC0017752 (S.D.W., P.M.S., B.R.O.). This work used facilities supported via the UC Santa Barbara NSF Quantum Foundry funded via the Q-AMASE-i program under Award No. DMR-1906325. The research made use of the shared experimental facilities of the NSF Materials Research Science and Engineering Center at UC Santa Barbara (Grant No. DMR-1720256). The UC Santa Barbara MRSEC is a member of the Materials Research Facilities Network [387].

-
- [1] M. A. Subramanian, G. Aravamudan, and G. V. Subba Rao, Oxide pyrochlores – A review, *Prog. Solid State Chem.* **15**, 55 (1983).
 - [2] J. S. Gardner, M. J. P. Gingras, and J. E. Greedan, Magnetic pyrochlore oxides, *Rev. Mod. Phys.* **82**, 53 (2010).
 - [3] J. E. Greedan, Frustrated rare earth magnetism: Spin glasses, spin liquids and spin ices in pyrochlore oxides, *J. Alloys Compd.* **408**, 444 (2006).
 - [4] J. G. Rau and M. J. Gingras, Frustrated quantum rare-earth pyrochlores, *Annu. Rev. Condens. Matter Phys.* **10**, 357 (2019).
 - [5] A. M. Hallas, J. Gaudet, and B. D. Gaulin, Experimental insights into ground-state selection of quantum XY pyrochlores, *Annu. Rev. Condens. Matter Phys.* **9**, 105 (2018).
 - [6] A. F. Fuentes, S. M. Montemayor, M. Maczka, M. Lang, R. C. Ewing, and U. Amador, A critical review of existing criteria

- for the prediction of pyrochlore formation and stability, *Inorg. Chem.* **57**, 12093 (2018).
- [7] G. R. Lumpkin and R. D. Aughterson, Perspectives on pyrochlores, defect fluorites, and related compounds: Building blocks for chemical diversity and functionality, *Front. Chem.* **9**, 778140 (2021).
- [8] J. D. M. Champion, M. J. Harris, P. C. W. Holdsworth, A. S. Wills, G. Balakrishnan, S. T. Bramwell, E. Čížmár, T. Fennell, J. S. Gardner, J. Lago, D. F. McMorrow, M. Orendáč, A. Orendáčová, D. McK. Paul, R. I. Smith, M. T. F. Telling, and A. Wildes, $\text{Er}_2\text{Ti}_2\text{O}_7$: Evidence of quantum order by disorder in a frustrated antiferromagnet, *Phys. Rev. B* **68**, 020401(R) (2003).
- [9] L. Savary, K. A. Ross, B. D. Gaulin, J. P. C. Ruff, and L. Balents, Order by Quantum Disorder in $\text{Er}_2\text{Ti}_2\text{O}_7$, *Phys. Rev. Lett.* **109**, 167201 (2012).
- [10] M. E. Zhitomirsky, M. V. Gvozdikova, P. C. W. Holdsworth, and R. Moessner, Quantum Order by Disorder and Accidental Soft Mode in $\text{Er}_2\text{Ti}_2\text{O}_7$, *Phys. Rev. Lett.* **109**, 077204 (2012).
- [11] A. W. C. Wong, Z. Hao, and M. J. P. Gingras, Ground state phase diagram of generic XY pyrochlore magnets with quantum fluctuations, *Phys. Rev. B* **88**, 144402 (2013).
- [12] J. D. M. Champion and P. C. W. Holdsworth, Soft modes in the easy plane pyrochlore antiferromagnet, *J. Phys.: Condens. Matter* **16**, S665 (2004).
- [13] X. Li, Y. Q. Cai, Q. Cui, C. J. Lin, Z. L. Dun, K. Matsubayashi, Y. Uwatoko, Y. Sato, T. Kawae, S. J. Lv, C. Q. Jin, J.-S. Zhou, J. B. Goodenough, H. D. Zhou, and J.-G. Cheng, Long-range magnetic order in the Heisenberg pyrochlore antiferromagnets $\text{Gd}_2\text{Ge}_2\text{O}_7$ and $\text{Gd}_2\text{Pt}_2\text{O}_7$ synthesized under high pressure, *Phys. Rev. B* **94**, 214429 (2016).
- [14] N. P. Raju, M. Dion, M. J. P. Gingras, T. E. Mason, and J. E. Greedan, Transition to long-range magnetic order in the highly frustrated insulating pyrochlore antiferromagnet $\text{Gd}_2\text{Ti}_2\text{O}_7$, *Phys. Rev. B* **59**, 14489 (1999).
- [15] T. Subramani, A. Voskanyan, K. Jayanthi, M. Abramchuk, and A. Navrotsky, A comparison of order-disorder in several families of cubic oxides, *Front. Chem.* **9**, 719169 (2021).
- [16] J. N. Reimers, J. E. Greedan, and M. Sato, The crystal structure of the spin-glass pyrochlore, $\text{Y}_2\text{Mo}_2\text{O}_7$, *J. Solid State Chem.* **72**, 390 (1988).
- [17] L. Clark, G. J. Nilsen, E. Kermarrec, G. Ehlers, K. S. Knight, A. Harrison, J. P. Attfield, and B. D. Gaulin, From Spin Glass to Quantum Spin Liquid Ground States in Molybdate Pyrochlores, *Phys. Rev. Lett.* **113**, 117201 (2014).
- [18] N. P. Raju, E. Gmelin, and R. K. Kremer, Magnetic-susceptibility and specific-heat studies of spin-glass-like ordering in the pyrochlore compounds $R_2\text{Mo}_2\text{O}_7$ ($R=\text{Y}$, Sm , or Gd), *Phys. Rev. B* **46**, 5405 (1992).
- [19] H. D. Zhou, C. R. Wiebe, A. Harter, N. S. Dalal, and J. S. Gardner, Unconventional spin glass behavior in the cubic pyrochlore $\text{Mn}_2\text{Sb}_2\text{O}_7$, *J. Phys.: Condens. Matter* **20**, 325201 (2008).
- [20] D. K. Singh and Y. S. Lee, Nonconventional Spin Glass Transition in a Chemically Ordered Pyrochlore, *Phys. Rev. Lett.* **109**, 247201 (2012).
- [21] Y. M. Jana, O. Sakai, R. Higashinaka, H. Fukazawa, Y. Maeno, P. Dasgupta, and D. Ghosh, Spin-glass-like magnetic ground state of the geometrically frustrated pyrochlore niobate $\text{Tb}_2\text{Nb}_2\text{O}_7$, *Phys. Rev. B* **68**, 174413 (2003).
- [22] H. Shinaoka, Y. Tomita, and Y. Motome, Spin-Glass Transition in Bond-Disordered Heisenberg Antiferromagnets Coupled with Local Lattice Distortions on a Pyrochlore Lattice, *Phys. Rev. Lett.* **107**, 047204 (2011).
- [23] H. Zhou, C. Wiebe, J. Janik, B. Vogt, A. Harter, N. Dalal, and J. Gardner, Spin glass transitions in the absence of chemical disorder for the pyrochlores $A_2\text{Sb}_2\text{O}_7$ ($A=\text{Mn}$, Co , Ni), *J. Solid State Chem.* **183**, 890 (2010).
- [24] T. Taniguchi, T. Munenaka, and H. Sato, Spin glass behavior in metallic pyrochlore ruthenate $\text{Ca}_2\text{Ru}_2\text{O}_7$, *J. Phys.: Conf. Ser.* **145**, 012017 (2009).
- [25] J. N. Reimers, J. E. Greedan, R. K. Kremer, E. Gmelin, and M. A. Subramanian, Short-range magnetic ordering in the highly frustrated pyrochlore $\text{Yb}_2\text{Mn}_2\text{O}_7$, *Phys. Rev. B* **43**, 3387 (1991).
- [26] B. D. Gaulin, J. N. Reimers, T. E. Mason, J. E. Greedan, and Z. Tun, Spin Freezing in the Geometrically Frustrated Pyrochlore Antiferromagnet $\text{Tb}_2\text{Mo}_2\text{O}_7$, *Phys. Rev. Lett.* **69**, 3244 (1992).
- [27] M. J. P. Gingras, C. V. Stager, N. P. Raju, B. D. Gaulin, and J. E. Greedan, Static Critical Behavior of the Spin-Freezing Transition in the Geometrically Frustrated Pyrochlore Antiferromagnet $\text{Y}_2\text{Mo}_2\text{O}_7$, *Phys. Rev. Lett.* **78**, 947 (1997).
- [28] H.-M. Guo and M. Franz, Three-Dimensional Topological Insulators on the Pyrochlore Lattice, *Phys. Rev. Lett.* **103**, 206805 (2009).
- [29] H.-M. Guo and M. Franz, Topological insulator on the kagome lattice, *Phys. Rev. B* **80**, 113102 (2009).
- [30] D. Pesin and L. Balents, Mott physics and band topology in materials with strong spin-orbit interaction, *Nat. Phys.* **6**, 376 (2010).
- [31] Y. Otsuka, T. Yoshida, K. Kudo, S. Yunoki, and Y. Hatsugai, Higher-order topological Mott insulator on the pyrochlore lattice, *Sci. Rep.* **11**, 1 (2021).
- [32] L. Hozoi, H. Gretarsson, J. P. Clancy, B.-G. Jeon, B. Lee, K. H. Kim, V. Yushankhai, P. Fulde, D. Casa, T. Gog, J. Kim, A. H. Said, M. H. Upton, Y.-J. Kim, and J. van den Brink, Longer-range lattice anisotropy strongly competing with spin-orbit interactions in pyrochlore iridates, *Phys. Rev. B* **89**, 115111 (2014).
- [33] M. Kargarian, J. Wen, and G. A. Fiete, Competing exotic topological insulator phases in transition-metal oxides on the pyrochlore lattice with distortion, *Phys. Rev. B* **83**, 165112 (2011).
- [34] B.-J. Yang and Y. B. Kim, Topological insulators and metal-insulator transition in the pyrochlore iridates, *Phys. Rev. B* **82**, 085111 (2010).
- [35] M. Ezawa, Higher-Order Topological Insulators and Semimetals on the Breathing Kagome and Pyrochlore Lattices, *Phys. Rev. Lett.* **120**, 026801 (2018).
- [36] H. Shinaoka, Y. Tomita, and Y. Motome, Effect of magnetoelastic coupling on spin-glass behavior in Heisenberg pyrochlore antiferromagnets with bond disorder, *Phys. Rev. B* **90**, 165119 (2014).
- [37] M. J. Harris, S. T. Bramwell, D. F. McMorrow, T. Zeiske, and K. W. Godfrey, Geometrical Frustration in the Ferromagnetic Pyrochlore $\text{Ho}_2\text{Ti}_2\text{O}_7$, *Phys. Rev. Lett.* **79**, 2554 (1997).
- [38] S. T. Bramwell, M. J. Harris, B. C. den Hertog, M. J. P. Gingras, J. S. Gardner, D. F. McMorrow, A. R. Wildes, A. Cornelius, J. D. M. Champion, R. G. Melko, and T. Fennell,

- Spin Correlations in $\text{Ho}_2\text{Ti}_2\text{O}_7$: A Dipolar Spin Ice System, *Phys. Rev. Lett.* **87**, 047205 (2001).
- [39] M. Harris, S. Bramwell, T. Zeiske, D. McMorrow, and P. King, Magnetic structures of highly frustrated pyrochlores, *J. Magn. Magn. Mater.* **177-181**, 757 (1998).
- [40] A. P. Ramirez, A. Hayashi, R. J. Cava, R. Siddharthan, and B. Shastry, Zero-point entropy in ‘spin ice’, *Nature (London)* **399**, 333 (1999).
- [41] S. T. Bramwell and M. J. P. Gingras, Spin ice state in frustrated magnetic pyrochlore materials, *Science* **294**, 1495 (2001).
- [42] S. T. Bramwell and M. J. Harris, The history of spin ice, *J. Phys.: Condens. Matter* **32**, 374010 (2020).
- [43] B. C. den Hertog and M. J. P. Gingras, Dipolar Interactions and Origin of Spin Ice in Ising Pyrochlore Magnets, *Phys. Rev. Lett.* **84**, 3430 (2000).
- [44] P. W. Anderson, Ordering and antiferromagnetism in ferrites, *Phys. Rev.* **102**, 1008 (1956).
- [45] J. P. C. Ruff, R. G. Melko, and M. J. P. Gingras, Finite-Temperature Transitions in Dipolar Spin Ice in a Large Magnetic Field, *Phys. Rev. Lett.* **95**, 097202 (2005).
- [46] T. Yavors’kii, T. Fennell, M. J. P. Gingras, and S. T. Bramwell, $\text{Dy}_2\text{Ti}_2\text{O}_7$ Spin Ice: A Test Case for Emergent Clusters in a Frustrated Magnet, *Phys. Rev. Lett.* **101**, 037204 (2008).
- [47] R. G. Melko and M. J. P. Gingras, Monte Carlo studies of the dipolar spin ice model, *J. Phys.: Condens. Matter* **16**, R1277 (2004).
- [48] P. M. Sarte, A. A. Aczel, G. Ehlers, C. Stock, B. D. Gaulin, C. Mauws, M. B. Stone, S. Calder, S. E. Nagler, J. W. Hollett, H. D. Zhou, J. S. Gardner, J. P. Attfield, and C. R. Wiebe, Evidence for the confinement of magnetic monopoles in quantum spin ice, *J. Phys.: Condens. Matter* **29**, 45LT01 (2017).
- [49] D. J. P. Morris, D. A. Tennant, S. Grigera, B. Klemke, C. Castelnovo, R. Moessner, C. Czternasty, M. Meissner, K. Rule, J.-U. Hoffmann, K. Kiefer, S. Gerischer, D. Slobinsky, and R. S. Perry, Dirac strings and magnetic monopoles in the spin ice $\text{Dy}_2\text{Tb}_2\text{O}_7$, *Science* **326**, 411 (2009).
- [50] C. Castelnovo, R. Moessner, and S. L. Sondhi, Magnetic monopoles in spin ice, *Nature (London)* **451**, 42 (2008).
- [51] S. T. Bramwell, S. R. Giblin, S. Calder, R. Aldus, D. Prabhakaran, and T. Fennell, Measurement of the charge and current of magnetic monopoles in spin ice, *Nature (London)* **461**, 956 (2009).
- [52] C. Paulsen, S. R. Giblin, E. Lhotel, D. Prabhakaran, G. Balakrishnan, K. Matsuhira, and S. T. Bramwell, Experimental signature of the attractive Coulomb force between positive and negative magnetic monopoles in spin ice, *Nat. Phys.* **12**, 661 (2016).
- [53] B. Gao, T. Chen, D. W. Tam, C.-L. Huang, K. Sasmal, D. T. Adroja, F. Ye, H. Cao, G. Sala, M. B. Stone, C. Baines, J. A. T. Verezhab, H. Hu, C. J.-H. X. Xu, S.-W. Cheong, M. Nallaiyan, S. Spagna, M. B. Maple, A. H. Nevidomskyy *et al.*, Experimental signatures of a three-dimensional quantum spin liquid in effective spin- $\frac{1}{2}$ $\text{Ce}_2\text{Zr}_2\text{O}_7$ pyrochlore, *Nat. Phys.* **15**, 1052 (2019).
- [54] O. Benton, Instabilities of a U(1) Quantum Spin Liquid in Disordered Non-Kramers Pyrochlores, *Phys. Rev. Lett.* **121**, 037203 (2018).
- [55] J.-J. Wen, S. M. Koohpayeh, K. A. Ross, B. A. Trump, T. M. McQueen, K. Kimura, S. Nakatsuji, Y. Qiu, D. M. Pajerowski, J. R. D. Copley, and C. L. Broholm, Disordered Route to the Coulomb Quantum Spin Liquid: Random Transverse Fields on Spin Ice in $\text{Pr}_2\text{Zr}_2\text{O}_7$, *Phys. Rev. Lett.* **118**, 107206 (2017).
- [56] L. Savary and L. Balents, Disorder-Induced Quantum Spin Liquid in Spin Ice Pyrochlores, *Phys. Rev. Lett.* **118**, 087203 (2017).
- [57] R. Sibille, E. Lhotel, V. Pomjakushin, C. Baines, T. Fennell, and M. Kenzelmann, Candidate Quantum Spin Liquid in the Ce^{3+} Pyrochlore Stannate $\text{Ce}_2\text{Sn}_2\text{O}_7$, *Phys. Rev. Lett.* **115**, 097202 (2015).
- [58] S. B. Lee, S. Onoda, and L. Balents, Generic quantum spin ice, *Phys. Rev. B* **86**, 104412 (2012).
- [59] L. Balents, Spin liquids in frustrated magnets, *Nature (London)* **464**, 199 (2010).
- [60] K. A. Ross, L. Savary, B. D. Gaulin, and L. Balents, Quantum Excitations in Quantum Spin Ice, *Phys. Rev. X* **1**, 021002 (2011).
- [61] L. Savary and L. Balents, Spin liquid regimes at nonzero temperature in quantum spin ice, *Phys. Rev. B* **87**, 205130 (2013).
- [62] L. Savary and L. Balents, Quantum spin liquids: A review, *Rep. Prog. Phys.* **80**, 016502 (2016).
- [63] Y. Zhou, K. Kanoda, and T.-K. Ng, Quantum spin liquid states, *Rev. Mod. Phys.* **89**, 025003 (2017).
- [64] J. S. Gardner, S. R. Dunsiger, B. D. Gaulin, M. J. P. Gingras, J. E. Greedan, R. F. Kiefl, M. D. Lumsden, W. A. MacFarlane, N. P. Raju, J. E. Sonier, I. Swainson, and Z. Tun, Cooperative Paramagnetism in the Geometrically Frustrated Pyrochlore Antiferromagnet $\text{Tb}_2\text{Ti}_2\text{O}_7$, *Phys. Rev. Lett.* **82**, 1012 (1999).
- [65] J. S. Gardner, B. D. Gaulin, A. J. Berlinsky, P. Waldron, S. R. Dunsiger, N. P. Raju, and J. E. Greedan, Neutron scattering studies of the cooperative paramagnet pyrochlore $\text{Tb}_2\text{Ti}_2\text{O}_7$, *Phys. Rev. B* **64**, 224416 (2001).
- [66] B. G. Ueland, J. S. Gardner, A. J. Williams, M. L. Dahlberg, J. G. Kim, Y. Qiu, J. R. D. Copley, P. Schiffer, and R. J. Cava, Coexisting magnetic order and cooperative paramagnetism in the stuffed pyrochlore $\text{Tb}_{2+x}\text{Ti}_{2-2x}\text{Nb}_x\text{O}_7$, *Phys. Rev. B* **81**, 060408(R) (2010).
- [67] P. H. Conlon and J. T. Chalker, Spin Dynamics in Pyrochlore Heisenberg Antiferromagnets, *Phys. Rev. Lett.* **102**, 237206 (2009).
- [68] A. Keren, J. S. Gardner, G. Ehlers, A. Fukaya, E. Segal, and Y. J. Uemura, Dynamic Properties of a Diluted Pyrochlore Cooperative Paramagnet $(\text{Tb}_p\text{Y}_{1-p})_2\text{Ti}_2\text{O}_7$, *Phys. Rev. Lett.* **92**, 107204 (2004).
- [69] Y. Motome and N. Furukawa, Phase Competition in the Double-Exchange Model on the Frustrated Pyrochlore Lattice, *Phys. Rev. Lett.* **104**, 106407 (2010).
- [70] C. Liu, G. B. Halász, and L. Balents, Competing orders in pyrochlore magnets from a \mathbb{Z}_2 spin liquid perspective, *Phys. Rev. B* **100**, 075125 (2019).
- [71] V. M. Goldschmidt, Die gesetze der krystallochemie, *Sci. Nat.* **14**, 477 (1926).
- [72] C. R. Wiebe and A. M. Hallas, Frustration under pressure: Exotic magnetism in new pyrochlore oxides, *APL Mater.* **3**, 041519 (2015).
- [73] H. Zhou and C. R. Wiebe, High-pressure routes to new pyrochlores and novel magnetism, *Inorganics* **7**, 49 (2019).
- [74] A. M. Hallas, J. G. Cheng, A. M. Arevalo-Lopez, H. J. Silverstein, Y. Su, P. M. Sarte, H. D. Zhou, E. S. Choi, J. P. Attfield, G. M. Luke, and C. R. Wiebe, Incipient

- Ferromagnetism in $Tb_2Ge_2O_7$: Application of Chemical Pressure to the Enigmatic Spin-Liquid Compound $Tb_2Ti_2O_7$, *Phys. Rev. Lett.* **113**, 267205 (2014).
- [75] A. M. Hallas, J. A. M. Paddison, H. J. Silverstein, A. L. Goodwin, J. R. Stewart, A. R. Wildes, J. G. Cheng, J. S. Zhou, J. B. Goodenough, E. S. Choi, G. Ehlers, J. S. Gardner, C. R. Wiebe, and H. D. Zhou, Statics and dynamics of the highly correlated spin ice $Ho_2Ge_2O_7$, *Phys. Rev. B* **86**, 134431 (2012).
- [76] H. D. Zhou, J. G. Cheng, A. M. Hallas, C. R. Wiebe, G. Li, L. Balicas, J. S. Zhou, J. B. Goodenough, J. S. Gardner, and E. S. Choi, Chemical Pressure Effects on Pyrochlore Spin Ice, *Phys. Rev. Lett.* **108**, 207206 (2012).
- [77] X. Li, W. M. Li, K. Matsabayashi, Y. Sato, C. Q. Jin, Y. Uwatoko, T. Kawae, A. M. Hallas, C. R. Wiebe, A. M. Arevalo-Lopez, J. P. Attfield, J. S. Gardner, R. S. Freitas, H. D. Zhou, and J.-G. Cheng, Long-range antiferromagnetic order in the frustrated XY pyrochlore antiferromagnet $Er_2Ge_2O_7$, *Phys. Rev. B* **89**, 064409 (2014).
- [78] A. M. Hallas, J. Gaudet, M. N. Wilson, T. J. Munsie, A. A. Aczel, M. B. Stone, R. S. Freitas, A. M. Arevalo-Lopez, J. P. Attfield, M. Tachibana, C. R. Wiebe, G. M. Luke, and B. D. Gaulin, XY antiferromagnetic ground state in the effective $S = \frac{1}{2}$ pyrochlore $Yb_2Ge_2O_7$, *Phys. Rev. B* **93**, 104405 (2016).
- [79] A. M. Hallas, A. M. Arevalo-Lopez, A. Z. Sharma, T. Munsie, J. P. Attfield, C. R. Wiebe, and G. M. Luke, Magnetic frustration in lead pyrochlores, *Phys. Rev. B* **91**, 104417 (2015).
- [80] H. W. J. Blöte, R. F. Wielinga, and W. J. Huiskamp, Heat-capacity measurements on rare-earth double oxides $R_2M_2O_7$, *Physica (Amsterdam)* **43**, 549 (1969).
- [81] N. Martin, P. Bonville, E. Lhotel, S. Guitteny, A. Wildes, C. Decorse, M. Ciomaga Hatnean, G. Balakrishnan, I. Mirebeau, and S. Petit, Disorder and Quantum Spin Ice, *Phys. Rev. X* **7**, 041028 (2017).
- [82] S. J. Gomez, P. M. Sarte, M. Zelensky, A. M. Hallas, B. A. Gonzalez, K. H. Hong, E. J. Pace, S. Calder, M. B. Stone, Y. Su, E. Feng, M. D. Le, C. Stock, J. P. Attfield, S. D. Wilson, C. R. Wiebe, and A. A. Aczel, Absence of moment fragmentation in the mixed B -site pyrochlore Nd_2GaSbO_7 , *Phys. Rev. B* **103**, 214419 (2021).
- [83] P. M. Sarte, K. Cruz-Kan, B. R. Ortiz, K. H. Hong, M. M. Bordelon, D. Reig-i Plessis, M. Lee, E. S. Choi, M. B. Stone, S. Calder, D. M. Pajerowski, L. Mangin-Thro, Y. Qiu, J. P. Attfield, S. D. Wilson, C. Stock, H. D. Zhou, A. M. Hallas, J. A. M. Paddison, A. A. Aczel *et al.*, Dynamical ground state in the XY pyrochlore Yb_2GaSbO_7 , *npj Quantum Mater.* **6**, 42 (2021).
- [84] Y. M. Jana, A. Ghosal, S. Nandi, J. Alam, P. Bag, S. S. Islam, and R. Nath, Spin-ice behavior of mixed pyrochlore Dy_2GaSbO_7 exhibiting enhanced Pauling zero-point entropy, *J. Magn. Magn. Mater.* **562**, 169814 (2022).
- [85] M. R. Rutherford, Dy_2ScNbO_7 : A study of the effect of a disordered B-site on the spin ice magnetism typically seen in dysprosium pyrochlores, Master's thesis, McMaster University, Hamilton, ON, 2021.
- [86] J. Beare, Muon Spin Rotation, Relaxation, and Resonance, and AC Susceptibility as a probe of Frustrated Pyrochlore Magnets and Type-I Superconductivity, Ph.D. thesis, McMaster University, Hamilton, ON, 2021.
- [87] C. Mauws, N. Hiebert, M. L. Rutherford, H. D. Zhou, Q. Huang, M. B. Stone, N. P. Butch, Y. Su, E. S. Choi, Z. Yamani, and C. R. Wiebe, Magnetic ordering in the Ising antiferromagnetic pyrochlore Nd_2ScNbO_7 , *J. Phys.: Condens. Matter* **33**, 245802 (2021).
- [88] P. Strobel, S. Zouari, R. Ballou, A. Cheikh-Rouhou, J.-C. Jumas, and J. Olivier-Fourcade, Structural and magnetic properties of new rare-earth–antimony pyrochlore-type oxides Ln_2BSbO_7 ($B = Sc, Ga, In$), *Solid State Sci.* **12**, 570 (2010).
- [89] A. A. Coelho, *TOPAS* and *TOPAS-Academic*: An optimization program integrating computer algebra and crystallographic objects written in C++, *J. Appl. Crystallogr.* **51**, 210 (2018).
- [90] K. Momma and F. Izumi, *VESTA3* for three-dimensional visualization of crystal, volumetric and morphology data, *J. Appl. Crystallogr.* **44**, 1272 (2011).
- [91] M. V. Talanov and V. M. Talanov, Structural diversity of ordered pyrochlores, *Chem. Mater.* **33**, 2706 (2021).
- [92] B. A. Trump, S. M. Koohpayeh, K. J. Livi, J.-J. Wen, K. Arpino, Q. M. Ramasse, R. Brydson, M. Feygenson, H. Takeda, M. Takigawa, K. Kimura, S. Nakatsuji, C. L. Broholm, and T. M. McQueen, Universal geometric frustration in pyrochlores, *Nat. Commun.* **9**, 2619 (2018).
- [93] A. W. Sleight, Rare earth plumbates with pyrochlore structure, *Inorg. Chem.* **8**, 1807 (1969).
- [94] W. E. Klee and G. Weitz, Infrared spectra of ordered and disordered pyrochlore-type compounds in the series $RE_2Tb_2O_7$, $RE_2Zr_2O_7$, and $RE_2Hf_2O_7$, *J. Inorg. Nucl.* **31**, 2367 (1969).
- [95] D. Michel, M. Perez y Jorba, and R. Collongues, Étude de la transformation ordre-désordre de la structure fluorite à la structure pyrochlore pour des phases $(1-x)ZrO_2 \cdot xLn_2O_3$, *Mater. Res. Bull.* **9**, 1457 (1974).
- [96] M. Perez y Jorba, Contribution to the study of ZrO_2 -rare earth oxide systems, *Ann. Chim.* **7**, 479 (1962).
- [97] R. Collongues, M. Perez Y Jorba, and J. Lefevre, Diagrammes de phase des systèmes zircone-oxyde de terres rares, *Bull. Soc. Chim. France* **28**, 70 (1961).
- [98] R. S. Roth, Pyrochlore-type compounds containing double oxides of trivalent and tetravalent ions, *J. Res. Natl. Bur. Stand.* **56**, 17 (1956).
- [99] L. N. Fomina and S. F. Pal'guev, Formation mechanism of $Sm_2Zr_2O_7$ and $Gd_2Zr_2O_7$ compounds of pyrochlore structure, *Russ. J. Phys. Chem.* **22**, 326 (1977).
- [100] N. Gundovin, F. M. Spiridonov, L. N. Komissarova, and K. I. Petrov, *Russ. J. Inorg. Chem.* **20**, 325 (1975).
- [101] J. Besson, C. Deportes, and G. Robert, Conductibilité électrique dans le système oxyde de hafniumoxyde dyttrium à haute température, *C. R. (Paris)* **262C**, 527 (1966).
- [102] F. M. Spiridonov, V. Stepanov, L. N. Komissarova, and V. I. Spitsyn, The binary system $HfO_2-Gd_2O_3$, *J. Less-Common Met.* **14**, 435 (1968).
- [103] R. Sibile, T. Fennell, M. C. Hatnean, E. Lhotel, D. Keen, G. Balakrishnan, and M. Kenzelmann, Structural disorder in a magnetic pyrochlore oxide, *Acta Crystallogr. Sect. A* **72**, s306 (2016).
- [104] A. V. Shlyakhtina, M. V. Boguslavskii, S. Y. Stefanovich, I. V. Kolbanov, A. V. Knotko, O. K. Karyagina, S. A. Borisov, and L. G. Shcherbakova, Structure and electrical conductivity of

- $Ln_{2+x}Hf_{2-x}O_{7-x/2}$ (Ln = Sm-Tb; x = 0, 0.096), *Inorg. Mater.* **42**, 519 (2006).
- [105] A. V. Shlyakhtina, D. A. Belov, K. S. Pigalskiy, A. N. Shchegolikhin, I. V. Kolbanev, and O. K. Karyagina, Synthesis, properties and phase transitions of pyrochlore-and fluorite-like Ln_2RMO_7 (Ln = Sm, Ho; R= Lu, Sc; M= Nb, Ta), *Mater. Res. Bull.* **49**, 625 (2014).
- [106] A. V. Shlyakhtina, K. S. Pigalskiy, D. A. Belov, N. V. Lyskov, E. P. Kharitonova, I. V. Kolbanev, A. B. Borunova, O. K. Karyagina, E. M. Sadovskaya, V. A. Sadykov, and N. F. Eremeev, Proton and oxygen ion conductivity in the pyrochlore/fluorite family of $Ln_{2-x}Ca_xScMO_{7-\delta}$ (Ln = La, Sm, Ho, Yb; M = Nb, Ta; x = 0, 0.05, 0.1) niobates and tantalates, *Dalton Trans.* **47**, 2376 (2018).
- [107] *MLZ Conference: Neutrons for Information and Quantum Technologies*, edited by J. Song, V. Pecanha-Antonio, and Y. Su (ACM, New York, 2019).
- [108] K. Sato, G.-Y. Adachi, and J. Shiokawa, Preparation of new perovskite type oxide containing divalent europium, *J. Inorg. Nucl.* **38**, 1287 (1976).
- [109] T. M. McQueen, D. V. West, B. Muegge, Q. Huang, K. Noble, H. W. Zandbergen, and R. J. Cava, Frustrated ferroelectricity in niobate pyrochlores, *J. Phys.: Condens. Matter* **20**, 235210 (2008).
- [110] S. Zouari, R. Ballou, A. Cheikh-Rouhou, and P. Strobel, Synthesis and structure of new pyrochlore-type oxides Ln_2ScNbO_7 (Ln = Pr, Nd, Eu, Gd, Dy), *Mater. Lett.* **62**, 3767 (2008).
- [111] B. J. Kennedy, B. A. Hunter, and C. J. Howard, Structural and bonding trends in tin pyrochlore oxides, *J. Solid State Chem.* **130**, 58 (1997).
- [112] B. R. Ortiz, P. M. Sarte, G. Pokharel, and S. D. Wilson, (unpublished).
- [113] L. Clark, C. Ritter, A. Harrison, and J. P. Attfield, Oxygen miscibility gap and spin glass formation in the pyrochlore $Lu_2Mo_2O_7$, *J. Solid State Chem.* **203**, 199 (2013).
- [114] J. E. Greedan, M. Sato, N. Ali, and W. R. Datars, Electrical resistivity of pyrochlore compounds $R_2Mo_2O_7$ (R =Nd, Sm, Gd, Tb, Y), *J. Solid State Chem.* **68**, 300 (1987).
- [115] M. A. Subramanian, G. Aravamudan, and G. V. Subba Rao, Electrical properties of $Ln_2Mo_2O_7$ pyrochlores (Ln = Sm, Yb, Y), *Mater. Res. Bull.* **15**, 1401 (1980).
- [116] E. A. Tkachenko and P. P. Fedorov, Lower rare-earth molybdates, *Inorg. Mater.* **39**, S25 (2003).
- [117] G. J. McCarthy, Divalent europium compounds in the systems Eu–Mo–O and Eu–W–O, *Mater. Res. Bull.* **6**, 31 (1971).
- [118] R. Ranganathan, G. Rangarajan, R. Srinivasan, M. A. Subramanian, and G. V. Rao, Magnetic properties of $RE_2Mo_2O_7$ pyrochlores, *J. Low Temp. Phys.* **52**, 481 (1983).
- [119] I. Shaplygin and V. Lazarev, $Ln_2Os_2O_7$ A new family of pyrochlores, *Mater. Res. Bull.* **8**, 761 (1973).
- [120] A. W. Sleight, New ternary oxides of tetravalent platinum and palladium with the pyrochlore structure, *Mater. Res. Bull.* **3**, 699 (1968).
- [121] C. L. Chien and A. W. Sleight, Mössbauer effect studies of europium pyrochlores, *Phys. Rev. B* **18**, 2031 (1978).
- [122] K. Matsuhira, M. Wakushima, Y. Hinatsu, and S. Takagi, Metal-Insulator Transitions in Pyrochlore Oxides $Ln_2Ir_2O_7$, *J. Phys. Soc. Jpn.* **80**, 094701 (2011).
- [123] M. Klicpera, K. Vlašková, and M. Diviš, Characterization and Magnetic Properties of Heavy Rare-Earth $A_2Ir_2O_7$ Pyrochlore Iridates, the Case of $Tm_2Ir_2O_7$, *J. Phys. Chem. C* **124**, 20367 (2020).
- [124] K. Blacklock and H. W. White, Specific heats of the pyrochlore compounds $Eu_2Ir_2O_7$ and $Lu_2Ir_2O_7$, *J. Chem. Phys.* **72**, 2191 (1980).
- [125] D. Yanagishima and Y. Maeno, Metal-Nonmetal Changeover in Pyrochlore Iridates, *J. Phys. Soc. Jpn.* **70**, 2880 (2001).
- [126] V. B. Lazarev and I. S. Shaplygin, Electrical conductivity of platinum metal – nonplatinum metal double oxides, *Mater. Res. Bull.* **13**, 229 (1978).
- [127] D. Ismunandar, B. J. Kennedy, and B. A. Hunter, Structural and magnetic studies of manganese-containing pyrochlore oxides, *J. Alloys Compd.* **302**, 94 (2000).
- [128] G. Berndt, K. Silva, F. Ivashita, A. Paesano, M. Blanco, E. Miner, R. Carbonio, S. Dantas, A. Ayala, and O. Isnard, Structural, hyperfine and Raman properties of RE_2FeSbO_7 compounds, *J. Alloys Compd.* **618**, 635 (2015).
- [129] O. Knop, F. Brisse, R. E. Meads, and J. Bainbridge, Pyrochlores. IV. Crystallographic and Mössbauer studies of A_2FeSbO_7 pyrochlores, *Can. J. Chem.* **46**, 3829 (1968).
- [130] M.-C. Montmory and F. Bertaut, *Compt. Rend.* **252**, 4171 (1961).
- [131] N. Taira, M. Wakushima, and Y. Hinatsu, Magnetic properties of ruthenium pyrochlores $R_2Ru_2O_7$ (R = rare earth), *J. Phys.: Condens. Matter* **11**, 6983 (1999).
- [132] M. W. Gaultois, *Design Principles for Oxide Thermoelectric Materials* (University of California Press, Santa Barbara, 2015).
- [133] B. J. Kennedy, Structure Refinement of $Y_2Ru_2O_7$ by Neutron Powder Diffraction, *Acta Crystallogr., Sect. C* **51**, 790 (1995).
- [134] E. F. Bertaut, F. Forrat, and M. C. Montmory, *C. R. Hebd. Séances Acad. Sci.* **249**, 829 (1959).
- [135] Y. Kobayashi, T. Miyashita, T. Fukamachi, and M. Sato, NMR studies of Ga in magnetically frustrated pyrochlore system R_2GaSbO_7 (R = rare earth elements), *J. Phys. Chem. Solids* **62**, 347 (2001).
- [136] M. J. Whitaker and C. Greaves, Magnetic ordering in the pyrochlore Ho_2CrSbO_7 determined from neutron diffraction, and the magnetic properties of other RE_2CrSbO_7 phases (RE =Y, Tb, Dy, Er), *J. Solid State Chem.* **215**, 171 (2014).
- [137] P. F. Bongers and E. R. Van Meurs, Ferromagnetism in Compounds with Pyrochlore Structure, *J. Appl. Phys.* **38**, 944 (1967).
- [138] P. Casado, A. Mendiola, and I. Rasines, Preparation and crystallographic data of the pyrochlores Gd_2MSbO_7 (M = Cr,Mn, Fe, In), *J. Phys. Chem. Solids* **46**, 921 (1985).
- [139] P. Villars, K. Cenzual, and R. Gladyshevskii, *Handbook of Inorganic Substances* (Walter de Gruyter GmbH, Berlin, 2015).
- [140] C. T. F. and E. D. Copenhagen, *Bibliography of Magnetic Materials and Tabulation of Magnetic Transition Temperatures* (Springer, New York, 1972).
- [141] O. Knop, F. Brisse, and L. Castelliz, Pyrochlores. v. thermoanalytic, x-ray, neutron, infrared, and dielectric studies of $A_2Ti_2O_7$ titanates, *Can. J. Chem.* **47**, 971 (1969).
- [142] O. Knop, F. Brisse, and L. Castelliz, Determination of the crystal structure of erbium titanate, $Er_2Ti_2O_7$, by x-ray and neutron diffraction, *Can. J. Chem.* **43**, 2812 (1965).

- [143] Y. Haipeng, C. Xiaoge, Z. Hongsong, Z. Haoming, Z. Yongde, L. Yanxu, and T. An, Preparation and thermal properties of $\text{Sm}_2\text{AlTaO}_7$, *Cogent Phys.* **3**, 1244244 (2016).
- [144] C. Xiaoge, T. An, Z. Hongsong, L. Yanxu, Z. Haoming, and Z. Yongde, Thermal conductivity and expansion coefficient of $\text{Ln}_2\text{LaTaO}_7$ (Ln = Er and Yb) oxides for thermal barrier coating applications, *Ceram. Int.* **42**, 13491 (2016).
- [145] Y. Li, G. Chen, H. Zhang, and Z. Li, Photocatalytic water splitting of $\text{La}_2\text{AlTaO}_7$ and the effect of aluminum on the electronic structure, *J. Phys. Chem. Solids* **70**, 536 (2009).
- [146] K. Kitayama and T. Katsura, A New Compound, $\text{Lu}_2\text{V}_2\text{O}_7$, *Chem. Lett.* **5**, 815 (1976).
- [147] L. Soderholm, C. V. Stager, and J. E. Greedan, Crystal field effects on the magnetic behavior of $\text{Yb}_2\text{V}_2\text{O}_7$ and $\text{Tm}_2\text{V}_2\text{O}_7$, *J. Solid State Chem.* **43**, 175 (1982).
- [148] I. O. Troyanchuk, Preparation and properties of $\text{Er}_2\text{V}_2\text{O}_7$, $\text{Ho}_2\text{V}_2\text{O}_7$, $\text{Y}_2\text{V}_2\text{O}_7$, $\text{Dy}_2\text{V}_2\text{O}_7$ pyrochlore structure, *Inorg. Mater.* **26**, 182 (1990).
- [149] H. Yokokawa, N. Sakai, T. Kawada, and M. Dokiya, Thermodynamic stabilities of perovskite oxides for electrodes and other electrochemical materials, *Solid State Ion.* **52**, 43 (1992).
- [150] T. Shin-ike, G. Adachi, and J. Shiokawa, On the pyrochlore type $\text{Ln}_2\text{V}_2\text{O}_7$ (Ln : Rare-earth elements), *Mater. Res. Bull.* **12**, 1149 (1977).
- [151] Y. Shimakawa, Y. Kubo, N. Hamada, J. D. Jorgensen, Z. Hu, S. Short, M. Nohara, and H. Takagi, Crystal structure, magnetic and transport properties, and electronic band structure of $A_2\text{Mn}_2\text{O}_7$ pyrochlores (A = Y, In, Lu, and Tl), *Phys. Rev. B* **59**, 1249 (1999).
- [152] M. A. Subramanian, C. C. Torardi, D. C. Johnson, J. Pannetier, and A. W. Sleight, Ferromagnetic $R_2\text{Mn}_2\text{O}_7$ pyrochlores (R = Dy, Lu, Y), *J. Solid State Chem.* **72**, 24 (1988).
- [153] J. E. Greedan, N. P. Raju, A. Maingan, C. Simon, J. S. Pedersen, A. M. Niraimathi, E. Gmelin, and M. A. Subramanian, Frustrated pyrochlore oxides, $\text{Y}_2\text{Mn}_2\text{O}_7$, $\text{Ho}_2\text{Mn}_2\text{O}_7$, and $\text{Yb}_2\text{Mn}_2\text{O}_7$: Bulk magnetism and magnetic microstructure, *Phys. Rev. B* **54**, 7189 (1996).
- [154] T. Shimazaki, T. Yamazaki, K. Terayama, and M. Yoshimura, Phase relations in the Pr–Mn–O system at 1000 °C, *J. Mater. Sci. Lett.* **19**, 2029 (2000).
- [155] R. D. Shannon and A. W. Sleight, Synthesis of new high-pressure pyrochlore phases, *Inorg. Chem.* **7**, 1649 (1968).
- [156] U. W. Becker and J. Felsche, Phases and structural relations of the rare earth germanates $\text{RE}_2\text{Ge}_2\text{O}_7$, RE = La–Lu, *J. Less-Common Met.* **128**, 269 (1987).
- [157] G. M. Clark and R. Morley, Inorganic pyro-compounds $\text{M}[(\text{X}_2\text{O}_7)]$, *Chem. Soc. Rev.* **5**, 269 (1976).
- [158] F. Wells, *Structural Inorganic Chemistry* (Clarendon, Oxford, 1987).
- [159] T. Phraewphiphat, M. Iqbal, K. Suzuki, M. Hirayama, and R. Kanno, Synthesis and Lithium-Ion Conductivity of $\text{LiSrB}_2\text{O}_6\text{F}$ (B = Nb⁵⁺, Ta⁵⁺) with a Pyrochlore Structure, *J. Jpn. Soc. Powder Powder Metall.* **65**, 26 (2018).
- [160] K. A. Ross, J. M. Brown, R. J. Cava, J. W. Krizan, S. E. Nagler, J. A. Rodriguez-Rivera, and M. B. Stone, Single-ion properties of the $S_{\text{eff}} = \frac{1}{2}$ XY antiferromagnetic pyrochlores $\text{NaA}'\text{Co}_2\text{F}_7$ (A' = Ca²⁺, Sr²⁺), *Phys. Rev. B* **95**, 144414 (2017).
- [161] H. L. Che, Z. Y. Zhao, X. Rao, L. G. Chu, N. Li, W. J. Chu, P. Gao, X. Y. Yue, Y. Zhou, Q. J. Li, Q. Huang, E. S. Choi, Y. Y. Han, Z. Z. He, H. D. Zhou, X. Zhao, and X. F. Sun, Absence of long-range order in an XY pyrochlore antiferromagnet $\text{Er}_2\text{AlSbO}_7$, *Phys. Rev. Materials* **4**, 054406 (2020).
- [162] D. Simeone, G. J. Thorogood, D. Huo, L. Luneville, G. Baldinozzi, V. Petricek, F. Porcher, J. Ribis, L. Mazerolles, L. Largeau, J. F. Berar, and S. Surble, Intricate disorder in defect fluorite/pyrochlore: a concord of chemistry and crystallography, *Sci. Rep.* **7**, 1 (2017).
- [163] R. Sibille, E. Lhotel, M. Ciomaga Hatnean, G. J. Nilsen, G. Ehlers, A. Cervellino, E. Ressouche, M. Frontzek, O. Zaharko, V. Pomjakushin, U. Stuhr, H. C. Walker, D. T. Adroja, H. Luetkens, C. Baines, G. Amato, A. Balakrishnan, T. Fennell, and M. Kenzelmann, Coulomb spin liquid in anion-disordered pyrochlore $\text{Tb}_2\text{Hf}_2\text{O}_7$, *Nat. Commun.* **8**, 892 (2017).
- [164] P. E. R. Blanchard, R. Clements, B. J. Kennedy, C. D. Ling, E. Reynolds, M. Avdeev, A. P. J. Stampfl, Z. Zhang, and L.-Y. Jang, Does local disorder occur in the pyrochlore zirconates? *Inorg. Chem.* **51**, 13237 (2012).
- [165] L.-J. Chang, S. Onoda, Y. Su, Y.-J. Kao, K.-D. Tsuei, Y. Yasui, K. Kakurai, and M. R. Lees, Higgs transition from a magnetic Coulomb liquid to a ferromagnet in $\text{Yb}_2\text{Nb}_2\text{O}_7$, *Nat. Commun.* **3**, 992 (2012).
- [166] J. Gaudet, K. A. Ross, E. Kermarrec, N. P. Butch, G. Ehlers, H. A. Dabkowska, and B. D. Gaulin, Gapless quantum excitations from an icelike splayed ferromagnetic ground state in stoichiometric $\text{Yb}_2\text{Ti}_2\text{O}_7$, *Phys. Rev. B* **93**, 064406 (2016).
- [167] K. A. Ross, T. Proffen, H. A. Dabkowska, J. A. Quilliam, L. R. Yaraskavitch, J. B. Kycia, and B. D. Gaulin, Lightly stuffed pyrochlore structure of single-crystalline $\text{Yb}_2\text{Ti}_2\text{O}_7$ grown by the optical floating zone technique, *Phys. Rev. B* **86**, 174424 (2012).
- [168] Y. Yasui, M. Soda, S. Iikubo, M. Ito, M. Sato, N. Hamaguchi, T. Matsushita, N. Wada, T. Takeuchi, N. Aso, and K. Kakurai, Ferromagnetic Transition of Pyrochlore Compound $\text{Yb}_2\text{Nb}_2\text{O}_7$, *J. Phys. Soc. Jpn.* **72**, 3014 (2003).
- [169] A. Yaouanc, P. Dalmas de Réotier, C. Marin, and V. Glazkov, Single-crystal versus polycrystalline samples of magnetically frustrated $\text{Yb}_2\text{Ti}_2\text{O}_7$: Specific heat results, *Phys. Rev. B* **84**, 172408 (2011).
- [170] K. A. Ross, L. R. Yaraskavitch, M. Laver, J. S. Gardner, J. A. Quilliam, S. Meng, J. B. Kycia, D. K. Singh, T. Proffen, H. A. Dabkowska, and B. D. Gaulin, Dimensional evolution of spin correlations in the magnetic pyrochlore $\text{Yb}_2\text{Ti}_2\text{O}_7$, *Phys. Rev. B* **84**, 174442 (2011).
- [171] R. M. D'Ortenzio, H. A. Dabkowska, S. R. Dunsiger, B. D. Gaulin, M. J. P. Gingras, T. Goko, J. B. Kycia, L. Liu, T. Medina, T. J. Munsie, D. Pomaranski, K. A. Ross, Y. J. Uemura, T. J. Williams, and G. M. Luke, Unconventional magnetic ground state in $\text{Yb}_2\text{Ti}_2\text{O}_7$, *Phys. Rev. B* **88**, 134428 (2013).
- [172] L.-J. Chang, M. R. Lees, I. Watanabe, A. D. Hillier, Y. Yasui, and S. Onoda, Static magnetic moments revealed by muon spin relaxation and thermodynamic measurements in the quantum spin ice $\text{Yb}_2\text{Ti}_2\text{O}_7$, *Phys. Rev. B* **89**, 184416 (2014).
- [173] K. E. Arpino, B. A. Trump, A. O. Scheie, T. M. McQueen, and S. M. Koohpayeh, Impact of stoichiometry of $\text{Yb}_2\text{Ti}_2\text{O}_7$ on its physical properties, *Phys. Rev. B* **95**, 094407 (2017).
- [174] M. Ruminy, L. Bovo, E. Pomjakushina, M. K. Haas, U. Stuhr, A. Cervellino, R. J. Cava, M. Kenzelmann, and T. Fennell, Sample independence of magnetoelastic excitations in the

- rare-earth pyrochlore $Tb_2Ti_2O_7$, *Phys. Rev. B* **93**, 144407 (2016).
- [175] J. S. Gardner, A. Keren, G. Ehlers, C. Stock, E. Segal, J. M. Roper, B. Fåk, M. B. Stone, P. R. Hammar, D. H. Reich, and B. D. Gaulin, Dynamic frustrated magnetism in $Tb_2Ti_2O_7$ at 50 mK, *Phys. Rev. B* **68**, 180401(R) (2003).
- [176] M. J. P. Gingras, B. C. den Hertog, M. Faucher, J. S. Gardner, S. R. Dunsiger, L. J. Chang, B. D. Gaulin, N. P. Raju, and J. E. Greedan, Thermodynamic and single-ion properties of Tb^{3+} within the collective paramagnetic-spin liquid state of the frustrated pyrochlore antiferromagnet $Tb_2Ti_2O_7$, *Phys. Rev. B* **62**, 6496 (2000).
- [177] Y. Chapuis, A. Yaouanc, P. Dalmas de Réotier, C. Marin, S. Vanishri, S. H. Curnoe, C. Váju, and A. Forget, Evidence from thermodynamic measurements for a singlet crystal-field ground state in pyrochlore $Tb_2Sn_2O_7$ and $Tb_2Ti_2O_7$, *Phys. Rev. B* **82**, 100402(R) (2010).
- [178] H. Takatsu, H. Kadowaki, T. J. Sato, J. W. Lynn, Y. Tabata, T. Yamazaki, and K. Matsuhira, Quantum spin fluctuations in the spin-liquid state of $Tb_2Ti_2O_7$, *J. Phys.: Condens. Matter* **24**, 052201 (2011).
- [179] A. Yaouanc, P. Dalmas de Réotier, Y. Chapuis, C. Marin, S. Vanishri, D. Aoki, B. Fåk, L.-P. Regnault, C. Buisson, A. Amato, C. Baines, and A. D. Hillier, Exotic transition in the three-dimensional spin-liquid candidate $Tb_2Ti_2O_7$, *Phys. Rev. B* **84**, 184403 (2011).
- [180] N. Hamaguchi, T. Matsushita, N. Wada, Y. Yasui, and M. Sato, Low-temperature phases of the pyrochlore compound $Tb_2Ti_2O_7$, *Phys. Rev. B* **69**, 132413 (2004).
- [181] T. Fennell, M. Kenzelmann, B. Roessli, H. Mutka, J. Ollivier, M. Rumin, U. Stuhr, O. Zaharko, L. Bovo, A. Cervellino, M. K. Haas, and R. J. Cava, Magnetoelastic Excitations in the Pyrochlore Spin Liquid $Tb_2Ti_2O_7$, *Phys. Rev. Lett.* **112**, 017203 (2014).
- [182] R. Siddharthan, B. S. Shastry, A. P. Ramirez, A. Hayashi, R. J. Cava, and S. Rosenkranz, Ising Pyrochlore Magnets: Low-Temperature Properties, “Ice Rules,” and Beyond, *Phys. Rev. Lett.* **83**, 1854 (1999).
- [183] R. D. Shannon, Revised effective ionic radii and systematic studies of interatomic distances in halides and chalcogenides, *Acta Crystallogr.* **32**, 751 (1976).
- [184] E. E. Levin, J. H. Grebenkemper, T. M. Pollock, and R. Seshadri, Protocols for high temperature assisted-microwave preparation of inorganic compounds, *Chem. Mater.* **31**, 7151 (2019).
- [185] D. Michael P. Mingos and D. R. Baghurst, Tilden Lecture. Applications of microwave dielectric heating effects to synthetic problems in chemistry, *Chem. Soc. Rev.* **20**, 1 (1991).
- [186] K. J. Rao, B. Vaidhyanathan, M. Ganguli, and P. A. Ramakrishnan, Synthesis of inorganic solids using microwaves, *Chem. Mater.* **11**, 882 (1999).
- [187] D. M. P. Mingos, Microwave syntheses of inorganic materials, *Adv. Mater.* **5**, 857 (1993).
- [188] A. G. Whittaker and D. M. Mingos, The application of microwave heating to chemical syntheses, *J. Microwave Power Electromagn. Energy* **29**, 195 (1994).
- [189] P. S. Maram, S. V. Ushakov, R. J. K. Weber, C. J. Benmore, and A. Navrotsky, Probing disorder in pyrochlore oxides using in situ synchrotron diffraction from levitated solids—a thermodynamic perspective, *Sci. Rep.* **8**, 10658 (2018).
- [190] M. Ciomaga Hatnean, C. Decorse, M. R. Lees, O. A. Petrenko, and G. Balakrishnan, Zirconate pyrochlore frustrated magnets: Crystal growth by the floating zone technique, *Crystals* **6**, 79 (2016).
- [191] V. Popov, A. Menushenkov, A. Yaroslavtsev, Y. Zubavichus, B. Gaynanov, A. Yastrebtsev, D. Leshchev, and R. Chernikov, Fluorite-pyrochlore phase transition in nanostructured $Ln_2Hf_2O_7$ ($Ln = La-Lu$), *J. Alloys Compd.* **689**, 669 (2016).
- [192] B. Jiang, C. A. Bridges, R. R. Unocic, K. C. Pitike, V. R. Cooper, Y. Zhang, D.-Y. Lin, and K. Page, Probing the local site disorder and distortion in pyrochlore high-entropy oxides, *J. Am. Chem. Soc.* **143**, 4193 (2020).
- [193] S. T. Bramwell, M. N. Field, M. J. Harris, and I. P. Parkin, Bulk magnetization of the heavy rare earth titanate pyrochlores - a series of model frustrated magnets, *J. Phys.: Condens. Matter* **12**, 483 (1999).
- [194] A. Scheie, M. Sanders, X. Gui, Y. Qiu, T. R. Prisk, R. J. Cava, and C. Broholm, Beyond magnons in Nd_2ScNbO_7 : An Ising pyrochlore antiferromagnet with all-in-all-out order and random fields, *Phys. Rev. B* **104**, 134418 (2021).
- [195] A. Bertin, P. Dalmas de Réotier, B. Fåk, C. Marin, A. Yaouanc, A. Forget, D. Sheptyakov, B. Frick, C. Ritter, A. Amato, C. Baines, and P. J. C. King, $Nd_2Sn_2O_7$: An all-in-all-out pyrochlore magnet with no divergence-free field and anomalously slow paramagnetic spin dynamics, *Phys. Rev. B* **92**, 144423 (2015).
- [196] J. Xu, V. K. Anand, A. K. Bera, M. Frontzek, D. L. Abernathy, N. Casati, K. Siemensmeyer, and B. Lake, Magnetic structure and crystal-field states of the pyrochlore antiferromagnet $Nd_2Zr_2O_7$, *Phys. Rev. B* **92**, 224430 (2015).
- [197] E. Lhotel, S. Petit, S. Guitteny, O. Florea, M. Ciomaga Hatnean, C. Colin, E. Ressouche, M. R. Lees, and G. Balakrishnan, Fluctuations and All-In–All-Out Ordering in Dipole-Octupole $Nd_2Zr_2O_7$, *Phys. Rev. Lett.* **115**, 197202 (2015).
- [198] V. K. Anand, D. L. Abernathy, D. T. Adroja, A. D. Hillier, P. K. Biswas, and B. Lake, Muon spin relaxation and inelastic neutron scattering investigations of the all-in/all-out antiferromagnet $Nd_2Hf_2O_7$, *Phys. Rev. B* **95**, 224420 (2017).
- [199] V. K. Anand, A. K. Bera, J. Xu, T. Herrmannsdörfer, C. Ritter, and B. Lake, Observation of long-range magnetic ordering in pyrohafnate $Nd_2Hf_2O_7$: A neutron diffraction study, *Phys. Rev. B* **92**, 184418 (2015).
- [200] K. Matsuhira, M. Tokunaga, M. Wakushima, Y. Hinatsu, and S. Takagi, Giant Magnetoresistance Effect in the Metal-Insulator Transition of Pyrochlore Oxide $Nd_2Ir_2O_7$, *J. Phys. Soc. Jpn.* **82**, 023706 (2013).
- [201] K. Tomiyasu, K. Matsuhira, K. Iwasa, M. Watahiki, S. Takagi, M. Wakushima, Y. Hinatsu, M. Yokoyama, K. Ohoyama, and K. Yamada, Emergence of Magnetic Long-range Order in Frustrated Pyrochlore $Nd_2Ir_2O_7$ with Metal-Insulator Transition, *J. Phys. Soc. Jpn.* **81**, 034709 (2012).
- [202] Y. Yasui, Y. Kondo, M. Kanada, M. Ito, H. Harashina, M. Sato, and K. Kakurai, Magnetic Structure of $Nd_2Mo_2O_7$, *J. Phys. Soc. Jpn.* **70**, 284 (2001).
- [203] S. T. Ku, D. Kumar, M. R. Lees, W.-T. Lee, R. Aldus, A. Studer, P. Imperia, S. Asai, T. Masuda, S. W. Chen, J. M. Chen, and L. J. Chang, Low temperature magnetic properties of $Nd_2Ru_2O_7$, *J. Phys.: Condens. Matter* **30**, 155601 (2018).

- [204] M. E. Brooks-Bartlett, S. T. Banks, L. D. C. Jaubert, A. Harman-Clarke, and P. C. W. Holdsworth, Magnetic-Moment Fragmentation and Monopole Crystallization, *Phys. Rev. X* **4**, 011007 (2014).
- [205] O. Benton, Quantum origins of moment fragmentation in $\text{Nd}_2\text{Zr}_2\text{O}_7$, *Phys. Rev. B* **94**, 104430 (2016).
- [206] R. Sibille, N. Gauthier, H. Yan, M. Ciomaga Hatnean, J. Ollivier, B. Winn, U. Filges, G. Balakrishnan, M. Kenzelmann, N. Shannon, and T. Fennell, Experimental signatures of emergent quantum electrodynamics in $\text{Pr}_2\text{Hf}_2\text{O}_7$, *Nat. Phys.* **14**, 711 (2018).
- [207] S. Petit, E. Lhotel, B. Canals, M. Ciomaga Hatnean, J. Ollivier, H. Mutka, E. Ressouche, A. R. Wildes, M. R. Lees, and G. Balakrishnan, Observation of magnetic fragmentation in spin ice, *Nat. Phys.* **12**, 746 (2016).
- [208] E. Zoghlin, J. Schmehr, C. Holgate, R. Dally, Y. Liu, G. Laurita, and S. D. Wilson, Evaluating the effects of structural disorder on the magnetic properties of $\text{Nd}_2\text{Zr}_2\text{O}_7$, *Phys. Rev. Materials* **5**, 084403 (2021).
- [209] J. Xu, O. Benton, A. T. M. N. Islam, T. Guidi, G. Ehlers, and B. Lake, Order out of a Coulomb Phase and Higgs Transition: Frustrated Transverse Interactions of $\text{Nd}_2\text{Zr}_2\text{O}_7$, *Phys. Rev. Lett.* **124**, 097203 (2020).
- [210] K. Kimura, S. Nakatsuji, J. Wen, C. Broholm, M. B. Stone, E. Nishibori, and H. Sawa, Quantum fluctuations in spin-ice-like $\text{Pr}_2\text{Zr}_2\text{O}_7$, *Nat. Commun.* **4**, 1934 (2013).
- [211] J. Jensen and A. R. Mackintosh, *Rare Earth Magnetism* (Clarendon, Oxford, 1991).
- [212] J. D. Cashion, A. H. Cooke, M. J. M. Leask, T. L. Thorp, and M. R. Wells, Crystal growth and magnetic susceptibility of some rare-earth compounds, *J. Mater. Sci.* **3**, 402 (1968).
- [213] V. N. Glazkov, M. E. Zhitomirsky, A. I. Smirnov, H.-A. Krug von Nidda, A. Loidl, C. Marin, and J.-P. Sanchez, Single-ion anisotropy in the gadolinium pyrochlores studied by electron paramagnetic resonance, *Phys. Rev. B* **72**, 020409(R) (2005).
- [214] B. Canals and C. Lacroix, Pyrochlore Antiferromagnet: A Three-Dimensional Quantum Spin Liquid, *Phys. Rev. Lett.* **80**, 2933 (1998).
- [215] B. Canals and C. Lacroix, Quantum spin liquid: The heisenberg antiferromagnet on the three-dimensional pyrochlore lattice, *Phys. Rev. B* **61**, 1149 (2000).
- [216] R. Moessner and J. T. Chalker, Properties of a Classical Spin Liquid: The Heisenberg Pyrochlore Antiferromagnet, *Phys. Rev. Lett.* **80**, 2929 (1998).
- [217] R. Moessner and J. T. Chalker, Low-temperature properties of classical geometrically frustrated antiferromagnets, *Phys. Rev. B* **58**, 12049 (1998).
- [218] K. Nawa, D. Okuyama, M. Avdeev, H. Nojiri, M. Yoshida, D. Ueta, H. Yoshizawa, and T. J. Sato, Degenerate ground state in the classical pyrochlore antiferromagnet $\text{Na}_3\text{Mn}(\text{CO}_3)_2\text{Cl}$, *Phys. Rev. B* **98**, 144426 (2018).
- [219] J. N. Reimers, Absence of long-range order in a three-dimensional geometrically frustrated antiferromagnet, *Phys. Rev. B* **45**, 7287 (1992).
- [220] J. N. Reimers, A. J. Berlinsky, and A.-C. Shi, Mean-field approach to magnetic ordering in highly frustrated pyrochlores, *Phys. Rev. B* **43**, 865 (1991).
- [221] J. Villain, Insulating spin glasses, *Z. Phys. B* **33**, 31 (1979).
- [222] P. Bonville, J. A. Hodges, M. Ocio, J. P. Sanchez, P. Vulliet, S. Sosin, and D. Braithwaite, Low temperature magnetic properties of geometrically frustrated $\text{Gd}_2\text{Sn}_2\text{O}_7$ and $\text{Gd}_2\text{Ti}_2\text{O}_7$, *J. Phys.: Condens. Matter* **15**, 7777 (2003).
- [223] G. Luo, S. T. Hess, and L. Corruccini, Low temperature magnetic properties of the geometrically frustrated pyrochlores $\text{Tb}_2\text{Tb}_2\text{O}_7$, $\text{Gd}_2\text{Tb}_2\text{O}_7$, and $\text{Gd}_2\text{Sn}_2\text{O}_7$, *Phys. Lett. A* **291**, 306 (2001).
- [224] K. Matsuhira, Y. Hinatsu, K. Tenya, H. Amitsuka, and T. Sakakibara, Low-Temperature Magnetic Properties of Pyrochlore Stannates, *J. Phys. Soc. Jpn.* **71**, 1576 (2002).
- [225] A. M. Durand, P. Klavins, and L. R. Corruccini, Heat capacity of the frustrated magnetic pyrochlores $\text{Gd}_2\text{Zr}_2\text{O}_7$ and $\text{Gd}_2\text{Hf}_2\text{O}_7$, *J. Phys.: Condens. Matter* **20**, 235208 (2008).
- [226] R. S. Freitas and J. S. Gardner, The magnetic phase diagram of $\text{Gd}_2\text{Sn}_2\text{O}_7$, *J. Phys.: Condens. Matter* **23**, 164215 (2011).
- [227] J. A. Mydosh, *Spin Glasses: An Experimental Introduction* (Taylor & Francis, London, 1993).
- [228] A. S. Wills, M. E. Zhitomirsky, B. Canals, J. P. Sanchez, P. Bonville, P. D. de Réotier, and A. Yaouanc, Magnetic ordering in $\text{Gd}_2\text{Sn}_2\text{O}_7$: the archetypal Heisenberg pyrochlore antiferromagnet, *J. Phys.: Condens. Matter* **18**, L37 (2006).
- [229] J. D. M. Champion, A. S. Wills, T. Fennell, S. T. Bramwell, J. S. Gardner, and M. A. Green, Order in the Heisenberg pyrochlore: The magnetic structure of $\text{Gd}_2\text{Ti}_2\text{O}_7$, *Phys. Rev. B* **64**, 140407(R) (2001).
- [230] J. R. Stewart, G. Ehlers, A. S. Wills, S. T. Bramwell, and J. S. Gardner, Phase transitions, partial disorder and multi- k structures in $\text{Gd}_2\text{Ti}_2\text{O}_7$, *J. Phys.: Condens. Matter* **16**, L321 (2004).
- [231] J. R. Stewart, J. S. Gardner, Y. Qiu, and G. Ehlers, Collective dynamics in the Heisenberg pyrochlore antiferromagnet $\text{Gd}_2\text{Sn}_2\text{O}_7$, *Phys. Rev. B* **78**, 132410 (2008).
- [232] S. E. Palmer and J. T. Chalker, Order induced by dipolar interactions in a geometrically frustrated antiferromagnet, *Phys. Rev. B* **62**, 488 (2000).
- [233] A. M. Hallas, A. Z. Sharma, Y. Cai, T. J. Munsie, M. N. Wilson, M. Tachibana, C. R. Wiebe, and G. M. Luke, Relief of frustration in the heisenberg pyrochlore antiferromagnet $\text{Gd}_2\text{Pt}_2\text{O}_7$, *Phys. Rev. B* **94**, 134417 (2016).
- [234] J. A. M. Paddison, G. Ehlers, A. B. Cairns, J. S. Gardner, O. A. Petrenko, N. P. Butch, D. D. Khalyavin, P. Manuel, H. E. Fischer, H. Zhou, A. L. Goodwin, and J. R. Stewart, Suppressed-moment 2- k order in the canonical frustrated antiferromagnet $\text{Gd}_2\text{Ti}_2\text{O}_7$, *npj Quantum Mater.* **6**, 99 (2021).
- [235] O. A. Petrenko, M. R. Lees, G. Balakrishnan, and D. M. Paul, Magnetic phase diagram of the antiferromagnetic pyrochlore $\text{Gd}_2\text{Ti}_2\text{O}_7$, *Phys. Rev. B* **70**, 012402 (2004).
- [236] M. I. Brammall, A. K. R. Briffa, and M. W. Long, Magnetic structure of $\text{Gd}_2\text{Ti}_2\text{O}_7$, *Phys. Rev. B* **83**, 054422 (2011).
- [237] B. Javanparast, Z. Hao, M. Enjalran, and M. J. P. Gingras, Fluctuation-Driven Selection at Criticality in a Frustrated Magnetic System: The Case of Multiple- k Partial Order on the Pyrochlore Lattice, *Phys. Rev. Lett.* **114**, 130601 (2015).
- [238] J. Xu, Magnetic properties of rare earth zirconate pyrochlores, Ph.D. thesis, Technische Universität Berlin, Berlin, 2017.
- [239] O. Cépas and B. S. Shastry, Field-driven transitions in the dipolar pyrochlore antiferromagnet $\text{Gd}_2\text{Ti}_2\text{O}_7$, *Phys. Rev. B* **69**, 184402 (2004).
- [240] S. Guitteny, S. Petit, E. Lhotel, J. Robert, P. Bonville, A. Forget, and I. Mirebeau, Palmer-Chalker correlations in the

- XY pyrochlore antiferromagnet $\text{Er}_2\text{Sn}_2\text{O}_7$, *Phys. Rev. B* **88**, 134408 (2013).
- [241] Z. L. Dun, X. Li, R. S. Freitas, E. Arrighi, C. R. Dela Cruz, M. Lee, E. S. Choi, H. B. Cao, H. J. Silverstein, C. R. Wiebe, J. G. Cheng, and H. D. Zhou, Antiferromagnetic order in the pyrochlores $\text{R}_2\text{Ge}_2\text{O}_7$ ($\text{R}=\text{Er}, \text{Yb}$), *Phys. Rev. B* **92**, 140407(R) (2015).
- [242] A. Poole, A. S. Wills, and E. Lelièvre-Berna, Magnetic ordering in the XY pyrochlore antiferromagnet $\text{Er}_2\text{Ti}_2\text{O}_7$: A spherical neutron polarimetry study, *J. Phys.: Condens. Matter* **19**, 452201 (2007).
- [243] J. Lago, I. Živković, J. O. Piatek, P. Álvarez, D. Hüvonen, F. L. Pratt, M. Díaz, and T. Rojo, Glassy dynamics in the low-temperature inhomogeneous ferromagnetic phase of the quantum spin ice $\text{Yb}_2\text{Sn}_2\text{O}_7$, *Phys. Rev. B* **89**, 024421 (2014).
- [244] A. Yaouanc, P. D. Dalmas de Réotier, P. Bonville, J. A. Hodges, V. Glazkov, L. Keller, V. Sikolenko, M. Bartkowiak, A. Amato, C. Baines, P. J. C. King, P. C. M. Gubbens, and A. Forget, Dynamical Splayed Ferromagnetic Ground State in the Quantum Spin Ice $\text{Yb}_2\text{Sn}_2\text{O}_7$, *Phys. Rev. Lett.* **110**, 127207 (2013).
- [245] Y. Q. Cai, Q. Cui, X. Li, Z. L. Dun, J. Ma, C. de la Cruz, Y. Y. Jiao, J. Liao, P. J. Sun, Y. Q. Li, J. S. Zhou, J. B. Goodenough, H. D. Zhou, and J.-G. Cheng, High-pressure synthesis and characterization of the effective pseudospin $s = 1/2$ XY pyrochlores $\text{R}_2\text{Pt}_2\text{O}_7$ ($\text{R}=\text{Er}, \text{Yb}$), *Phys. Rev. B* **93**, 014443 (2016).
- [246] H. Yan, O. Benton, L. Jaubert, and N. Shannon, Theory of multiple-phase competition in pyrochlore magnets with anisotropic exchange with application to $\text{Yb}_2\text{Ti}_2\text{O}_7$, $\text{Er}_2\text{Ti}_2\text{O}_7$, and $\text{Er}_2\text{Sn}_2\text{O}_7$, *Phys. Rev. B* **95**, 094422 (2017).
- [247] L. D. C. Jaubert, O. Benton, J. G. Rau, J. Oitmaa, R. R. P. Singh, N. Shannon, and M. J. P. Gingras, Are Multiphase Competition and Order by Disorder the Keys to Understanding $\text{Yb}_2\text{Ti}_2\text{O}_7$? *Phys. Rev. Lett.* **115**, 267208 (2015).
- [248] K. Guratinder, J. G. Rau, V. Tsurkan, C. Ritter, J. Embs, T. Fennell, H. C. Walker, M. Medarde, T. Shang, A. Cervellino, C. Rüegg, and O. Zaharko, Multiphase competition in the quantum XY pyrochlore antiferromagnet CdYb_2Se_4 : Zero and applied magnetic field study, *Phys. Rev. B* **100**, 094420 (2019).
- [249] A. Scheie, J. Kindervater, S. Zhang, H. J. Changlani, G. Sala, G. Ehlers, A. Heinemann, G. S. Tucker, S. M. Koohpayeh, and C. Broholm, Multiphase magnetism in $\text{Yb}_2\text{Ti}_2\text{O}_7$, *Proc. Natl. Acad. Sci. USA* **117**, 27245 (2020).
- [250] A. M. Hallas, J. Gaudet, N. P. Butch, G. Xu, M. Tachibana, C. R. Wiebe, G. M. Luke, and B. D. Gaulin, Phase Competition in the Palmer-Chalker XY Pyrochlore $\text{Er}_2\text{Pt}_2\text{O}_7$, *Phys. Rev. Lett.* **119**, 187201 (2017).
- [251] S. Petit, E. Lhotel, F. Damay, P. Boutrouille, A. Forget, and D. Colson, Long-Range Order in the Dipolar X Y Antiferromagnet $\text{Er}_2\text{Sn}_2\text{O}_7$, *Phys. Rev. Lett.* **119**, 187202 (2017).
- [252] J. G. Rau, S. Petit, and M. J. P. Gingras, Order by virtual crystal field fluctuations in pyrochlore XY antiferromagnets, *Phys. Rev. B* **93**, 184408 (2016).
- [253] D. R. Yahne, D. Pereira, L. D. C. Jaubert, L. D. Sanjeewa, M. Powell, J. W. Kolis, G. Xu, M. Enjalran, M. J. P. Gingras, and K. A. Ross, Understanding Reentrance in Frustrated Magnets: The Case of the $\text{Er}_2\text{Sn}_2\text{O}_7$ Pyrochlore, *Phys. Rev. Lett.* **127**, 277206 (2021).
- [254] J. Gaudet, A. M. Hallas, D. D. Maharaj, C. R. C. Buhariwalla, E. Kermarrec, N. P. Butch, T. J. S. Munsie, H. A. Dabkowska, G. M. Luke, and B. D. Gaulin, Magnetic dilution and domain selection in the XY pyrochlore antiferromagnet $\text{Er}_2\text{Ti}_2\text{O}_7$, *Phys. Rev. B* **94**, 060407(R) (2016).
- [255] H. Cao, A. Gukasov, I. Mirebeau, P. Bonville, C. Decorse, and G. Dhaleine, Ising versus XY Anisotropy in frustrated $\text{R}_2\text{Ti}_2\text{O}_7$ Compounds as “Seen” by Polarized Neutrons, *Phys. Rev. Lett.* **103**, 056402 (2009).
- [256] P. Bonville, S. Petit, I. Mirebeau, J. Robert, E. Lhotel, and C. Paulsen, Magnetization process in $\text{Er}_2\text{Ti}_2\text{O}_7$ at very low temperature, *J. Phys.: Condens. Matter* **25**, 275601 (2013).
- [257] O. A. Petrenko, M. R. Lees, and G. Balakrishnan, Titanium pyrochlore magnets: How much can be learned from magnetization measurements? *J. Phys.: Condens. Matter* **23**, 164218 (2011).
- [258] P. M. Sarte, H. J. Silverstein, B. T. K. V. Wyk, J. S. Gardner, Y. Qiu, H. D. Zhou, and C. R. Wiebe, Absence of long-range magnetic ordering in the pyrochlore compound $\text{Er}_2\text{Sn}_2\text{O}_7$, *J. Phys.: Condens. Matter* **23**, 382201 (2011).
- [259] V. Bondah-Jagalu and S. T. Bramwell, Magnetic susceptibility study of the heavy rare-earth stannate pyrochlores, *Can. J. Phys.* **79**, 1381 (2001).
- [260] N. Al Ghandi, A. Orendáčová, V. Pavlík, and M. Orendáč, Thermodynamic Properties of Geometrically Frustrated $s = \frac{1}{2}$ XY Antiferromagnet $\text{Er}_2\text{Sn}_2\text{O}_7$, *Acta Phys. Pol.* **126**, 264 (2014).
- [261] M. Shirai, R. S. Freitas, J. Lago, S. T. Bramwell, C. Ritter, and I. Živković, Doping-induced quantum crossover in $\text{Er}_2\text{Ti}_{2-x}\text{Sn}_x\text{O}_7$, *Phys. Rev. B* **96**, 180411(R) (2017).
- [262] S. Tardif, S. Takeshita, H. Ohsumi, J.-i. Yamaura, D. Okuyama, Z. Hiroi, M. Takata, and T.-h. Arima, All-In-All-Out Magnetic Domains: X-Ray Diffraction Imaging and Magnetic Field Control, *Phys. Rev. Lett.* **114**, 147205 (2015).
- [263] E. Lhotel, V. Simonet, J. Ortloff, B. Canals, C. Paulsen, E. Suard, T. Hansen, D. J. Price, P. T. Wood, A. K. Powell, and R. Ballou, Domain-Wall Spin Dynamics in Kagome Antiferromagnets, *Phys. Rev. Lett.* **107**, 257205 (2011).
- [264] J. Snyder, B. G. Ueland, A. Mizel, J. S. Slusky, H. Karunadasa, R. J. Cava, and P. Schiffer, Quantum and thermal spin relaxation in the diluted spin ice $\text{Dy}_{2-x}\text{M}_x\text{Ti}_2\text{O}_7$ ($\text{M}=\text{Lu}, \text{Y}$), *Phys. Rev. B* **70**, 184431 (2004).
- [265] J. Snyder, J. S. Slusky, R. J. Cava, and P. Schiffer, How ‘spin ice’ freezes, *Nature (London)* **413**, 48 (2001).
- [266] G. Ehlers, J. S. Gardner, C. H. Booth, M. Daniel, K. C. Kam, A. K. Cheetham, D. Antonio, H. E. Brooks, A. L. Cornelius, S. T. Bramwell, J. Lago, W. Häussler, and N. Rosov, Dynamics of diluted Ho spin ice $\text{Ho}_{2-x}\text{Y}_x\text{Ti}_2\text{O}_7$ studied by neutron spin echo spectroscopy and ac susceptibility, *Phys. Rev. B* **73**, 174429 (2006).
- [267] X. Ke, B. G. Ueland, D. V. West, M. L. Dahlberg, R. J. Cava, and P. Schiffer, Spin-ice behavior in $\text{Dy}_2\text{Sn}_{2-x}\text{Sb}_x\text{O}_{7+x/2}$ and $\text{Dy}_2\text{NbScO}_7$, *Phys. Rev. B* **76**, 214413 (2007).
- [268] M. J. Gingras and P. A. McClarty, Quantum spin ice: a search for gapless quantum spin liquids in pyrochlore magnets, *Rep. Prog. Phys.* **77**, 056501 (2014).
- [269] R. Applegate, N. R. Hayre, R. R. P. Singh, T. Lin, A. G. R. Day, and M. J. P. Gingras, Vindication of $\text{Yb}_2\text{Ti}_2\text{O}_7$ as a Model Exchange Quantum Spin Ice, *Phys. Rev. Lett.* **109**, 097205 (2012).

- [270] S. Petit, On the way to understanding $\text{Yb}_2\text{Ti}_2\text{O}_7$, *Proc. Natl. Acad. Sci. USA* **117**, 29263 (2020).
- [271] L. Pan, N. J. Laurita, K. A. Ross, B. D. Gaulin, and N. P. Armitage, A measure of monopole inertia in the quantum spin ice $\text{Yb}_2\text{Ti}_2\text{O}_7$, *Nat. Phys.* **12**, 361 (2016).
- [272] M. Baenitz, P. Schlender, J. Sichelschmidt, Y. A. Onykiienko, Z. Zangeneh, K. M. Ranjith, R. Sarkar, L. Hozoi, H. C. Walker, J.-C. Orain, H. Yasuoka, J. van den Brink, H. H. Klauss, D. S. Inosov, and T. Doert, NaYbS_2 : A planar spin- $\frac{1}{2}$ triangular-lattice magnet and putative spin liquid, *Phys. Rev. B* **98**, 220409(R) (2018).
- [273] W. Liu, Z. Zhang, J. Ji, Y. Liu, J. Li, X. Wang, H. Lei, G. Chen, and Q. Zhang, Rare-earth chalcogenides: A large family of triangular lattice spin liquid candidates, *Chin. Phys. Lett.* **35**, 117501 (2018).
- [274] K. M. Ranjith, D. Dmytrieva, S. Khim, J. Sichelschmidt, S. Luther, D. Ehlers, H. Yasuoka, J. Wosnitza, A. A. Tsirlin, H. Kühne, and M. Baenitz, Field-induced instability of the quantum spin liquid ground state in the $J_{\text{eff}} = \frac{1}{2}$ triangular-lattice compound NaYbO_2 , *Phys. Rev. B* **99**, 180401(R) (2019).
- [275] M. M. Bordelon, E. Kenney, C. Liu, T. Hogan, L. Posthuma, M. Kavand, Y. Lyu, M. Sherwin, N. P. Butch, C. Brown, M. J. Graf, L. Balents, and S. D. Wilson, Field-tunable quantum disordered ground state in the triangular-lattice antiferromagnet NaYbO_2 , *Nat. Phys.* **15**, 1058 (2019).
- [276] K. M. Ranjith, S. Luther, T. Reimann, B. Schmidt, P. Schlender, J. Sichelschmidt, H. Yasuoka, A. M. Strydom, Y. Skourski, J. Wosnitza, H. Kühne, T. Doert, and M. Baenitz, Anisotropic field-induced ordering in the triangular-lattice quantum spin liquid NaYbSe_2 , *Phys. Rev. B* **100**, 224417 (2019).
- [277] B. Schmidt, J. Sichelschmidt, K. M. Ranjith, T. Doert, and M. Baenitz, Yb delafossites: Unique exchange frustration of 4f spin- $\frac{1}{2}$ moments on a perfect triangular lattice, *Phys. Rev. B* **103**, 214445 (2021).
- [278] Y. Li, G. Chen, W. Tong, L. Pi, J. Liu, Z. Yang, X. Wang, and Q. Zhang, Rare-Earth Triangular Lattice Spin Liquid: A Single-Crystal Study of YbMgGaO_4 , *Phys. Rev. Lett.* **115**, 167203 (2015).
- [279] J. A. M. Paddison, M. Daum, Z. Dun, G. Ehlers, Y. Liu, M. B. Stone, H. Zhou, and M. Mourigal, Continuous excitations of the triangular-lattice quantum spin liquid YbMgGaO_4 , *Nat. Phys.* **13**, 117 (2017).
- [280] B. Sriram Shastry and B. Sutherland, Exact ground state of a quantum mechanical antiferromagnet, *Physica B+C* **108**, 1069 (1981).
- [281] M. S. Kim and M. C. Aronson, Spin Liquids and Antiferromagnetic Order in the Shastry-Sutherland-Lattice Compound $\text{Yb}_2\text{Pt}_2\text{Pb}$, *Phys. Rev. Lett.* **110**, 017201 (2013).
- [282] B. H. Bernhard, B. Coqblin, and C. Lacroix, Frustration in the Kondo lattice model: Local versus extended singlet phases, *Phys. Rev. B* **83**, 214427 (2011).
- [283] F. Kikuchi, K. Hara, E. Matsuoka, H. Onodera, S. Nakamura, T. Nojima, K. Katoh, and A. Ochiai, $\text{Yb}_2(\text{Pd}_{1-x}\text{Ni}_x)_2\text{Sn}$: Interplay of Geometrical Frustration and Kondo Effect in Quantum Spin System, *J. Phys. Soc. Jpn.* **78**, 083708 (2009).
- [284] H.-D. Liu, Y.-H. Chen, H.-F. Lin, H.-S. Tao, and W.-M. Liu, Antiferromagnetic metal and Mott transition on Shastry-Sutherland lattice, *Sci. Rep.* **4**, 1 (2014).
- [285] Y. I. Dublenych, Ground States of the Ising Model on the Shastry-Sutherland Lattice and the Origin of the Fractional Magnetization Plateaus in Rare-Earth-Metal Tetraborides, *Phys. Rev. Lett.* **109**, 167202 (2012).
- [286] J. A. Hodges, P. Bonville, A. Forget, M. Rams, K. Królas, and G. Dhaleine, The crystal field and exchange interactions in $\text{Yb}_2\text{Ti}_2\text{O}_7$, *J. Phys.: Condens. Matter* **13**, 9301 (2001).
- [287] J. Gaudet, D. D. Maharaj, G. Sala, E. Kermarrec, K. A. Ross, H. A. Dabkowska, A. I. Kolesnikov, G. E. Granroth, and B. D. Gaulin, Neutron spectroscopic study of crystalline electric field excitations in stoichiometric and lightly stuffed $\text{Yb}_2\text{Ti}_2\text{O}_7$, *Phys. Rev. B* **92**, 134420 (2015).
- [288] B. Z. Malkin, A. R. Zakirov, M. N. Popova, S. A. Klimin, E. P. Chukalina, E. Antic-Fidancev, P. Goldner, P. Aschehoug, and G. Dhaleine, Optical spectroscopy of $\text{Yb}_2\text{Ti}_2\text{O}_7$ and $\text{Y}_2\text{Ti}_2\text{O}_7$: Yb^{3+} and crystal-field parameters in rare-earth titanate pyrochlores, *Phys. Rev. B* **70**, 075112 (2004).
- [289] M. Hermele, M. P. A. Fisher, and L. Balents, Pyrochlore photons: The $U(1)$ spin liquid in a $S = \frac{1}{2}$ three-dimensional frustrated magnet, *Phys. Rev. B* **69**, 064404 (2004).
- [290] A. Banerjee, S. V. Isakov, K. Damle, and Y. B. Kim, Unusual Liquid State of Hard-Core Bosons on the Pyrochlore Lattice, *Phys. Rev. Lett.* **100**, 047208 (2008).
- [291] L. Savary and L. Balents, Coulombic Quantum Liquids in Spin-1/2 Pyrochlores, *Phys. Rev. Lett.* **108**, 037202 (2012).
- [292] O. Benton, O. Sikora, and N. Shannon, Seeing the light: Experimental signatures of emergent electromagnetism in a quantum spin ice, *Phys. Rev. B* **86**, 075154 (2012).
- [293] Z. L. Dun, M. Lee, E. S. Choi, A. M. Hallas, C. R. Wiebe, J. S. Gardner, E. Arrighi, R. S. Freitas, A. M. Arevalo-Lopez, J. P. Attfield, H. D. Zhou, and J. G. Cheng, Chemical pressure effects on magnetism in the quantum spin liquid candidates $\text{Yb}_2\text{X}_2\text{O}_7$ ($\text{X} = \text{Sn}, \text{Ti}, \text{Ge}$), *Phys. Rev. B* **89**, 064401 (2014).
- [294] A. M. Hallas, J. Gaudet, N. P. Butch, M. Tachibana, R. S. Freitas, G. M. Luke, C. R. Wiebe, and B. D. Gaulin, Universal dynamic magnetism in Yb pyrochlores with disparate ground states, *Phys. Rev. B* **93**, 100403(R) (2016).
- [295] E. Lhotel, S. R. Giblin, M. R. Lees, G. Balakrishnan, L. J. Chang, and Y. Yasui, First-order magnetic transition in $\text{Yb}_2\text{Ti}_2\text{O}_7$, *Phys. Rev. B* **89**, 224419 (2014).
- [296] A. Yaouanc, A. Maisuradze, and P. Dalmas de Réotier, Influence of short-range spin correlations on the μSR polarization functions in the slow dynamic limit: Application to the quantum spin-liquid system $\text{Yb}_2\text{Ti}_2\text{O}_7$, *Phys. Rev. B* **87**, 134405 (2013).
- [297] D. F. Bowman, E. Cemal, T. Lehner, A. R. Wildes, L. Mangin-Thro, G. J. Nilsen, M. J. Gutmann, D. Voneshen, D. Prabhakaran, A. T. Boothroyd, D. G. Porter, C. castelnovo, K. Refson, and J. P. Goff, Role of defects in determining the magnetic ground state of ytterbium titanate, *Nat. Commun.* **10**, 637 (2019).
- [298] G. Sala, M. J. Gutmann, D. Prabhakaran, D. Pomaranski, C. Mitchelitis, J. B. Kycia, D. G. Porter, C. Castelnovo, and J. P. Goff, Vacancy defects and monopole dynamics in oxygen-deficient pyrochlores, *Nat. Mater.* **13**, 488 (2014).
- [299] A. Mostaed, G. Balakrishnan, M. R. Lees, Y. Yasui, L.-J. Chang, and R. Beanland, Atomic structure study of the pyrochlore $\text{Yb}_2\text{Ti}_2\text{O}_7$ and its relationship with low-temperature magnetic order, *Phys. Rev. B* **95**, 094431 (2017).

- [300] E. Kermarrec, J. Gaudet, K. Fritsch, R. Khasanov, Z. Guguchia, C. Ritter, K. A. Ross, H. A. Dabkowska, and B. D. Gaulin, Ground state selection under pressure in the quantum pyrochlore magnet $\text{Yb}_2\text{Ti}_2\text{O}_7$, *Nat. Commun.* **8**, 14810 (2017).
- [301] Z. L. Dun, E. S. Choi, H. D. Zhou, A. M. Hallas, H. J. Silverstein, Y. Qiu, J. R. D. Copley, J. S. Gardner, and C. R. Wiebe, $\text{Yb}_2\text{Sn}_2\text{O}_7$: A magnetic Coulomb liquid at a quantum critical point, *Phys. Rev. B* **87**, 134408 (2013).
- [302] J. A. Hodges, P. Bonville, A. Forget, A. Yaouanc, P. Dalmas de Réotier, G. André, M. Rams, K. Królas, C. Ritter, P. C. M. Gubbens, C. T. Kaiser, P. J. C. King, and C. Baines, First-Order Transition in the Spin Dynamics of Geometrically Frustrated $\text{Yb}_2\text{Ti}_2\text{O}_7$, *Phys. Rev. Lett.* **88**, 077204 (2002).
- [303] J. A. Hodges, P. D. De Réotier, A. Yaouanc, P. C. M. Gubbens, P. J. C. King, and C. Baines, Magnetic frustration in the disordered pyrochlore $\text{Yb}_2\text{GaSbO}_7$, *J. Phys.: Condens. Matter* **23**, 164217 (2011).
- [304] E. Kermarrec, D. D. Maharaj, J. Gaudet, K. Fritsch, D. Pomaranski, J. B. Kycia, Y. Qiu, J. R. D. Copley, M. M. P. Couchman, A. O. R. Morningstar, H. A. Dabkowska, and B. D. Gaulin, Gapped and gapless short-range-ordered magnetic states with $(\frac{1}{2}, \frac{1}{2}, \frac{1}{2})$ wave vectors in the pyrochlore magnet $\text{Tb}_{2+x}\text{Ti}_{2-x}\text{O}_{7-\delta}$, *Phys. Rev. B* **92**, 245114 (2015).
- [305] T. Taniguchi, H. Kadowaki, H. Takatsu, B. Fåk, J. Ollivier, T. Yamazaki, T. J. Sato, H. Yoshizawa, Y. Shimura, T. Sakakibara, T. Hong, K. Goto, L. R. Yaraskavitch, and J. B. Kycia, Long-range order and spin-liquid states of polycrystalline $\text{Tb}_{2+x}\text{Ti}_{2-x}\text{O}_{7+y}$, *Phys. Rev. B* **87**, 060408(R) (2013).
- [306] H. Kadowaki, M. Wakita, B. Fåk, J. Ollivier, S. Ohira-Kawamura, K. Nakajima, H. Takatsu, and M. Tamai, Continuum excitation and pseudospin wave in quantum spin-liquid and quadrupole ordered states of $\text{Tb}_{2+x}\text{Ti}_{2-x}\text{O}_{7+y}$, *J. Phys. Soc. Jpn.* **87**, 064704 (2018).
- [307] M. Kanada, Y. Yasui, M. Ito, H. Harashina, M. Sato, H. Okumura, and K. Kakurai, Neutron Inelastic Scattering Study on a Single Crystal of $\text{Yb}_2\text{Ti}_2\text{O}_7$, a Magnetically Frustrated Pyrochlore System, *J. Phys. Soc. Jpn.* **68**, 3802 (1999).
- [308] V. K. Anand, L. Opherden, J. Xu, D. T. Adroja, A. D. Hillier, P. K. Biswas, T. Herrmannsdörfer, M. Uhlärz, J. Hornung, J. Wosnitza, E. Canévet, and B. Lake, Evidence for a dynamical ground state in the frustrated pyrohafnate $\text{Tb}_2\text{Hf}_2\text{O}_7$, *Phys. Rev. B* **97**, 094402 (2018).
- [309] B. D. Gaulin, E. Kermarrec, M. L. Dahlberg, M. J. Matthews, F. Bert, J. Zhang, P. Mendels, K. Fritsch, G. E. Granroth, P. Jiramongkolchai, A. Amato, C. Baines, R. J. Cava, and P. Schiffer, Quenched crystal-field disorder and magnetic liquid ground states in $\text{Tb}_2\text{Sn}_{2-x}\text{Ti}_x\text{O}_7$, *Phys. Rev. B* **91**, 245141 (2015).
- [310] A. Scheie, J. Kindervater, S. Säubert, C. Duvinage, C. Pfleiderer, H. J. Changlani, S. Zhang, L. Harriger, K. Arpino, S. M. Koohpayeh, O. Tchernyshyov, and C. Broholm, Reentrant Phase Diagram of $\text{Yb}_2\text{Ti}_2\text{O}_7$ in a $\langle 111 \rangle$ Magnetic Field, *Phys. Rev. Lett.* **119**, 127201 (2017).
- [311] A. Yaouanc, P. D. De Réotier, L. Keller, B. Roessli, and A. Forget, A novel type of splayed ferromagnetic order observed in $\text{Yb}_2\text{Ti}_2\text{O}_7$, *J. Phys.: Condens. Matter* **28**, 426002 (2016).
- [312] A. J. Princep, H. C. Walker, D. T. Adroja, D. Prabhakaran, and A. T. Boothroyd, Crystal field states of Tb^{3+} in the pyrochlore spin liquid $\text{Tb}_2\text{Ti}_2\text{O}_7$ from neutron spectroscopy, *Phys. Rev. B* **91**, 224430 (2015).
- [313] J. Zhang, K. Fritsch, Z. Hao, B. V. Bagheri, M. J. P. Gingras, G. E. Granroth, P. Jiramongkolchai, R. J. Cava, and B. D. Gaulin, Neutron spectroscopic study of crystal field excitations in $\text{Tb}_2\text{Ti}_2\text{O}_7$ and $\text{Tb}_2\text{Sn}_2\text{O}_7$, *Phys. Rev. B* **89**, 134410 (2014).
- [314] I. Mirebeau, P. Bonville, and M. Hennion, Magnetic excitations in $\text{Tb}_2\text{Sn}_2\text{O}_7$ and $\text{Tb}_2\text{Ti}_2\text{O}_7$ as measured by inelastic neutron scattering, *Phys. Rev. B* **76**, 184436 (2007).
- [315] H. R. Molavian, M. J. P. Gingras, and B. Canals, Dynamically Induced Frustration as a Route to a Quantum Spin Ice State in $\text{Tb}_2\text{Ti}_2\text{O}_7$ via virtual Crystal Field Excitations and Quantum Many-Body Effects, *Phys. Rev. Lett.* **98**, 157204 (2007).
- [316] H. R. Molavian, P. A. McClarty, and M. J. P. Gingras, Towards an Effective Spin Hamiltonian of the Pyrochlore Spin Liquid $\text{Tb}_2\text{Ti}_2\text{O}_7$, *arXiv:0912.2957*.
- [317] A. M. Hallas, W. Jin, J. Gaudet, E. M. Tonita, D. Pomaranski, C. R. C. Buhariwalla, M. Tachibana, N. P. Butch, S. Calder, M. B. Stone, G. M. Luke, C. R. Wiebe, J. B. Kycia, M. J. P. Gingras, and B. D. Gaulin, Intertwined Magnetic Dipolar and Electric Quadrupolar Correlations in the Pyrochlore $\text{Tb}_2\text{Ge}_2\text{O}_7$, *arXiv:2009.05036*.
- [318] C. Liu, F.-Y. Li, and G. Chen, Upper branch magnetism in quantum magnets: Collapses of excited levels and emergent selection rules, *Phys. Rev. B* **99**, 224407 (2019).
- [319] Y.-J. Kao, M. Enjalran, A. Del Maestro, H. R. Molavian, and M. J. P. Gingras, Understanding paramagnetic spin correlations in the spin-liquid pyrochlore $\text{Tb}_2\text{Ti}_2\text{O}_7$, *Phys. Rev. B* **68**, 172407 (2003).
- [320] H. R. Molavian and M. J. P. Gingras, Proposal for a $\langle 111 \rangle$ magnetization plateau in the spin liquid state of $\text{Tb}_2\text{Ti}_2\text{O}_7$, *J. Phys.: Condens. Matter* **21**, 172201 (2009).
- [321] H. Takatsu, S. Onoda, S. Kittaka, A. Kasahara, Y. Kono, T. Sakakibara, Y. Kato, B. Fåk, J. Ollivier, J. W. Lynn, T. Taniguchi, M. Wakita, and H. Kadowaki, Quadrupole Order in the Frustrated Pyrochlore $\text{Tb}_{2+x}\text{Ti}_{2-x}\text{O}_{7+y}$, *Phys. Rev. Lett.* **116**, 217201 (2016).
- [322] S. Guitteny, J. Robert, P. Bonville, J. Ollivier, C. Decorse, P. Steffens, M. Boehm, H. Mutka, I. Mirebeau, and S. Petit, Anisotropic Propagating Excitations and Quadrupolar Effects in $\text{Tb}_2\text{Ti}_2\text{O}_7$, *Phys. Rev. Lett.* **111**, 087201 (2013).
- [323] S. Petit, P. Bonville, J. Robert, C. Decorse, and I. Mirebeau, Spin liquid correlations, anisotropic exchange, and symmetry breaking in $\text{Tb}_2\text{Ti}_2\text{O}_7$, *Phys. Rev. B* **86**, 174403 (2012).
- [324] M. Wakita, T. Taniguchi, H. Edamoto, H. Takatsu, and H. Kadowaki, Quantum spin liquid and electric quadrupolar states of single crystal $\text{Tb}_{2+x}\text{Ti}_{2-x}\text{O}_{7+y}$, *J. Phys.: Conf. Ser.* **683**, 012023 (2016).
- [325] H. Kadowaki, H. Takatsu, T. Taniguchi, B. Fåk, and J. Ollivier, Composite spin and quadrupole wave in the ordered phase of frustrated pyrochlore $\text{Tb}_{2+x}\text{Ti}_{2-x}\text{O}_{7+y}$, *SPIN* **05**, 1540003 (2015).
- [326] I. Mirebeau, A. Apetrii, J. Rodríguez-Carvajal, P. Bonville, A. Forget, D. Colson, V. Glazkov, J. P. Sanchez, O. Isnard, and E. Suard, Ordered Spin Ice State and Magnetic Fluctuations in $\text{Tb}_2\text{Sn}_2\text{O}_7$, *Phys. Rev. Lett.* **94**, 246402 (2005).
- [327] F. Bert, P. Mendels, A. Olariu, N. Blanchard, G. Collin, A. Amato, C. Baines, and A. D. Hillier, Direct Evidence for a

- Dynamical Ground State in the Highly Frustrated $Tb_2Sn_2O_7$ Pyrochlore, *Phys. Rev. Lett.* **97**, 117203 (2006).
- [328] M. L. Dahlberg, M. J. Matthews, P. Jiramongkolchai, R. J. Cava, and P. Schiffer, Low-temperature dynamic freezing and the fragility of ordering in $Tb_2Sn_2O_7$, *Phys. Rev. B* **83**, 140410(R) (2011).
- [329] Y. Chapuis, A. Yaouanc, P. D. de Réotier, S. Pouget, P. Fouquet, A. Cervellino, and A. Forget, Ground state of the geometrically frustrated compound $Tb_2Sn_2O_7$, *J. Phys.: Condens. Matter* **19**, 446206 (2007).
- [330] P. Dalmas de Réotier, A. Yaouanc, L. Keller, A. Cervellino, B. Roessli, C. Baines, A. Forget, C. Vaju, P. C. M. Gubbens, A. Amato, and P. J. C. King, Spin Dynamics and Magnetic Order in Magnetically Frustrated $Tb_2Sn_2O_7$, *Phys. Rev. Lett.* **96**, 127202 (2006).
- [331] K. C. Rule, G. Ehlers, J. R. Stewart, A. L. Cornelius, P. P. Deen, Y. Qiu, C. R. Wiebe, J. A. Janik, H. D. Zhou, D. Antonio, B. W. Woytko, J. P. Ruff, H. A. Dabkowska, B. D. Gaulin, and J. S. Gardner, Polarized inelastic neutron scattering of the partially ordered $Tb_2Sn_2O_7$, *Phys. Rev. B* **76**, 212405 (2007).
- [332] K. C. Rule, G. Ehlers, J. S. Gardner, Y. Qiu, E. Moskvin, K. Kiefer, and S. Gerischer, Neutron scattering investigations of the partially ordered pyrochlore $Tb_2Sn_2O_7$, *J. Phys.: Condens. Matter* **21**, 486005 (2009).
- [333] E. Lhotel, C. Paulsen, P. D. de Réotier, A. Yaouanc, C. Marin, and S. Vanishri, Low-temperature magnetization in geometrically frustrated $Tb_2Ti_2O_7$, *Phys. Rev. B* **86**, 020410(R) (2012).
- [334] C. Mauws, A. M. Hallas, G. Sala, A. A. Aczel, P. M. Sarte, J. Gaudet, D. Ziat, J. A. Quilliam, J. A. Lussier, M. Bieringer, H. D. Zhou, A. Wildes, M. B. Stone, D. Abernathy, G. M. Luke, B. D. Gaulin, and C. R. Wiebe, Dipolar-octupolar ising antiferromagnetism in $Sm_2Ti_2O_7$: A moment fragmentation candidate, *Phys. Rev. B* **98**, 100401(R) (2018).
- [335] V. Peçanha-Antonio, E. Feng, X. Sun, D. Adroja, H. C. Walker, A. S. Gibbs, F. Orlandi, Y. Su, and T. Brückel, Intermultiplet transitions and magnetic long-range order in Sm-based pyrochlores, *Phys. Rev. B* **99**, 134415 (2019).
- [336] S. Singh, S. Saha, S. K. Dhar, R. Suryanarayanan, A. K. Sood, and A. Revcolevschi, Manifestation of geometric frustration on magnetic and thermodynamic properties of the pyrochlores $Sm_2X_2O_7$ ($X=Ti,Zr$), *Phys. Rev. B* **77**, 054408 (2008).
- [337] B. Z. Malkin, T. T. A. Lummen, P. H. M. van Loosdrecht, G. Dhaleine, and A. R. Zakirov, Static magnetic susceptibility, crystal field and exchange interactions in rare earth titanate pyrochlores, *J. Phys.: Condens. Matter* **22**, 276003 (2010).
- [338] C. Donnerer, M. C. Rahn, M. M. Sala, J. G. Vale, D. Pincini, J. Strempfer, M. Krisch, D. Prabhakaran, A. T. Boothroyd, and D. F. McMorrow, All-in-all-Out Magnetic Order and Propagating Spin Waves in $Sm_2Ir_2O_7$, *Phys. Rev. Lett.* **117**, 037201 (2016).
- [339] P. C. Guruciaga, S. A. Grigera, and R. A. Borzi, Monopole ordered phases in dipolar and nearest-neighbors ising pyrochlore: From spin ice to the all-in-all-out antiferromagnet, *Phys. Rev. B* **90**, 184423 (2014).
- [340] A. Ikeda and H. Kawamura, Ordering of the pyrochlore ising model with the long-range rkky interaction, *J. Phys. Soc. Jpn.* **77**, 073707 (2008).
- [341] S. T. Bramwell and M. J. Harris, Frustration in Ising-type spin models on the pyrochlore lattice, *J. Phys.: Condens. Matter* **10**, L215 (1998).
- [342] L. Opherden, J. Hornung, T. Herrmannsdörfer, J. Xu, A. T. M. N. Islam, B. Lake, and J. Wosnitza, Evolution of anti-ferromagnetic domains in the all-in-all-out ordered pyrochlore $Nd_2Zr_2O_7$, *Phys. Rev. B* **95**, 184418 (2017).
- [343] S. R. Giblin, M. Twengström, L. Bovo, M. Ruminy, M. Bartkowiak, P. Manuel, J. C. Andresen, D. Prabhakaran, G. Balakrishnan, E. Pomjakushina, C. Paulsen, E. Lhotel, L. Keller, M. Frontzek, S. C. Capelli, O. Zaharko, P. A. McClarty, S. T. Bramwell, P. Henelius, and T. Fennell, Pauling Entropy, Metastability, and Equilibrium in $Dy_2Ti_2O_7$ Spin Ice, *Phys. Rev. Lett.* **121**, 067202 (2018).
- [344] H. T. Diep, *Frustrated Spin Systems*, 2nd ed. (World Scientific, Singapore, 2013).
- [345] S. Rosenkranz, A. P. Ramirez, A. Hayashi, R. J. Cava, R. Siddharthan, and B. S. Shastry, Crystal-field interaction in the pyrochlore magnet $Ho_2Tb_2O_7$, *J. Appl. Phys.* **87**, 5914 (2000).
- [346] H. Fukazawa, R. G. Melko, R. Higashinaka, Y. Maeno, and M. J. P. Gingras, Magnetic anisotropy of the spin-ice compound $Dy_2Ti_2O_7$, *Phys. Rev. B* **65**, 054410 (2002).
- [347] D. J. Flood, Magnetization and magnetic entropy of $Dy_2Tb_2O_7$, *J. Appl. Phys.* **45**, 4041 (1974).
- [348] Y. Jana, A. Sengupta, and D. Ghosh, Estimation of single ion anisotropy in pyrochlore $Dy_2Tb_2O_7$, a geometrically frustrated system, using crystal field theory, *J. Magn. Magn. Mater.* **248**, 7 (2002).
- [349] K. Matsuhira, Y. Hinatsu, K. Tenya, and T. Sakakibara, Low temperature magnetic properties of frustrated pyrochlore ferromagnets $Ho_2Sn_2O_7$ and $Ho_2Ti_2O_7$, *J. Phys.: Condens. Matter* **12**, L649 (2000).
- [350] T. Fennell, O. A. Petrenko, B. Fåk, S. T. Bramwell, M. Enjalran, T. Yavors'kii, M. J. P. Gingras, R. G. Melko, and G. Balakrishnan, Neutron scattering investigation of the spin ice state in $Dy_2Ti_2O_7$, *Phys. Rev. B* **70**, 134408 (2004).
- [351] H. Kadowaki, Y. Ishii, K. Matsuhira, and Y. Hinatsu, Neutron scattering study of dipolar spin ice $Ho_2Sn_2O_7$: Frustrated pyrochlore magnet, *Phys. Rev. B* **65**, 144421 (2002).
- [352] K. Matsuhira, Y. Hinatsu, and T. Sakakibara, Novel dynamical magnetic properties in the spin ice compound $Dy_2Ti_2O_7$, *J. Phys. Condens. Matter* **13**, L737 (2001).
- [353] J. Snyder, B. G. Ueland, J. S. Slusky, H. Karunadasa, R. J. Cava, A. Mizel, and P. Schiffer, Quantum-Classical Reentrant Relaxation Crossover in $Dy_2Ti_2O_7$ Spin Ice, *Phys. Rev. Lett.* **91**, 107201 (2003).
- [354] G. Ehlers, A. L. Cornelius, M. O. c, M. Kajnakov, T. Fennell, S. T. Bramwell, and J. S. Gardner, Dynamical crossover in hot spin ice, *J. Phys.: Condens. Matter* **15**, L9 (2002).
- [355] H. D. Zhou, C. R. Wiebe, J. A. Janik, L. Balicas, Y. J. Yo, Y. Qiu, J. R. D. Copley, and J. S. Gardner, Dynamic Spin Ice: $Pr_2Sn_2O_7$, *Phys. Rev. Lett.* **101**, 227204 (2008).
- [356] J. S. Gardner, G. Ehlers, P. Fouquet, B. Farago, and J. R. Stewart, Slow and static spin correlations in $Dy_{2+x}Ti_{2-x}O_{7-\delta}$, *J. Phys.: Condens. Matter* **23**, 164220 (2011).
- [357] G. Ehlers, A. L. Cornelius, T. Fennell, M. Koza, S. T. Bramwell, and J. S. Gardner, Evidence for two distinct spin relaxation mechanisms in hot spin ice $Ho_2Ti_2O_7$, *J. Phys.: Condens. Matter* **16**, S635 (2004).

- [358] J. Snyder, S. Slusky, R. J. Cava, and P. Schiffer, Dirty spin ice: The effect of dilution on spin freezing in $\text{Dy}_2\text{Ti}_2\text{O}_7$, *Phys. Rev. B* **66**, 064432 (2002).
- [359] K. Matsuhira, M. Wakshima, Y. Hinatsu, C. Sekine, C. Paulsen, T. Sakakibara, and S. Takagi, Slow dynamics of Dy pyrochlore oxides $\text{Dy}_2\text{Sn}_2\text{O}_7$ and $\text{Dy}_2\text{Ir}_2\text{O}_7$, *J. Phys.: Conf. Ser.* **320**, 012050 (2011).
- [360] J. Snyder, B. G. Ueland, J. S. Slusky, H. Karunadasa, R. J. Cava, and P. Schiffer, Low-temperature spin freezing in the $\text{Dy}_2\text{Ti}_2\text{O}_7$ spin ice, *Phys. Rev. B* **69**, 064414 (2004).
- [361] L. R. Yaraskavitch, H. M. Revell, S. Meng, K. A. Ross, H. M. L. Noad, H. A. Dabkowska, B. D. Gaulin, and J. B. Kycia, Spin dynamics in the frozen state of the dipolar spin ice material $\text{Dy}_2\text{Ti}_2\text{O}_7$, *Phys. Rev. B* **85**, 020410(R) (2012).
- [362] J. A. Quilliam, L. R. Yaraskavitch, H. A. Dabkowska, B. D. Gaulin, and J. B. Kycia, Dynamics of the magnetic susceptibility deep in the Coulomb phase of the dipolar spin ice material $\text{Ho}_2\text{Ti}_2\text{O}_7$, *Phys. Rev. B* **83**, 094424 (2011).
- [363] G. C. Lau, R. S. Freitas, B. Ueland, B. D. Muegge, E. L. Duncan, P. Schiffer, and R. J. Cava, Zero-point entropy in stuffed spin-ice, *Nat. Phys.* **2**, 249 (2006).
- [364] R. J. Aldus, T. Fennell, P. P. Deen, E. Ressouche, G. C. Lau, R. J. Cava, and S. T. Bramwell, Ice rule correlations in stuffed spin ice, *New J. Phys.* **15**, 013022 (2013).
- [365] G. Lau, B. Muegge, T. McQueen, E. Duncan, and R. Cava, Stuffed rare earth pyrochlore solid solutions, *J. Solid State Chem.* **179**, 3126 (2006).
- [366] H. D. Zhou, C. R. Wiebe, Y. J. Jo, L. Balicas, Y. Qiu, J. R. D. Copley, G. Ehlers, P. Fouquet, and J. S. Gardner, The origin of persistent spin dynamics and residual entropy in the stuffed spin ice $\text{Ho}_{2.3}\text{Ti}_{1.7}\text{O}_{7-\delta}$, *J. Phys.: Condens. Matter* **19**, 342201 (2007).
- [367] G. Ehlers, J. S. Gardner, Y. Qiu, P. Fouquet, C. R. Wiebe, L. Balicas, and H. D. Zhou, Dynamic spin correlations in stuffed spin ice $\text{Ho}_{2+x}\text{Ti}_{2-x}\text{O}_{7-\delta}$, *Phys. Rev. B* **77**, 052404 (2008).
- [368] B. G. Ueland, G. C. Lau, R. S. Freitas, J. Snyder, M. L. Dahlberg, B. D. Muegge, E. L. Duncan, R. J. Cava, and P. Schiffer, Magnetothermal study of a Dy-stuffed spin ice: $\text{Dy}_2(\text{Dy}_x\text{Ti}_{2-x})\text{O}_{7-x/2}$, *Phys. Rev. B* **77**, 144412 (2008).
- [369] J. G. A. Ramon, C. W. Wang, L. Ishida, P. L. Bernardo, M. M. Leite, F. M. Vichi, J. S. Gardner, and R. S. Freitas, Absence of spin-ice state in the disordered fluorite $\text{Dy}_2\text{Zr}_2\text{O}_7$, *Phys. Rev. B* **99**, 214442 (2019).
- [370] H. Liu, Y. Zou, L. Ling, L. Zhang, W. Tong, C. Zhang, and Y. Zhang, Frustrated magnetism and dynamical properties in pyrochlore-type magnet $\text{Dy}_2\text{Ti}_{2-x}\text{Fe}_x\text{O}_7$, *J. Magn. Magn. Mater.* **369**, 107 (2014).
- [371] S. Nandi, Y. Jana, D. Swarnakar, J. Alam, P. Bag, and R. Nath, Magnetization process and specific heat properties of geometrically frustrated pyrochlores R_2FeSbO_7 ($\text{R}^{3+} = \text{Dy}, \text{Y}$) and spin-ice magnetic phase in $\text{Dy}_2\text{FeSbO}_7$, *J. Alloys Compd.* **714**, 318 (2017).
- [372] A. Pal, A. Singh, A. K. Ghosh, and S. Chatterjee, High temperature spin-freezing transition in pyrochlore $\text{Eu}_2\text{Tb}_2\text{O}_7$: A new observation from ac-susceptibility, *J. Magn. Magn. Mater.* **462**, 1 (2018).
- [373] P. Dasgupta, Y. Jana, A. Nag Chattopadhyay, R. Higashinaka, Y. Maeno, and D. Ghosh, Low-temperature measurements of magnetic susceptibility and specific heat of $\text{Eu}_2\text{Tb}_2\text{O}_7$ —An XY pyrochlore, *J. Phys. Chem. Solids* **68**, 347 (2007).
- [374] M. P. Zinkin, M. J. Harris, Z. Tun, R. A. Cowley, and B. M. Wanklyn, Lifting of the ground-state degeneracy by crystal-field interactions in the pyrochlore $\text{Tm}_2\text{Ti}_2\text{O}_7$, *J. Phys.: Condens. Matter* **8**, 193 (1996).
- [375] A. Chattopadhyay, P. Dasgupta, Y. Jana, and D. Ghosh, A study on crystal field effect and single ion anisotropy in pyrochlore europium titanate $\text{Eu}_2\text{Tb}_2\text{O}_7$, *J. Alloys Compd.* **384**, 6 (2004).
- [376] Sheetal and C. Yadav, Structure and magnetic studies of geometrically frustrated disordered pyrochlores $\text{A}_2\text{Zr}_2\text{O}_7$: ($\text{A} = \text{Eu}, \text{Gd}, \text{Er}$), *J. Magn. Magn. Mater.* **553**, 169255 (2022).
- [377] N. Taira, M. Wakshima, and Y. Hinatsu, Magnetic susceptibility and specific heat studies on heavy rare earth ruthenate pyrochlores $\text{R}_2\text{Ru}_2\text{O}_7$ ($\text{R} = \text{Gd-Yb}$), *J. Mater. Chem.* **12**, 1475 (2002).
- [378] K. R. Lea, M. J. M. Leask, and W. Wolf, The raising of angular momentum degeneracy of f -Electron terms by cubic crystal fields, *J. Phys. Chem. Solids* **23**, 1381 (1962).
- [379] J. E. Greedan, *Oxides with Trirutile and Pyrochlore Structures, Landolt-Börnstein-Group III Condensed Matter*, edited by H. Wijn, Vol. 27, Part g (Springer, Berlin, 1992).
- [380] R. Sibille, E. Lhotel, M. C. Hatnean, G. Balakrishnan, B. Fåk, N. Gauthier, T. Fennell, and M. Kenzelmann, Candidate quantum spin ice in the pyrochlore $\text{Pr}_2\text{Hf}_2\text{O}_7$, *Phys. Rev. B* **94**, 024436 (2016).
- [381] V. K. Anand, L. Opherden, J. Xu, D. T. Adroja, A. T. M. N. Islam, T. Herrmannsdörfer, J. Hornung, R. Schönemann, M. Uhlarz, H. C. Walker, N. Casati, and B. Lake, Physical properties of the candidate quantum spin-ice system $\text{Pr}_2\text{Hf}_2\text{O}_7$, *Phys. Rev. B* **94**, 144415 (2016).
- [382] S. Petit, E. Lhotel, S. Guitteny, O. Florea, J. Robert, P. Bonville, I. Mirebeau, J. Ollivier, H. Mutka, E. Ressouche, C. Decorse, M. Ciomaga Hatnean, and G. Balakrishnan, Antiferroquadrupolar correlations in the quantum spin ice candidate $\text{Pr}_2\text{Zr}_2\text{O}_7$, *Phys. Rev. B* **94**, 165153 (2016).
- [383] P. Bonville, S. Guitteny, A. Gukasov, I. Mirebeau, S. Petit, C. Decorse, M. C. Hatnean, and G. Balakrishnan, Magnetic properties and crystal field in $\text{Pr}_2\text{Zr}_2\text{O}_7$, *Phys. Rev. B* **94**, 134428 (2016).
- [384] S. Onoda and Y. Tanaka, Quantum fluctuations in the effective pseudospin- $\frac{1}{2}$ model for magnetic pyrochlore oxides, *Phys. Rev. B* **83**, 094411 (2011).
- [385] S. Koohpayeh, J.-J. Wen, B. Trump, C. Broholm, and T. McQueen, Synthesis, floating zone crystal growth and characterization of the quantum spin ice $\text{Pr}_2\text{Zr}_2\text{O}_7$ pyrochlore, *J. Cryst. Growth* **402**, 291 (2014).
- [386] C. Mauws and C. R. Wiebe (private communication).
- [387] <https://www.mrfn.org/>